POLITECNICO
MILANO 1863

SCUOLA DI INGEGNERIA INDUSTRIALE
E DELL'INFORMAZIONE

Reconciling theory, experiments and models for hydrogen combustion: an integrated theoretical and optimization approach

TESI DI LAUREA MAGISTRALE IN
CHEMICAL ENGINEERING-INGEGNERIA CHIMICA

Author: **Claudio Averoldi**

Student ID:	944627
Advisor:	Prof. Matteo Pelucchi
Co-advisor:	Dr. Andrea Bertolino
Academic Year:	2020-21

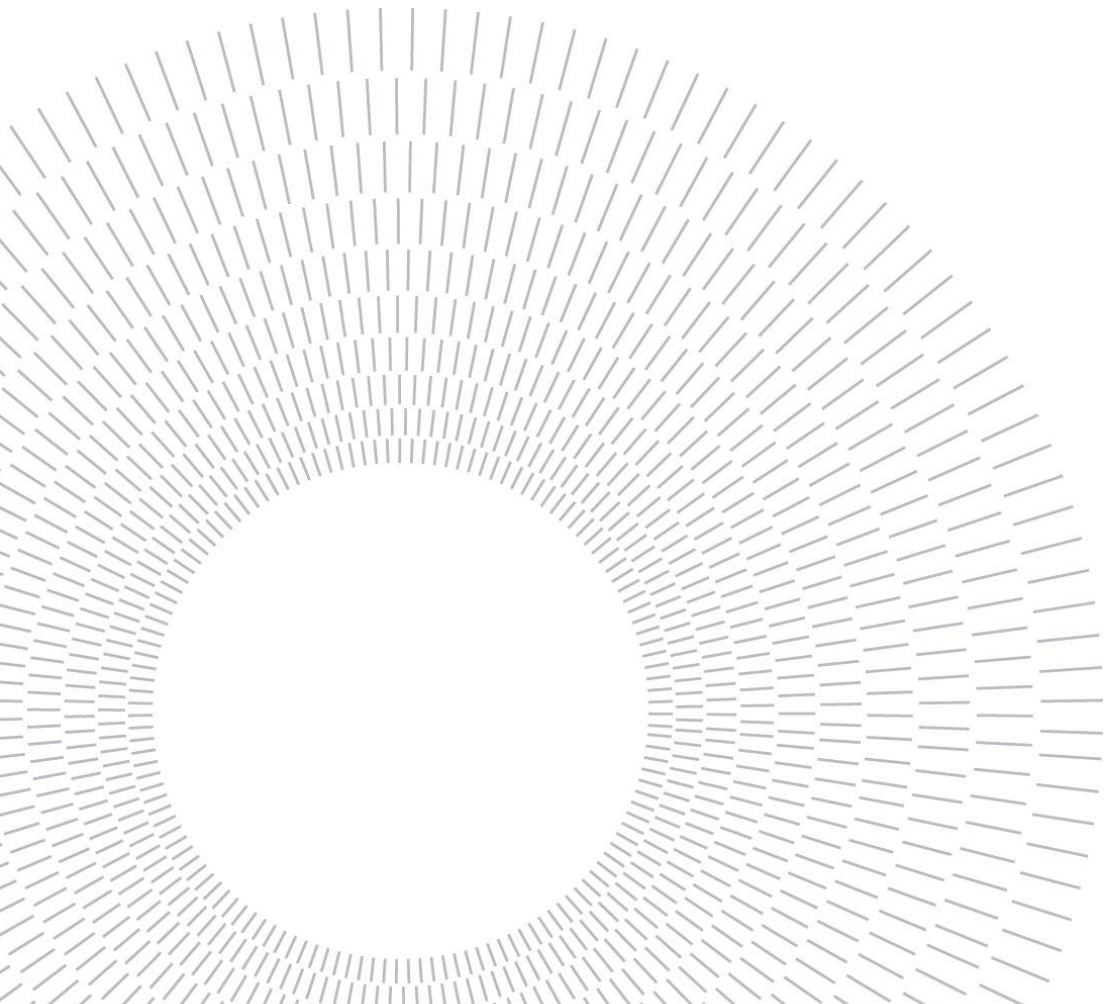

Abstract

Pollutant emissions related to productive activities have caused serious consequences, one of them is climate change, consequently, many countries have decided to gradually quit using fossil fuels, opting for the use of green energy. This change leads to growing attention on the development of renewable sources, and smart energy carriers, as hydrogen is, with this in mind, the study on the kinetic model for hydrogen combustion gains great importance in the development of new technologies. This work, in continuity with a previous project of Politecnico di Milano with other international universities, is finalized to the realization of a state of the art predictive model for hydrogen combustion, based on Ab initio theoretical calculations, then optimized with respect to the experimental data collected. Given theoretical results for a kinetic constant evaluation, provided by Argonne National Laboratory, they are used, together with the experimental data obtained analyzing scientific literature for every reaction, as an input in OptiSMOKE++, the result is an optimized model for every reaction analyzed. The same process is repeated on every reaction of interest, and a revised model is obtained, subsequently, in validation step, this model has been tested simulating operative conditions of various macroscopical experiments collected on flames and different kind of reactors, working with OpenSMOKE++, the results are compared with the previous model, CRECK2003, and with the measured experimental data.

The results obtained from this work show a valid model that, in some cases, have provided better results with respect to the original model, furthermore, if further both theoretical analyses and experimental data will be provided in future, it will be possible to continuously improve the new model, using the same methods proposed during this work.

Key-words: Hydrogen; Optimization; kinetic modeling; Ab initio calculations; PES; OptiSMOKE++; OpenSMOKE++;

Sommario

Le emissioni inquinanti legate alle attività produttive hanno portato gravi conseguenze, tra cui i cambiamenti climatici, per questo motivo vari paesi hanno deciso di abbandonare gradualmente l'uso dei combustibili fossili, optando per l'uso di energia pulita. Questo cambiamento porta ad una crescente attenzione verso lo sviluppo di fonti rinnovabili e vettori energetici puliti come l'idrogeno, in quest'ottica, lo studio del modello cinetico di combustione dell'idrogeno assume una grande importanza nello sviluppo di nuove tecnologie. Questo lavoro, in continuità con un precedente progetto del Politecnico di Milano in collaborazione con altre università internazionali, è finalizzato alla realizzazione di un modello predittivo per la combustione dell'idrogeno, basato su calcoli teorici Ab initio, poi ottimizzati sui dati sperimentali raccolti. I risultati teorici, forniti dall'Argonne National Laboratory, per la determinazione di una costante cinetica, uniti ai dati sperimentali ottenuti analizzando la letteratura scientifica per ogni reazione, sono usati come input in OptiSMOKE++, il risultato è un modello ottimizzato per ogni reazione studiata. Ripetuto questo processo su ogni reazione di interesse, si ottiene un modello revisionato, successivamente, in fase di validazione, questo modello è stato testato simulando le condizioni operative di vari esperimenti macroscopici raccolti su fiamme e diversi tipi di reattori, utilizzando OpenSMOKE++, i risultati sono confrontati con il modello precedente, CRECK2003, e con i dati sperimentali misurati.

I risultati ottenuti in questo lavoro mostrano un modello valido che, per alcuni casi, ha fornito risultati migliori rispetto al modello originale, inoltre, se supportato con un approfondimento della ricerca sia dal lato teorico che sperimentale, sarà possibile in futuro un ulteriore miglioramento del modello realizzato, utilizzando gli stessi metodi proposti in questo lavoro.

Parole chiave: Idrogeno; Ottimizzazione; modellazione cinetica; calcoli Ab initio; PES; OptiSMOKE++; OpenSMOKE++;

Contents

1. Introduction

1.1 Energetic scenario and hydrogen role

Nowadays, one of the most important challenges that have to be faced is the compromise between energy provision and sustainability.

For centuries, human activities have recklessly produced energy and other commodities, without thinking on the possible consequences on the environment, as a result of this, many criticalities have raised, in particular the phenomenon of climate change.

Indeed, the production of greenhouse gases (CO_2 mostly, but also N_2O, chlorofluorocarbons…) by human sources, have contributed to global temperature rise, that has many consequences like ice melting, rise of the sea level, ocean acidification, extreme meteorological events etc., these effects are already evident nowadays [1], and make clear that current system is not sustainable anymore.

For this reason, United Nations Member States, in 2015, fixed 17 sustainable development goals that should be reached within 2030, concerning wellness, more equality, and more attention to the environment, one of those is to afford green and sustainable energy.

In this perspective, a rising interest is expected in next years for renewable energy sources (i.e. solar, wind, hydroelectric…), and for the use of green fuels, such as hydrogen, gradually replacing the widely used fossil fuels.

Hydrogen is called a Smart Energy Carrier (SEC), since molecular hydrogen is not present on earth, it must be recovered from other molecules, this step demands some energy, then hydrogen guarantees an energy efficient fuel, useful for applications for which the use of renewable sources wouldn't be possible, i.e. it is a way to produce a fuel from the surplus of renewable energy.

Since hydrogen is present in many molecules, there are many possibilities to produce it, hydrogen is characterized with a color to define its origins, i.e. grey hydrogen that is produced from steam reforming, blue hydrogen has the same origin, but a carbon capture process is done on subproducts, of course, in order to have green energy, also hydrogen production must be sustainable: a clean way to produce it is from electrolysis of water, taking the energy needed from renewable sources, hydrogen produced in this process is named green, another possibility is the production of hydrogen from methane pyrolysis, this is called turquoise hydrogen, and doesn't produce CO_2 as a byproduct but solid carbon, therefore it is considered a carbon-free process[2].

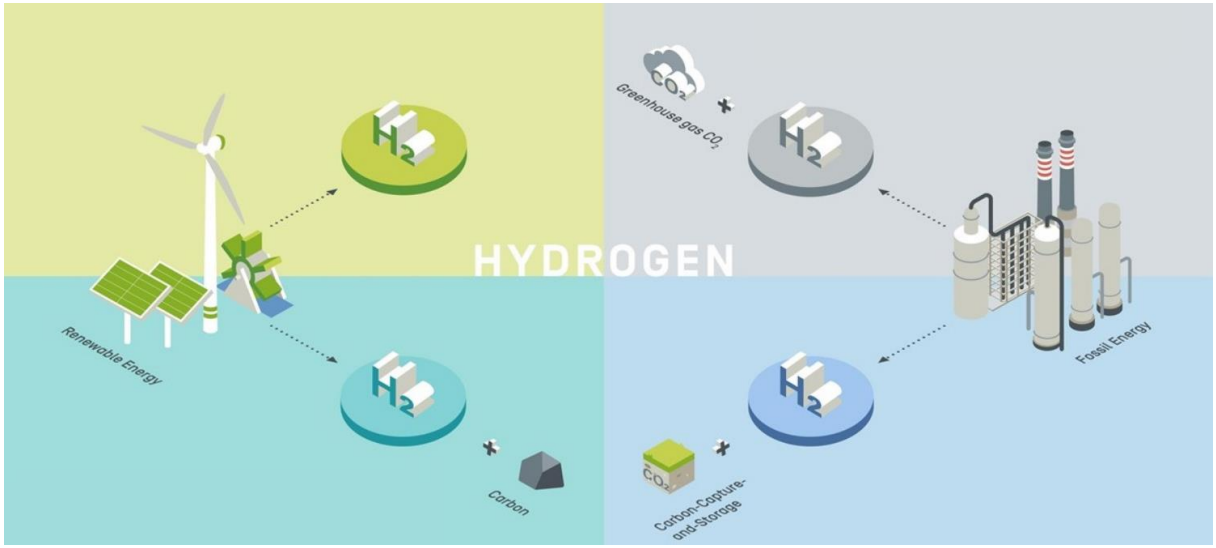

Figure 1.1: *Possible paths in hydrogen production [2]*

Once hydrogen is produced, obviously, the combustion reaction is totally green, water and energy are the only products.

The oxidation of hydrogen grants a very high adiabatic flame temperature, especially in oxy-combustion conditions, this makes it viable as a fuel for many applications, hydrogen is more energy efficient compared to fossil fuels, still, some issues arise in terms of storage, and energy density, that impose the use of high pressure and special tanks to store it, it is also an extremely flammable molecule, as can be seen in Figure 1.2, it is flammable in air at a concentration between 4% to 75% v/v, this could lead to safety issues.

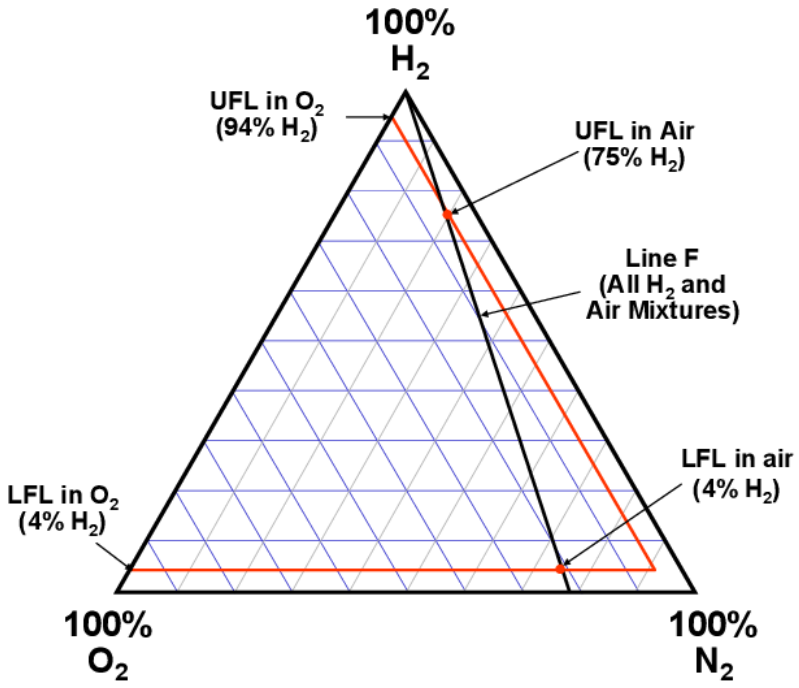

Figure 1.2: *Flammability limits of a H_2-O_2-N_2 mixture [3]*

Many sectors are already investing on hydrogen for future development, e.g. steel mills [4] (which now are responsible of 7% of global CO_2 emissions) are already at development stage, aviation sector aims to launch hydrogen fueled airbuses by 2035 [5], this occurs also to transport sector, with projects for trains, buses and cars powered by hydrogen, moreover, many companies are focusing on hydrogen production, this will hopefully reduce its cost, making it economically viable as a fuel.

In other words: more and more interest is growing on hydrogen combustion, thus, experimental research will focus in developing new facilities, and kinetic modeling will play a major role in the design and optimization of new technologies.

The goal of this work is to define a state of the art kinetic model for hydrogen combustion, that reconciles high-level theoretical analysis and experimental data available from literature, i.e. a predictive and reliable model to be used in simulations.

1.2 Topics of this thesis

This work inherits the efforts of a choral project by Politecnico di Milano, RWTH Aachen University, Argonne National Laboratory, National University of Ireland Galway, Technical University of Denmark and Eötvös Loránd University, whose goal is to define a common state of the art model for hydrogen combustion, starting from theoretical consideration and a large collection of data, both macroscopic (i.e. model validation targets) and microscopic (rate constant measurements) then reconciling experimental data, theory and kinetic models.

In particular, the evaluation for the kinetic constant of a specific reaction starts from Ab Initio Transition State Theory based Master Equation (ME) and Potential Energy Surface (PES) investigation [6], provided by Argonne National Laboratory, to get the kinetic constant of the considered elementary reaction, as a function of temperature and pressure, these high-level theoretical calculations grant very accurate results (i.e. typically well below a factor of 2).

At the same time, the scientific literature for each reaction has been examined, collecting all the existing data concerning the kinetic constants, the operative conditions where data were acquired and, if available, the related uncertainty.

For the following step, working with OptiSMOKE++ [7], an optimization routine has been performed starting from the outputs of theoretical calculations and ME simulations to better fit the data collected from the experimental papers, thus also identifying possible outliers.

Repeating this scheme for all the reactions, a new model is obtained and therefore has to be validated; in order to do that, other data were collected, this time concerning macroscopic experiments on flames, shock tubes, PFR, … and simulated the same experiments with OpenSMOKE++ [8] using an updated version of the CRECK kinetic model, comparing the results with both the original model and the experimental observations.

It must be specified that, in data collection, two categories of data are evidenced:

- Microscopic data: those are data collected from experiments focused on evaluating the kinetic constant of a single reaction, trying to measure it in a direct way, without adding external uncertainty; those are data that will be presented in Chapter 4.

- Macroscopic data: data on flame velocities, ignition delay times, concentration trends and so on, those data will be part of the model validation in Chapter 5.

In Chapter 2, some important aspects of hydrogen combustion model and some fundamentals of kinetics will be outlined.

In Chapter 3, the methods and protocols of the workflow will be discussed.

Chapter 4 is dedicated to assembling the new model, thus determining the "best" rate constants obtained either by direct fitting of the experimental measurements for temperature dependent kinetic rate constants, and by an optimization routine based on ME simulation outputs in the case of pressure and temperature dependent rate constants.

Chapter 5 presents the validation of the new model.

Lastly, Chapter 6 draws conclusion of the present work.

2. Kinetic modeling

2.1 The importance of a model for hydrogen

For what said in Chapter 1, the oxidation of hydrogen is interesting by itself, as a way to achieve decarbonization, indeed a deep knowledge of chemical kinetics phenomena allows to predict how the system evolves changing the operative conditions, and therefore to optimize the design of new technologies by means of detailed kinetics coupled with Computational Fluid Dynamics simulations.

Furthermore, since in general kinetic models for pyrolysis and combustion are hierarchical in nature and in the way they are typically developed, hydrogen plays an important role also in every oxidation process that involves higher molecular weight hydrocarbons, thus an improved hydrogen model should positively impact also combustion kinetic subsets of different fuels. For this reason, the hydrogen/oxygen subset of gas-phase kinetic models is often referred to as the "core mechanism".

It should be noted that the complexity typically increases opposed to the hierarchy (Figure 2.1). Thus, while hydrogen contains a relatively small number of species and reactions, the workflow here proposed is relatively easy to be managed in this specific case. The lack of data, in particular the microscopic ones, for higher molecular weight molecules poses some additional challenges if the same approach here presented was to be extended to other subsets.

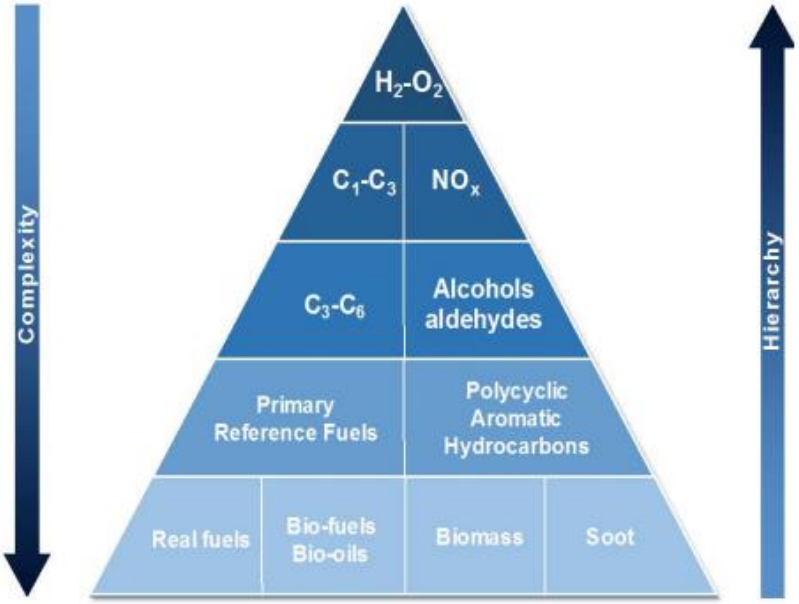

Figure 2.1: *Hierarchy and complexity "pyramid" of combustion chemical kinetics*

At a first sight, hydrogen oxidation may seem a very simple global reaction,

$$H_2 + \frac{1}{2}O_2 \rightarrow H_2O$$

But, in practice, things are more complicated, i.e. that overall reaction is made by many elementary reactions that happens simultaneously:

$$H_2 + M = 2H + M$$
$$H_2 + O = H + OH$$
$$H_2 + OH = H + H_2O$$
$$2O + M = O_2 + M$$
$$H + O_2 = O + OH$$
$$H + OH + M = H_2O + M$$
$$O + H_2O = 2OH$$
$$H + O + M = OH + M$$
$$H_2O_2 = 2OH$$
$$H + H_2O_2 = H_2O + OH$$

$$H + H_2O_2 = H_2 + HO_2$$
$$O + H_2O_2 = OH + HO_2$$
$$OH + H_2O_2 = H_2O + HO_2$$
$$OH + H_2O_2 = H_2O + HO_2$$
$$H + HO_2 = 2OH$$
$$H + HO_2 = H_2 + O_2$$
$$O + HO_2 = O_2 + OH$$
$$OH + HO_2 = O_2 + H_2O$$
$$OH + HO_2 = O_2 + H_2O$$
$$2HO_2 = O_2 + H_2O_2$$
$$2HO_2 = O_2 + H_2O_2$$
$$H + O_2 = HO_2$$

In addition to this, other reaction channels can emerge from analysis such as the one here presented. For example, an additional pathway for HO_2 radicals recombination (i.e. $HO_2+HO_2=O_2+OH+OH$) was recently highlighted by Klippenstein and co-workers involved in the present project.

A radical chain mechanism typically occurs through a series of reactions that can be classified according to the following:

- Initiation reactions: reactions that start from the (relatively) stable reactants to generate unstable and very reactive radicals, species created by the homolytic scission of a covalent bond in a molecule. As a consequence of this, the electrons that created the bond are equally divided in the products, generating new species with unpaired electrons, those are very unstable and tend to react with other species:

$$H \cdot\cdot H = \ H \cdot + H \cdot$$

- Propagation reactions: reactions in which the number of radicals is kept constant:

$$H_2 + OH\cdot = H\cdot + H_2O$$

- Branching reactions: reactions that increase the overall number of radicals, e.g.:

$$H_2 + O\cdot = H\cdot + OH\cdot$$
$$H\cdot + O_2 = OH\cdot + O:$$

In particular, O: is a double radical, because it has two unpaired electrons, so in this case three radicals are obtained starting from a single initial radical.

- Termination reactions: reactions in which the number of radicals is reduced:

$$H\cdot + OH\cdot = H_2O$$

The original model developed by the CRECK group at Politecnico di Milano relies on a well validated and trained state-of-the-art hydrogen model, i.e. the so called Aramco mech 2.0 [9]. Recent advances in theoretical techniques [6] allows this reconciliation effort, thus allowing detailed kinetic models to be predictive, a priori, without need of tuning or optimization over extensive database of macroscopic experimental targets.

The original model developed by CRECK is here improved based on an accurate revision of some of the elementary reactions.

2.2 Fundamentals of kinetics

While thermodynamics just deals with the initial and final state (i.e. the equilibrium state) of a system, chemical kinetics describes the rate of that process, called reaction rate.

$$\mathrm{R\,(T,P,Ci)} \;=\; \mathrm{k\,(T,P)} \;\cdot\; \mathrm{f\,(Ci)}\;[\frac{kmol}{m^3}\cdot \mathrm{s}]$$

f(Ci) is a function of the concentration of chemical species involved, for an elementary reaction it can be written as:

$$f(Ci) = \prod_{i=1}^{Nspecies} Ci^{\alpha i}$$

Where α is the stoichiometric coefficient of the selected species; Nspecies just refers to the reactants, i.e. in reaction

$$aA + bB \rightarrow products$$

It is:

$$f(Ci) = C_A^a \cdot C_B^b$$

When there are gas species involved, Ci can be rewritten as a function of pressure using ideal gas law:

$$Ci = \frac{P}{R \cdot T} \cdot xi$$

With

P: pressure of the system

R: universal gas constant

xi: molar fraction of the i-th species in the system.

k(T,P) is called kinetic constant, in order to define it, two different classes of reactions must be specified:

- Pressure independent reactions: for those reactions the kinetic constant is defined using an Arrhenius expression:

$$k(T) = A \cdot \exp\left(-\frac{Ea}{R \cdot T}\right)$$

Where A is pre exponential factor or frequency factor, it is related to the collision frequency and the steric properties of the reactants.

Ea is the activation energy of the system, the energy reactants need to overcome to generate products:

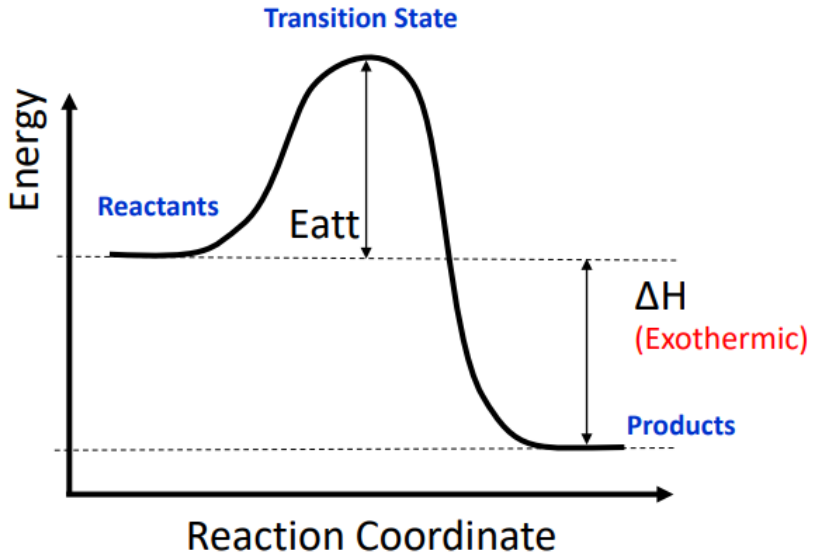

Figure 2.2: *Typical energy level diagram for an exothermic reaction*

Actually, in many cases a modified Arrhenius expression is used, that is:

$$k(T) = A \cdot T^n \cdot \exp\left(-\frac{Eact}{R \cdot T}\right)$$

In order to make explicit the temperature dependence in the pre exponential factor and better fit the experimental data.

- Third body reactions: these are some particular reactions in which a collision with a third body is necessary to carry on the reaction, let's consider a generic reaction

$$A + B + M \rightleftharpoons AB + M$$

Where M indicates the third body, in direct reaction, collision with M is needed to dissipate some energy and stabilize the product, in inverse reaction, collision with M breaks the AB bond.

For those reactions, k expression is more difficult than before, since it is a function of both temperature and pressure of the system, pressure dependence is described in Figure 2.3:

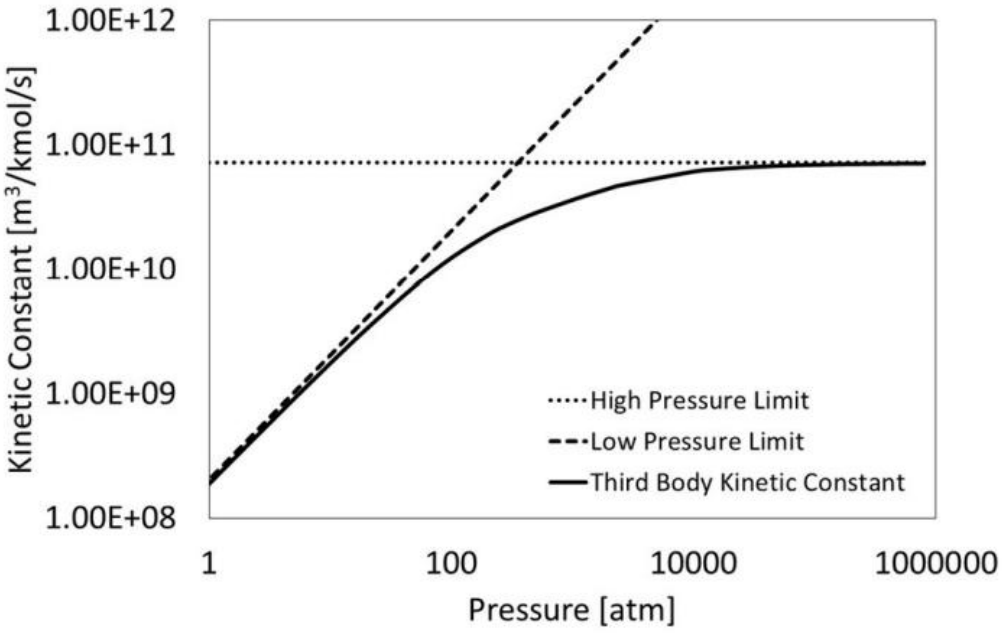

Figure 2.3: *Pressure dependence of the kinetic constant for a third body reaction*

As can be seen from this figure, there are 3 different regions:

1. Low pressure limit: an initial region in which pressure dependence is linear.
2. High pressure limit: it is the final region, over a certain pressure, in which the kinetic constant becomes pressure independent.
3. Intermediate region: also called fall-off behavior, typically at high temperatures, in this zone, pressure dependence has a complex nonlinear behavior.

Pressure dependence can be written as a function of the concentration of the third body M (also called bath gas) via the ideal gas law, in a general case with N species involved, it can be written as:

$$[M] = \frac{P}{R \cdot T} \cdot \sum_{i=1}^{N} x_i \cdot \varepsilon_i$$

The quantity ε_i is called third body efficiency, every different species has its relative efficiency in order to stabilize the designed molecule.

3. Methods

3.1 OpenSMOKE ++

OpenSMOKE++ is the framework used to simulate the macroscopical experiments to validate the new model in Chapter 5.

Developed by Cuoci et al. [8], OpenSMOKE++ is designed to perform numerical simulations on combustion processes, it allows to simulate flames and other ideal reactors such as Continuous Stirred Tank Reactors (CSTRs), Plug Flow Reactors (PFRs), shock tubes or batch reactors.

Working with its postprocessor, it is possible to directly plot the output results, or to perform some kinetic analysis on the mechanism, for example ROPA or sensitivity analyses.

To run a simulation, first of all what is needed is a kinetics folder, this is generated in a pre-processing phase, where a kinetic mechanism, a thermodynamic database, and a file with transport properties are needed as an input.

Once the kinetic model is generated, one can define the input of the simulation, specifying the type of simulation (i.e. premixed flame, plug flow reactor…), then the kinetics folder and the simulation conditions, i.e. reactor dimensions, temperature, pressure, species involved…

In order to define the mixture, it is possible either to give the total moles (or mole fractions/masses/mass fractions) of the system, or to define a fuel, an oxidizer and the equivalence ratio, defined as:

$$\phi = \frac{n_{fuel}}{n_{fuel,stoichiometric}}$$

In a combustion process, 3 different cases can be distinguished:

- If ϕ=1, combustion is in stoichiometric conditions.

- If ϕ<1, fuel moles are lower than in stoichiometric conditions, in this case the mixture is in lean condition.
- If ϕ>1, fuel moles are higher than in stoichiometric conditions, this is a rich condition.

Let's now focus on the kinetic mechanism, this file contains:

1. A list of elements

$ELEMENTS$
C
H
O
N
...
END

2. A list of species involved:

$SPECIES$

$H2$	H	$O2$
O	$H2O$	OH
$N2$	...	END

3. A list of reactions, for pressure independent reactions those are written as:

$H2 + O = H + OH$ $\quad$ $5.0800e+04 \quad 2.670 \quad 6292.00$

Where the three terms are the parameters of the modified Arrhenius equation (respectively A [mol/cm3/s], n [-] and Eact [cal/mol]).

While pressure dependent reactions may be written in different ways, for this work they are written with a PLOG formalism, different Arrhenius parameters are given at different pressures like this:

$$HOCO = OH + CO \qquad 6.3000e+32 \quad -5.960 \quad 32470.00$$
$$PLOG\ /\ 1.000000e-03 \quad 1.550000e-08 \quad 2.930000e+00 \quad 8.768000e+03 \quad /$$
$$PLOG\ /\ 3.000000e-03 \quad 1.770000e+03 \quad 3.400000e-01 \quad 1.807600e+04 \quad /$$
$$PLOG\ /\ 2.960000e-02 \quad 2.020000e+13 \quad -1.870000e+00 \quad 2.275500e+04 \quad /$$
$$\ldots$$
$$PLOG\ /\ 9.869000e+02 \quad 6.300000e+32 \quad -5.960000e+00 \quad 3.247000e+04 \quad /$$

Then using logarithmic interpolation it is possible to define the kinetic constants at intermediate pressures:

$$\ln(k_{int}) = \ln(k_i) + [\ln(k_{i+1}) - \ln(k_i)]\frac{\ln(P_{int}) - \ln(P_i)}{\ln(P_{i+1}) - \ln(P_i)}$$

Since PLOG formalism doesn't take into account third body efficiencies, for a single reaction a different PLOG must be written for every bath gas, and then a PLOG mix, like this:

PLOGMX / 0.493000 1.00268e+21 -3.24701 1785.38 /

…

PLOGSP / AR 0.493000 1.26692e+21 -3.40945 536.167 /

…

PLOGSP / KR 0.493462 1.32907e+21 -3.40035 478.122 /

…

Then, the reaction rate is calculated as follows:

$$r = r_{mx} \times \left(1 - \sum_{i=1}^{N} x_i\right) + \sum_{i=1}^{N} r_i \times x_i$$

Where:

xi is the molar fraction of the i-th bath gas

N is the total number of bath gases defined

r_{mx} and r_i are respectively the reaction rates calculated with the mix coefficients and with the coefficients for the i-th species.

The final goal of this work is to modify this file for H2 oxidation.

Concerning the thermodynamic file, it contains the list of species involved in the mechanism, with their properties expressed as NASA polynomials, i.e. for hydrogen:

H2	ATcT3EH	2	0	0	0G	200	6000	1000	1
2,90E+00	8,69E-04	-1,66E-07	1,91E-11	-9,31E-16	2				
-7,98E+02	-8,46E-01	2,38E+00	7,74E-03	-1,89E-05	3				
1,96E-08	-7,17E-12	-9,21E+02	5,47E-01	0,00E+00	4				

These polynomials are used by the code to calculate thermodynamic properties of the different species as a function of temperature, using the following formulae:

$$\frac{\tilde{C}_{p,i}}{R} = a_{i,1} + a_{i,2}T + a_{i,3}T^2 + a_{i,4}T^3 + a_{i,5}T^4$$

$$\frac{\widetilde{H}_i}{RT} = a_{i,1} + \frac{a_{i,2}}{2}T + \frac{a_{i,3}}{3}T^2 + \frac{a_{i,4}}{4}T^3 + \frac{a_{i,5}}{5}T^4 + \frac{a_{i,6}}{T}$$

$$\frac{\tilde{S}_i}{R} = a_{i,1}\ln T + a_{i,2}T + \frac{a_{i,3}}{2}T^2 + \frac{a_{i,4}}{3}T^3 + \frac{a_{i,5}}{4}T^4 + a_{i,7}$$

As can be seen, in a NASA polynomial two sets of coefficients are present (14 coefficients in total), those are valid in two different temperature intervals, the limits of the intervals are indicated on the top right side of the NASA formulation (continuity between the two intervals must be guaranteed).

3.2 OptiSMOKE ++

This paragraph is based on the PhD thesis:

- Optimization and Uncertainty Quantification of kinetic mechanisms for renewable fuels and sustainable combustion technologies, Andrea Bertolino

OptiSMOKE++ [7] is a toolbox developed by Fürst, Bertolino et al. used for the optimization of chemical kinetics, it can use different optimization methodologies, and deal with many uncertain parameters simultaneously.

Algorithms used for the optimization are taken from DAKOTA (Design analysis kit for optimization and terascale applications) toolkit [10], while input files are taken directly from OpenSMOKE++.

For each reaction rate constant, an uncertainty exists, also starting from theoretical calculations.

That uncertainty is, in general, both temperature and pressure dependent, in OptiSMOKE++, this is represented with the f factor:

$$\mathrm{f} = \frac{k_{max} - k_0}{\ln(10)} = \frac{k_0 - k_{min}}{\ln(10)}$$

(Where k_0 is the nominal value of the kinetic constant)

In order to optimize the kinetic constant, the uncertainty factor must be transferred to the Arrhenius parameters, in order to do that, the bounds for every parameter are defined as follows:

$$\alpha_0 + \ln(10^{-\mathrm{f}}) < \alpha < \alpha_0 + \ln(10^{\mathrm{f}})$$

$$\mathcal{E}_{a,0} - \mathrm{T_{min}}\,\mathrm{f}\ln(10) < \mathcal{E}_a < \mathcal{E}_{a,0} + \mathrm{T_{min}}\,\mathrm{f}\ln(10)$$

$$\beta_0 - \mathrm{f}\frac{\ln(10)}{\ln(\mathrm{T_{max}})} < \beta < \beta_0 + \mathrm{f}\frac{\ln(10)}{\ln(\mathrm{T_{max}})}$$

Where α refers to A, $\mathrm{E_a}$ to Eact, β to n.

If, during optimization, the kinetic constant goes out of these bounds, then a penalty function is applied.

In order to optimize PLOG reactions, some more considerations need to be done: in this case, multiple Arrhenius coefficients are provided at different pressure values, this implies that the three Arrhenius parameters for each pressure value cannot be optimized independently from the others, this would cause a loss in physical meaning for the result, having a non-monotonic behavior for the kinetic constant.

Therefore, Arrhenius parameters for all the pressures have to be optimized simultaneously, to do that, three new uniformly distributed random values are defined, their average value is zero, and they are constrained in these ranges:

$$X_1 \in [-f ln(10), f ln(10)]$$

$$X_2 \in [-R\ T_{min}\ f \ln(10)\ , R\ T_{min}\ f \ln(10)]$$

$$X_3 \in \left[-f\ \frac{\ln(10)}{\ln(T_{max})}, f\ \frac{\ln(10)}{\ln(T_{max})}\right]$$

Those 3 values are related to the Arrhenius parameters by the following formulae:

$$\ln(\boldsymbol{A_i}) = \ln(\boldsymbol{A_0}) + X_{1,i}$$

$$\boldsymbol{E_i} = \boldsymbol{E}_0 + X_{2,i}$$

$$\boldsymbol{n_i} = \boldsymbol{n}_0 + X_{3,i}$$

N.B. Independently from the number of pressures (np) involved in the PLOG, the active variables remain 3, but the optimized parameters are 3*np.

Since the PLOG formalism doesn't take into account the bath gas efficiency, and n PLOG must be written for every different bath gas, in the same way an optimization routine occurs for each bath gas.

The algorithm used for this work are called evolutionary algorithms [11], summarizing this method when applied to a kinetic model, an individual "DNA" string, composed of random values of Arrhenius parameters A,n,Ea is generated for every reaction rate involved, this process is repeated S times to generate a population of randomly generated DNA strings.

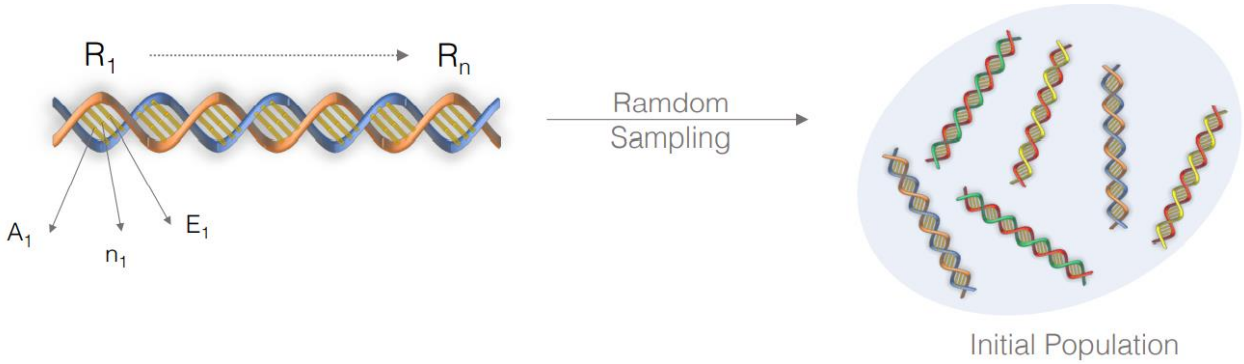

Figure 3.1: *Graphical representation of a DNA string in an evolutionary algorithm applied to chemical kinetics, Courtesy of Andrea Bertolino*

Starting from this, the algorithm begins the first iteration, the objective function is evaluated for every string, the strings are ranked with respect to the value returned.

Then the cross-over sequency begins, chromosomes are selected from the original strings and mixed, from these new strings (called Off-springs) are produced, during this process, each off-spring has a probability to mutate, given by a mutation rate.

At the end of this process, a 2S population of strings is finally produced, from this, S/2 strings are taken as the best individuals, and another S/2 is taken randomly, so a new S population is selected, and the procedure restarts, this happens until a good accuracy is achieved.

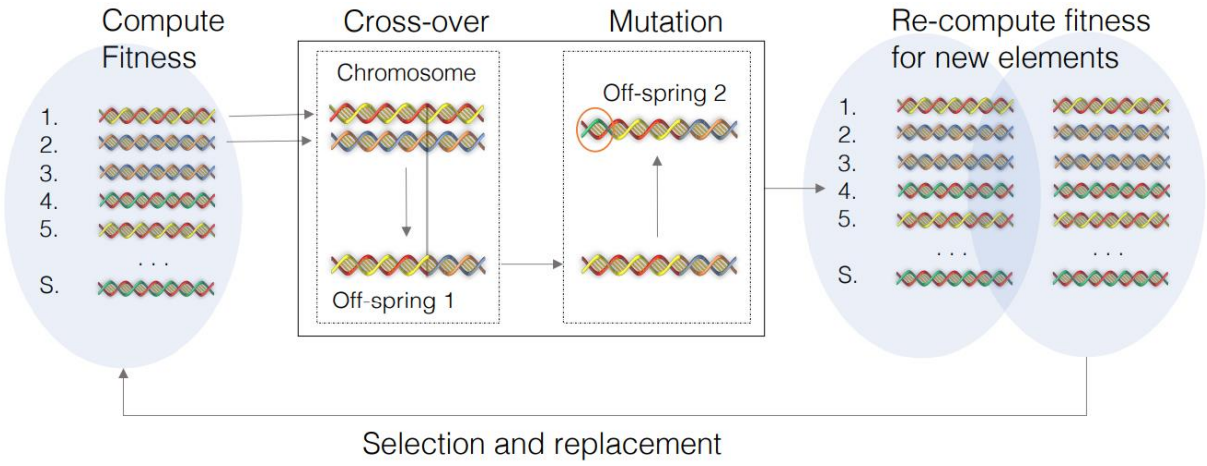

Figure 3.2: *Graphical representation of an example generation in Evolutionary Algorithms, Courtesy of Andrea Bertolino*

Let's now talk about the objective functions used in this work.

Assume to have a set of experiments y^e and a mathematical model f(θ), where θ is the vector of model parameters, the goal of parameters estimation is to maximize the probability of obtaining experimental data from model responses.

Data have their intrinsic uncertainty, so they can be regarded as random variables with a joint probability distribution like this:

$$P(y^e, y, \varepsilon)$$

With y intended as the real unknown values, and ε the experimental error; in this work, y is intended as ln(k), this is to avoid problems related to the scale of absolute values, which can be very large.

The vector of model parameters θ described above, can be estimated by maximizing the probability function P, this can be written as an objective function θ, that has to be minimized.

In this work, two objective functions are used, the L1-norm and the L2-norm, that are, respectively:

$$Obj(\theta)=\sum_{i=1}^{NE}\sum_{j=1}^{NY}\frac{|f_{i,j}-y_{i,j}^{e}|}{\sigma_{i,j}(y_{i,j}^{e})}$$

$$Obj(\theta)=\sum_{i=1}^{NE}\sum_{j=1}^{NY}\frac{(f_{i,j}-y_{i,j}^{e})^{2}}{\sigma_{i,j}(y_{i,j}^{e})^{2}}$$

Where:

NE: number if experiments

NY: number of dependent variables

$\sigma_{i,j}$: experimental variance of the j-th dependent variable in the i-th experiment, all the measured variable values are assumed to be with mean $y^{e}_{i,j}$ and standard deviation $\sigma_{i,j}$..

3.3 Workflow

Now that the methods are defined, let's see the workflow of this thesis:

- Select a reaction.
- External inputs: theoretical ab initio calculations are re-arranged in PLOG format for the kinetic mechanism, original mechanism file is modified and given as an input to OptiSMOKE++, together with experimental data, previously collected and organized. As already said, for pressure dependent reactions, an optimization routine must occur for every bath gas.
- An f factor must be specified, then the optimization routine can start, OptiSMOKE++ gives back an optimal mechanism as an output.
- The same process must be repeated for every bath gas (for which both theoretical calculation and experimental data are available), then a new reaction is selected and the same routine occurs.
- At the end of this step, all the results are put together, the new mechanism is constructed.
- New mechanism is used in OpenSMOKE++, simulating the operative conditions obtained from macroscopical experimental data, the results obtained are compared to the data and to the original model.

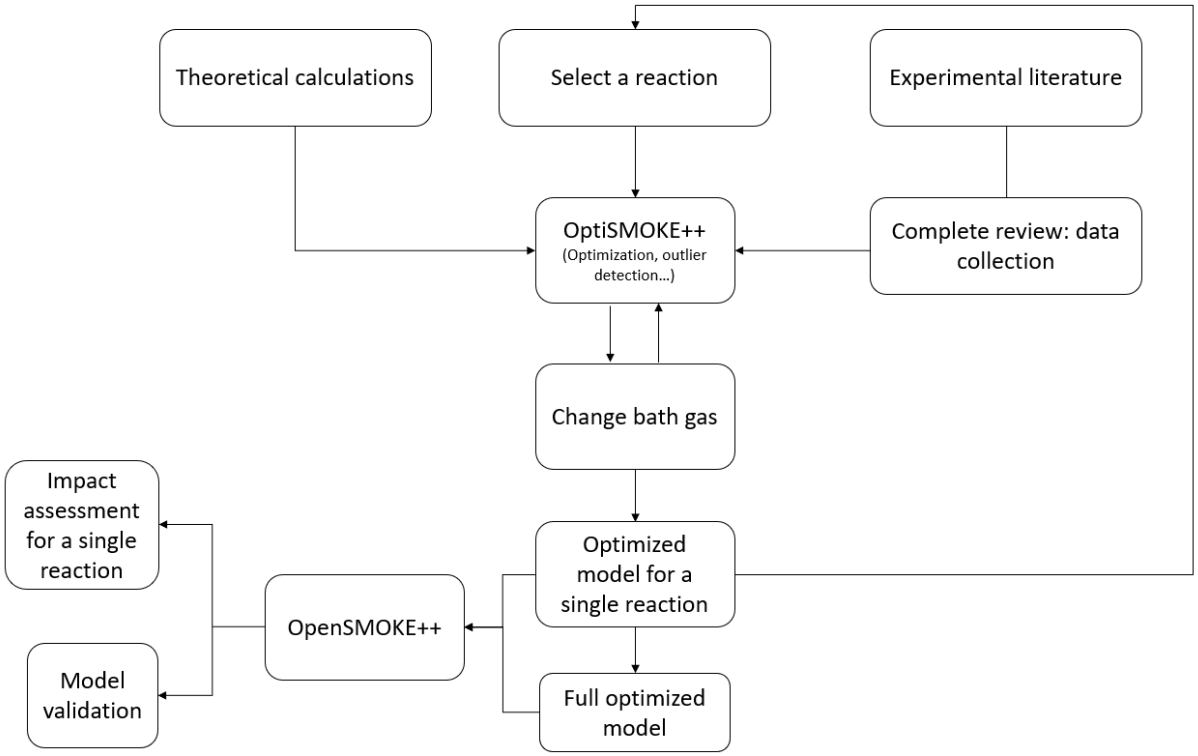

Figure 3.3: *Schematic workflow of this thesis*

4. New model construction

4.1 Introduction

In this chapter, the focus is the generation of the new model; to do that, the kinetic constants of the reactions of interest must be defined.

The reactions are organized in potential energy surfaces (PES), that represent the variation in energy of a system as a function of its geometrical properties.

Each of the following PES is named with an "R" followed by the number of valence electrons involved (i.e. "R2" will be the PES containing two valence electrons …).

For each PES analyzed, the procedure is the following:

1- PES is presented, and the reactions involved are outlined.

2- All the theoretical and experimental works for every reaction are reported.

3- Experimental data, theoretical calculations for k and optimized results are plotted, the new expression for k is reported.

4- The old model is modified, and the impact of the revised reaction is assessed for a sample of the macroscopical experiments (i.e. an anticipation of what will be done in Chapter 5).

For pressure dependent reactions, the starting point for optimization is from theoretical calculations, while for pressure independent reactions the input used is the original polimi mechanism (CRECK2003).

Concerning experimental data, it must be sad that all the following papers have been examined, however not all the data have been used for model validation, since not all of them are considered reliable, for different reasons:

- Old works, they often show inaccurate measures, due to instrumentation limits or to inappropriate interpretations of the observed phenomena
- Very indirect or too inaccurate measurements

- Sometimes data collection is difficult, not always operative pressure is provided, and just a range is given

Proceeding with this work, some other criticalities arose, in particular, there are reactions that still require some computational efforts on the ME side, so, the optimization step couldn't take place, and the Arrhenius coefficients used for these reactions are still the ones of Aramco mech 2.0.

In particular, those reactions are:

- $H_2 + M \rightarrow H\cdot + H\cdot + M$
- $H\cdot + O\colon + M \rightarrow OH\cdot + M$
- $O_2 + M \rightarrow O\colon + O\colon + M$
- $O_2 + O\colon + M \rightarrow O_3 + M$

However, data collection on both experimental and theoretical side is reported also for these reactions.

Another problem that will be evident in future paragraphs, is the inhomogeneity in analysis of the different reaction paths, with reactions that report poor datasets, thus introducing some doubts in the reliability of final results, also, for some pressure dependent reactions, only few bath gases are analyzed.

Of course, deepening the database for those reactions will help in improving the effectiveness of the new model.

To resume, these are the reactions presented in this work:

Reaction	Progress
R2: $H_2 + M \rightarrow H\cdot + H\cdot + M$	Data collected, theory in progress
R9: $H\cdot + O\colon + M \rightarrow OH\cdot + M$	Data collected, theory in progress
R10a: $H\cdot + OH\cdot + M \rightarrow H_2O + M$	Reaction optimized
R16: $O_2 + M \rightarrow O\colon + O\colon + M$	Data collected, theory in progress
R17a: $H\cdot + O_2 + M \rightarrow HO_2\cdot + M$	Reaction optimized
R17b: $H\cdot + O_2 \rightarrow O(^3P) + OH\cdot$	Reaction optimized
R18a: $OH\cdot + OH\cdot + M \rightarrow H_2O_2 + M$	Reaction optimized

$R18c: H\cdot + HO_2\cdot \rightarrow H_2 + O_2$	*Reaction optimized*
$R18d: H\cdot + HO_2\cdot \rightarrow OH\cdot + OH\cdot$	*Reaction optimized*
$R24: O_2 + O: + M \rightarrow O_3 + M$	*Data collected,* theory in progress
$R26b: H_2O_2 + O(^3P) \rightarrow OH\cdot + HO_2\cdot$	*Reaction optimized*
$R34a: HO_2\cdot + HO_2\cdot \rightarrow H_2O_2 + O_2$	*Arrhenius parameters revised*
$R34b: HO_2\cdot + HO_2\cdot \rightarrow OH\cdot + OH\cdot + O_2$	*New reaction added to mechanism*

Table 4.1: *Reactions presented and progress made in this work*

Sensitivity analyses have been performed working with OpenSMOKE++ for a flame velocity and a Shock tube at conditions that are exemplary of the macroscopic database, and the effects of the reactions studied in this work has been reported, normalized to the effect of the most impacting, these are the results obtained:

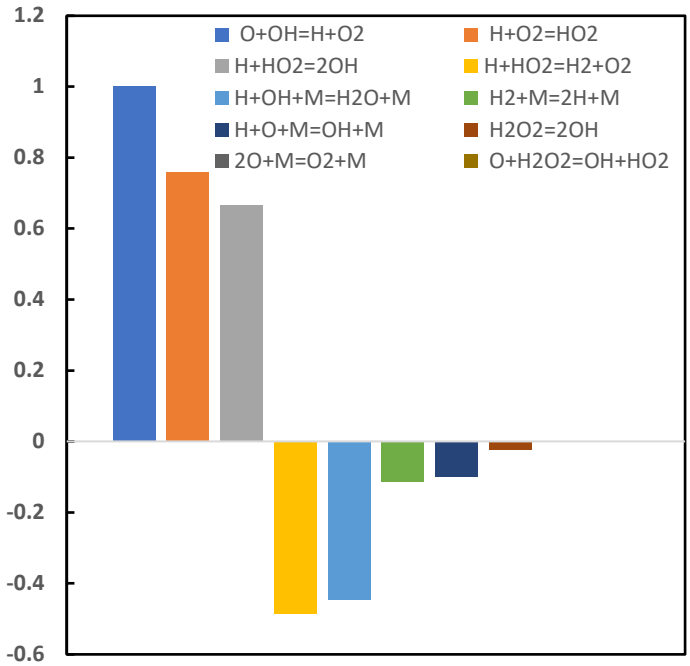

Figure 4.1: *Sensitivity analysis in an H2-Air flame in stoichiometric conditions, at room temperature and atmospheric pressure*

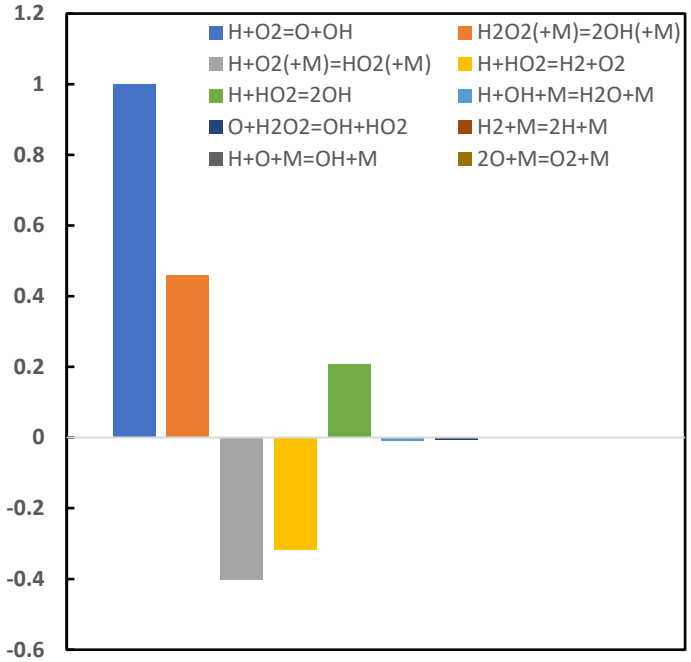

Figure 4.2: *Sensitivity analysis for a Shock Tube at T=1300K and P=110 atm*

It looks clear that $R17b: H\cdot + O_2 \rightarrow O(^3P) + OH\cdot$ is in both cases the most important reaction, and also its competitive reaction, $R17a: H\cdot + O_2 + M \rightarrow HO_2\cdot + M$, plays an important role in both cases.

Concerning PES R18, reactions $R18c: H\cdot + HO_2\cdot \rightarrow H_2 + O_2$ and $R18d: H\cdot + HO_2\cdot \rightarrow OH\cdot + OH\cdot$ play an important and competitive role in both cases, while $R18a: OH\cdot + OH\cdot + M \rightarrow H_2O_2 + M$ is relevant only in shock tube case.

These are the fundamental reactions for Shock Tube case, while for flames also $R10a: H\cdot + OH\cdot + M \rightarrow H_2O + M$ has an important contribution, other reactions play a minor but non-negligible role.

4.2 R2 PES

For what said, the first PES has 2 valence electrons, thus it contains the reaction of hydrogen dissociation:

R2: $H_2 + M \rightarrow H\cdot + H\cdot + M$

Which is one of the already discussed initiation reactions.

This reaction has a third body behavior, i.e. a collision is needed to break up molecular hydrogen into two radicals.

4.2.1 R2: Collected works

Theoretical papers: 34STE [12] is a study on recombination of hydrogen atoms with wall effects, and difference in efficiency when the third body is a hydrogen molecule or atomic hydrogen; 52_COO_AND [13] that studies this reaction in the presence of hydrogen bromine, and 10_GE_GOR [14], a study on many reactions using Canonical Variational Transition State Theory (CVTST).

Experimental papers:

Author	Reactor/Technique	T range [K]	P range [atm]	Bath gas
58_BUL_SUG [15]	Burner	2085 - 2270	1	H2O
58_PAD_SUG [16]	Burner	1400 – 2500	1	H2O
61_AVR_KOL [17]	Flow tube	298	1	H2

62_DIX_SUT [18]	Burner	1070	1	H2,H2O,N2
62_MAR [19]	Electron beam	300	0.0079	H2
62_PAT [20]	Shock tube	2950 – 5330	0.058	AR,H2,H
62_RIN [21]	Shock tube	2800 - 5000	0.047	AR,XE,KR,H2,H
63_KRE_PET [22]	Flow tube	300 - 350	0.0017	H2
64_LAR_THR [23]	Flow tube	293	0.0046	H2,AR
64_ROS_SUG [24]	Burner	1300 - 1600	1	H2,N2
64_SCH_BIR [25]	Shock tube	1700	0.164	AR
65_JAC_GIE [26]	Shock tube	3800 - 5300	1.63	AR
65_LAR_THR [27]	Flow tube	200 - 350	0.0052	H2,AR
67_JAC_GIE [28]	Shock tube	2900 - 4700	1.2	AR,H2
68_AZA_ROM [29]	Electron beam	296	0.0056	HE
68_BEN_BLA [30]	Flow tube	298	0.064 – 0.197	H2
68_MYE_WAT [31]	Shock tube	2290 - 3790	0.2 - 1	AR
69_EBE_HOY [32]	Electron beam	303	0.0055 – 0.0275	H2O
69_GET_BLA [33]	Shock tube	1260 – 1910	2.37	N2

69_HAL_JEN [34]	Burner	1800 - 2000	1	N2,HE,AR,CO2
69_HUR_JON [35]	Shock tube	2500 – 7000	1	H2
70_BEN_BLA [36]	Flow tube	298	0.0048	H2
70_DIX [37]	Burner	1050	1	N2
70_HAL_JEN [38]	Burner	1800 - 2000	1	AR,HE,N2,CO2
70_HAM_TRA [39]	Flow tube	77 - 300	0.0092	H2
71_BEN_BLA [40]	Flow tube	298	0.196	H2,HE,AR,N2,CO2,N2O,CH4
71_GAY_PRA [41]	Shock tube	1220 – 2580	2.645	AR
73_AZA_BOR [42]	Electron beam	298	0.0043	AR
73_BRE_BIR [43]	Shock tube	3500 – 8000	0.066 - 0.6	AR,XE
73_TEN_WIN [44]	Flow tube	298	0.002 – 0.006	NH3
73_TRA_HAM [45]	Flow tube	77 - 298	0.0079 – 0.012	H2,HE,AR,D2
74_MAL_OWE [46]	Shock tube	1300 - 1700	0.0267	AR
75_WAL_KAU [47]	Burner	77 – 298	0.0079	H2,HE,N2,AR,CH4,CO2,SF6
76_LYN_SCH [48]	Photolysis	298	0.8 - 2	H2,HE,NE,AR,KR,N2

77_MIT_LER [49]	Flow tube	296.5	0.016	HE
92_DU_HES [50]	Shock tube	3400 - 5300	0.9 – 1.48	KR

Table 4.2: Experimental data collection for R2

4.3 R9 PES

This is the PES with 9 valence electrons involved, therefore with one H atom and one O atom, giving the following reaction:

$$R9: H\cdot + O: + M \rightarrow OH\cdot + M$$

Which is considered the main source of hydroxyl radical.

This radical has two configuration states, a ground state with an excited state:

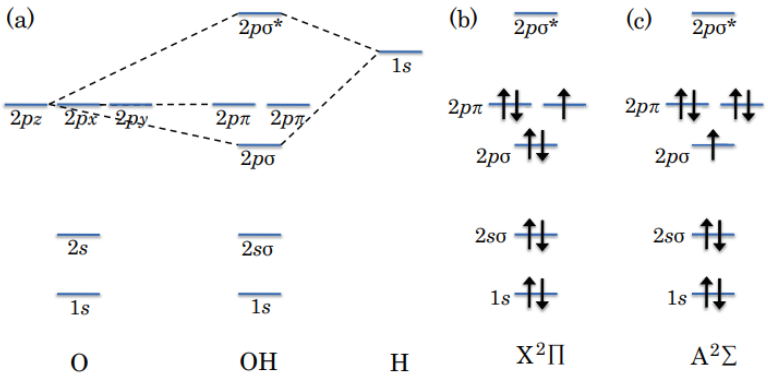

Figure 4.3: *Electronic configuration of the ground state (b) and the excited state in hydroxyl radical [51]*

The transition from excited state to ground state may occur with the collision with a third boy, or by chemiluminescence:

$$OH * + M \rightarrow OH + M$$

$$OH * \rightarrow OH + h\nu$$

The analysis of OH chemiluminescence is useful to make measurements on laminar flames and shock tubes.

Both data for OH and OH* evaluation are reported in literature.

4.3.1 R9: Collected works

No theoretical works dealing with this reaction have been found.

Experimental papers:

Author	Reactor/Technique	T range [K]	P range [atm]	Bath gas
82_HID_TAK [52]	Shock tube	1200 – 3200	0.0987	AR
82_KOI_MOR [53]	Shock tube	1250 – 3450	0.0237	AR
01_NAU_JAV [54]	Shock tube	2950 – 3700	2.2 – 3.1	AR
03_JAV_NAU [55]	Shock tube	2950 – 3700	2.2 – 3.1	AR
05_HAL_PET [56]	Shock tube	1200 – 2500	1	AR
10_KAT_FIK [57]	Shock tube	1400 – 3300	1	AR

Table 4.3: *Experimental data collection for R9*

4.4 R10 PES

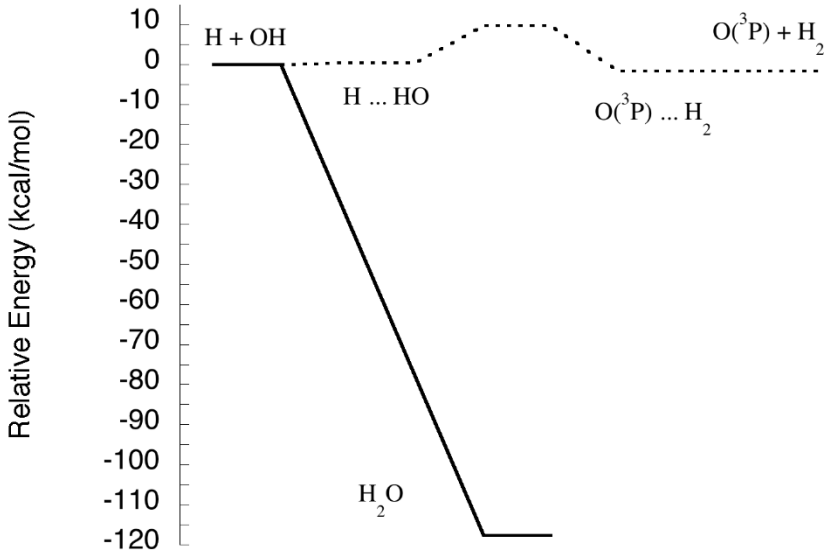

Figure 4.4: *Energy level representation for R10 PES*

Looking at Figure 4.4, two reaction paths are possible:

$$R10a: \quad H\cdot + OH\cdot + M \rightarrow H_2O + M$$

A termination reaction, which appears to be an important reaction in describing laminar flames at elevated pressures [58].

For that reaction, the product is way lower in energy (-120 kcal/mol) than the reactants, part of that energy is dissipated by the collision with a third body.

The other reaction path consists in:

$$R10b: \quad H\cdot + OH\cdot \rightarrow O(^3P) + H_2$$

That is an abstraction; final products are few kcal/mol lower in energy than the reactants, and a transition state (~10 kcal/mol with respect to the reactants) is present. Balakrishnan (in a study on the reverse reaction) reports an energy barrier for this reaction of 0.56 eV [59].

This reaction has already been studied in previous works done by Politecnico, and its new parameters are already fitted, so this work presents only R10a.

4.4.1 R10a: Collected works

Theoretical papers: two theoretical works are reported for R10a: 79TRO, which used simplified adiabatic channel calculations [60] and 08SEL-GEO, that adopts high-level quantum chemistry methods [58].

Experimental papers: all the collected papers with a brief description are resumed in the following table:

Author	Reactor	T range [K]	P range [atm]	Bath gas
39_OLD_RIE [61]	Flow tube	573.15	1	H2O,HE
58_BUL_SUG [15]	Burner	2085 - 2270	1	H2O
58_PAD_SUG [16]	Burner	2085 - 2460	0.267 - 0.335	H2O
61_BLA_POR [62]	Flow tube	298	0.06	HE,AR,XE,N2,H2O
62_DIX_SUT [63]	Burner	1072	1	N2,H2O
64_ROS_SUG [64]	Burner	1400	1	N2,H2O
64_SCH_BIR [65]	Shock tube	1550 - 1850	1 – 3	AR
67_GET [66]	Shock tube	1550 - 1800	2.95 – 5	AR
69_GET_BLA [33]	Shock tube	1585	2.4	H2,H2O,N2,AR
69_HAL_JEN [34]	Burner	1900	1	AR,HE,N2
70_HAL_JEN [38]	Burner	1900	1	AR,HE,N2,H2O

70_HOM_HUR [67]	Shock tube	2570 - 3274	2.151 - 7.302	AR
71_GAY_PRA [41]	Shock tube	1795 - 2265	2.645	AR
72_FRI_SUT [68]	Burner	2130	1	N2
74_DAV_MCG [69]	Burner	1740 - 1860	0.5	AR,HE,N2
77_ZEL_ERL [70]	Flow tube	300	0.008 - 0.015	HE,AR,N2,CO2
88_GOO_HAY [71]	Burner	1600 - 2200	0.7 - 0.9	N2
03_JAV_NAU [55]	Shock tube	2628 - 3350	2.467	AR,H2O
06_SRI_MIC [72]	Shock tube	2196 - 2792	0.411 - 0.988	KR

Table 4.4: *Experimental data collection for R10a*

4.4.2 R10a: Theoretical calculations and optimization

Theoretical calculations were provided for H2, AR and KR as third bodies, since no data were found for H2, optimization just occurs for AR and KR.

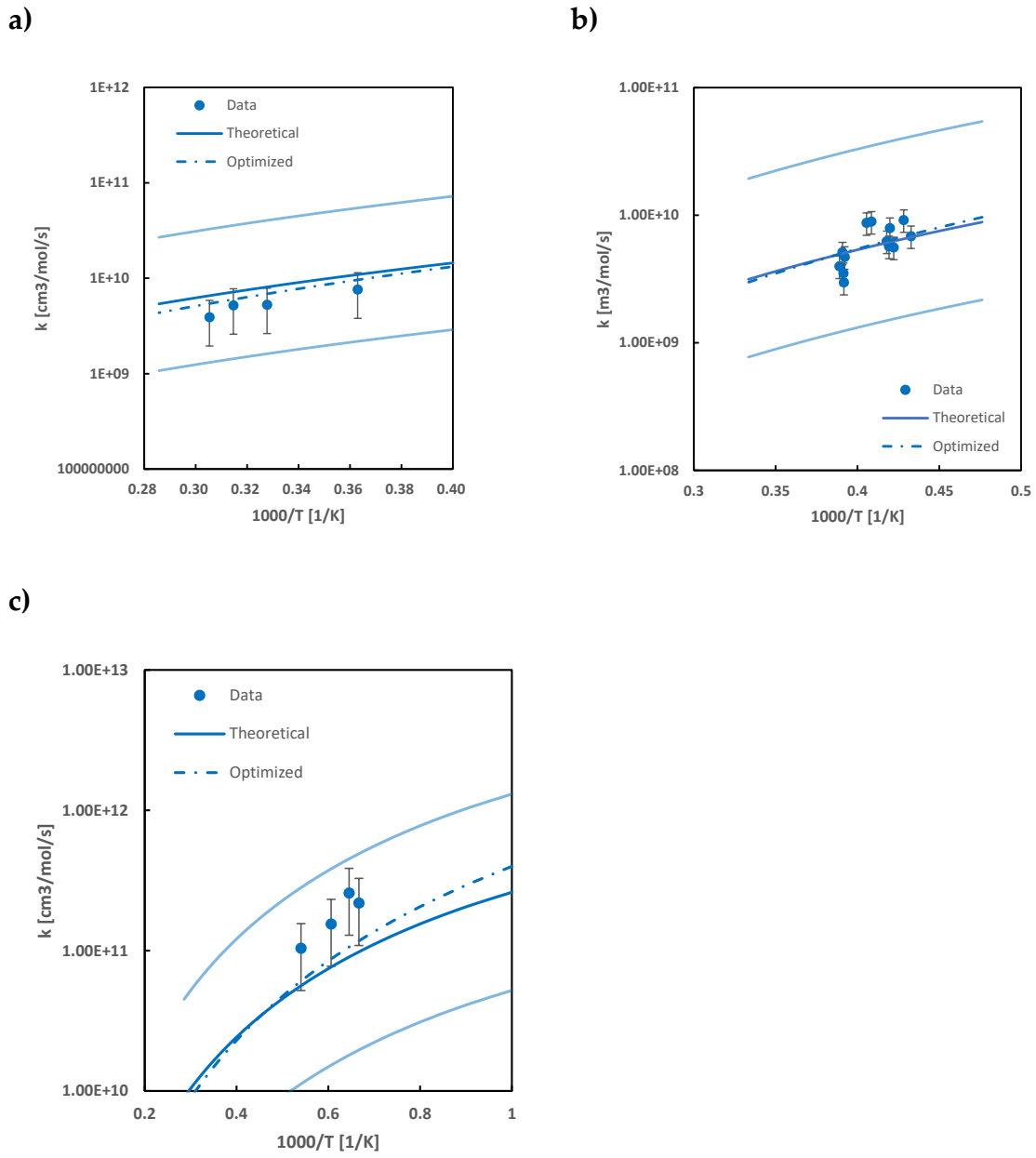

Figure 4.5: *Theoretical predictions and optimization with experimental data for R10a, fig. a) and b) refers to AR, respectively at 2.25 and 4 atm fig.c) refers to KR, at p fixed at 0.9 atm;*

straight line represents theoretical calculations, dashed line is the optimized curve, light blue lines are the limits in which the optimizer works

As can be seen from Figure 4.5, optimization makes a noticeable effect for AR, while for KR the optimized line is basically overlapped with the theoretical previsions.

After the optimization step, these appear to be the new coefficients for the final model:

Reaction	A	n	Ea
H+OH=H2O	3.5000e+22	-2.000	0.00(dummy values)
PLOGMX / 0.493000	1.00268e+21	-3.24701	1785.38
PLOGMX / 0.987000	2.80364e+21	-3.28479	2026.15
PLOGMX / 1.97000	8.28595e+21	-3.32925	2306.03
PLOGMX / 3.95000	2.27148e+22	-3.36544	2564.40
PLOGMX / 987.000	2.27333e+13	0.252521	-129.067
PLOGSP / H2 0.493000	1.00268e+21	-3.24701	1785.38
PLOGSP / H2 0.987000	2.80364e+21	-3.28479	2026.15
PLOGSP / H2 1.9700	8.28595e+21	-3.32925	2306.03
PLOGSP / H2 3.95000	2.27148e+22	-3.36544	2564.40
PLOGSP / H2 987.000	2.27333e+13	0.252521	-129.067
PLOGSP / AR 0.493000	1.26692e+21	-3.40945	536.167
PLOGSP / AR 0.987000	3.05716e+21	-3.43025	689.280
PLOGSP / AR 1.97000	8.54628e+21	-3.46799	929.880
PLOGSP / AR 3.95000	2.53358e+22	-3.51279	1211.29
PLOGSP / AR 987.000	8.66434e+13	0.0465141	-1089.87
PLOGSP / KR 0.493000	1.32907e+21	-3.40035	478.122
PLOGSP / KR 0.987000	3.23676e+21	-3.42220	636.738
PLOGSP / KR 1.9700	9.11360e+21	-3.46077	881.704
PLOGSP / KR 3.95000	2.70356e+22 -	3.50565	1164.22
PLOGSP / KR 987.000	9.55897e+13	0.0465141	-1089.87

Table 4.5: Optimized PLOG for R10a

4.4.3 R10a: Impact on the model

Let's see now the impact of that changed reaction in the original POLIMI model:

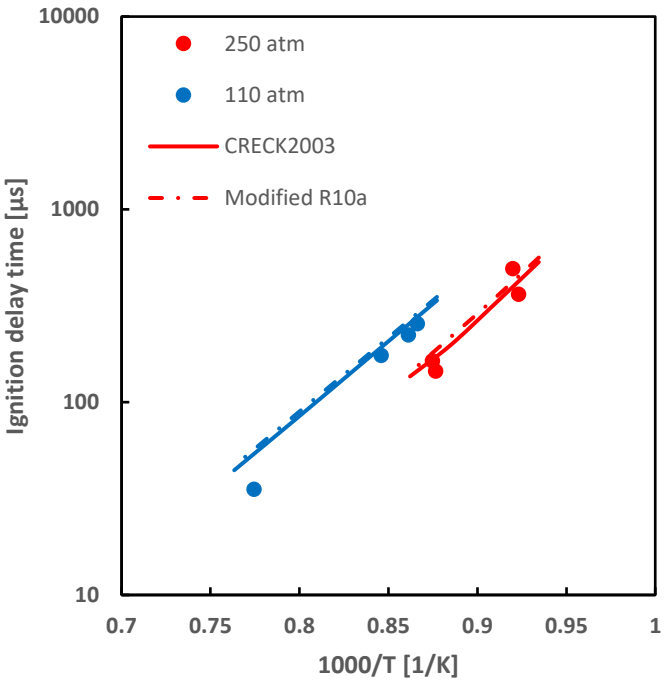

Figure 4.6: *Effect of the R10a reaction modify on a shock tube, data are from a work by Shao et al. [73]*

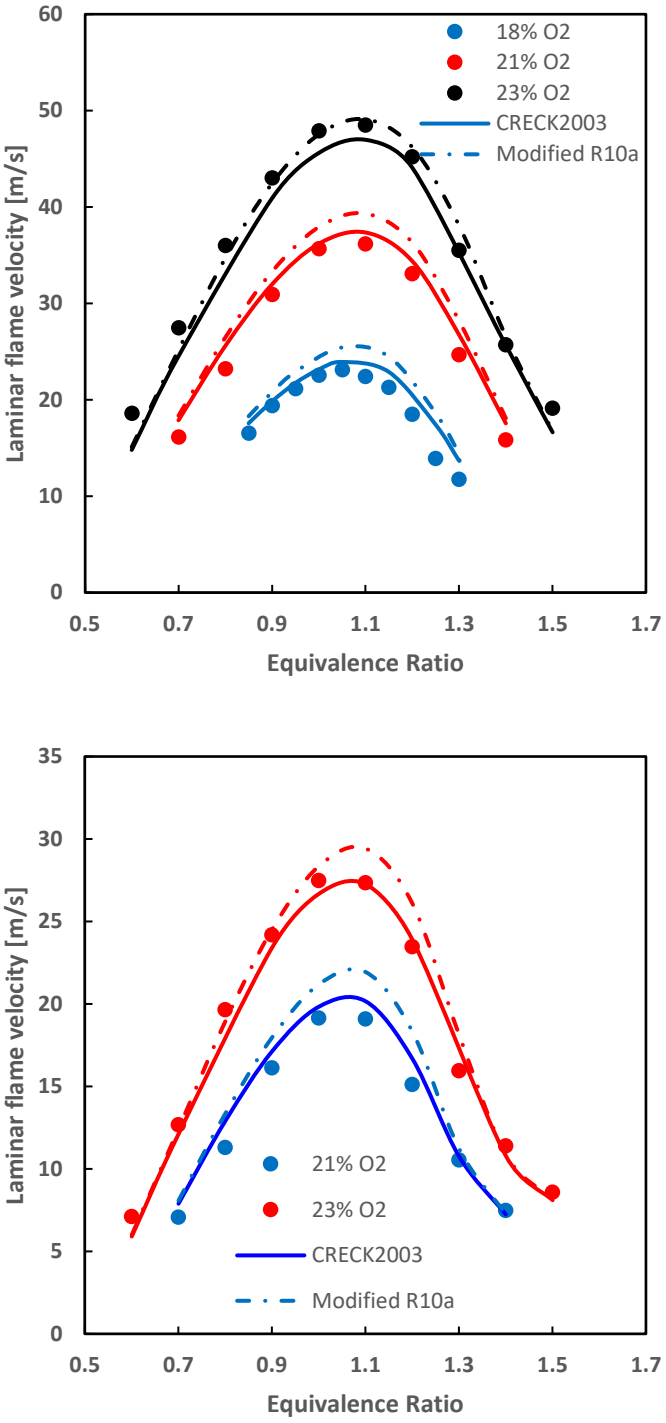

Figure 4.7: *Effect of the R10a reaction modify on a flame velocity, data are taken from a work by Wang-Costa et al. [74], respectively at 0.1 and 0.5 MPa*

A modest effect of this modify can be seen in the shock tubes experiments, while the impact on the flames is more evident, especially in stoichiometric or quasi-stoichiometric conditions (equivalence ratio=1), where higher flame velocities are predicted with respect to the original model.

4.5 R16 PES

This is the PES that involves 16 valence electrons, i.e. two oxygen atoms.

The reaction of interest is the following:

$$R16: O_2 + M \rightarrow O: + O: + M$$

Molecular oxygen dissociation, that is a third body reaction, in analogy with hydrogen dissociation, this is an initiation reaction, that produces two oxygen radicals from an initial oxygen molecule.

4.5.1 R16: Collected works

Theoretical papers: No theoretical works have been reported for this reaction.

Experimental papers:

Author	Reactor/Technique	T range [K]	P range [atm]	Bath gas
59_MATT [75]	Shock tube	2450 - 5000	0.024	O2
60_KRE_PET [76]	Electron beam	350	0.00263	O2
60_MOR_ELI [77]	Electron beam	300	0.003 - 0.0063	N2
60_REE_MAN [78]	Electron beam	300	0.0004 – 0.00178	AR
61_RIN_KNI [79]	Shock tube	3500	0.0263	O2,O,AR,XE
62_MAR [19]	Electron beam	300	0.0043 – 0.008	O2,N2,AR
62_RIN [21]	Shock tube	300	0.04	AR,KR,XE
63_WRA [80]	Shock tube	1340 - 2950	0.262 - 1.05	AR

65_WRA [81]	Shock tube	5000 – 18000	0.00065 – 0.0131	AR
65_KIE_LUT [82]	Shock tube	1480 - 2820	0.757 – 1.603	AR,KR,O2
66_KON_NIK [83]	Shock tube	300 - 3500	Not found	AR
67_CAM_THR [84]	Electron beam	196 - 327	0.0038 – 0.0107	N2
68_CAM_THR [85]	Electron beam	196	0.0042 – 0.0057	H2
73_CAM_GRA [86]	Flow tube	196 - 298	0.0113	N2
03_NAV_JAU [55]	Shock tube	2740 - 3460	1.15 – 4.45	AR,N2

Table 4.6: *Experimental data collection for R16*

4.6 R17 PES

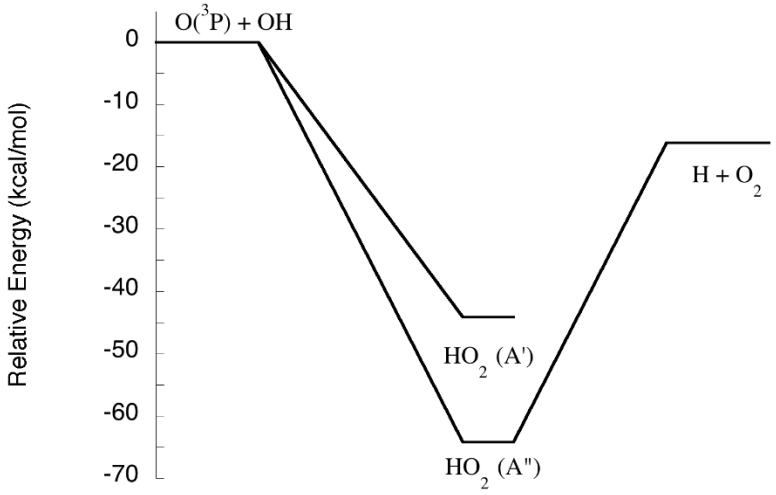

Figure 4.8: *Energy level representation for R17 PES*

First of all, it can be noticed that this reaction path passes through an HO2 well that can be stabilized by a third body, to give a stable HO2 intermediate:

$$R17a: H\cdot + O_2 + M \rightarrow HO_2\cdot + M$$

The HO2 radical also plays an important role in reaction path, i.e. it can lead to termination reactions such as:

$$2HO_2\cdot \rightarrow H_2O_2 + O_2$$

(this reaction will be investigated later on)

The other reaction path is the following:

$$R17b: H\cdot + O_2 \rightarrow O(^3P) + OH\cdot$$

That is one of the most important branching reactions that occur in combustion, because 3 radicals are generated starting from a single radical, and is also the main responsible of oxygen consumption; therefore this reaction has been deeply investigated and huge database is available for both the direct and the reverse reaction.

Data collection and optimization for this reaction has already been performed in previous Polimi project, what changed in this work is just the optimization method, i.e. OptiSmoke++ toolbox has been tested on this reaction, to validate the optimization routine for pressure independent reaction:

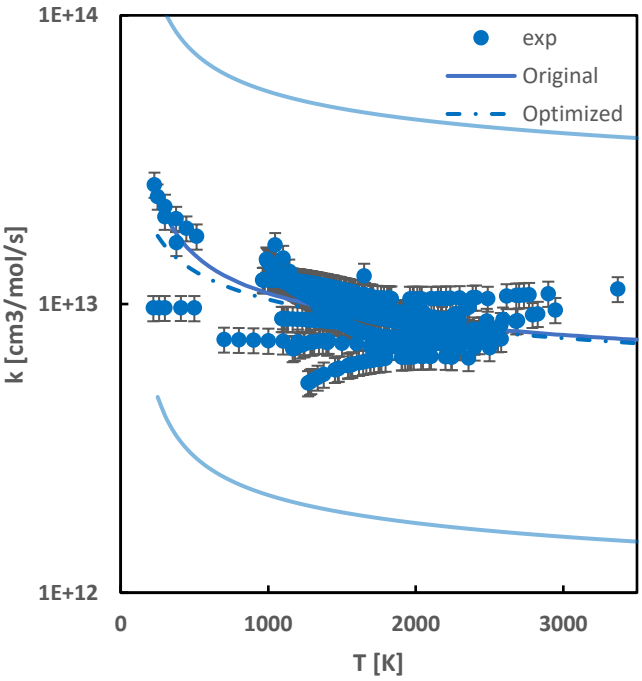

Figure 4.9: *Comparison between kinetic constant obtained in previous works vs optimization using OptiSmoke++ for R17b reaction, straight line represents the original rate constant, dashed line is the curve optimized with OptiSmoke++, light blue lines are the limits in which the optimizer works*

As can be seen, a slight difference is evident just in low temperature cases.

Actually, Figure 4.9 represents the kinetic constant of the reverse reaction (O+OH -> H+O2), i.e. the reaction is studied in its exothermic direction, this allows to smooth the effect of temperature dependence, and to obtain a better fit.

Since R17b in particular is a very important reaction, a large dataset is reported for both this reaction and R17a, i.e. the competitor reaction.

The revised coefficient for this reaction is:

Reaction	A	n	Ea
O+OH=H+O2	3.6670e+13	-0.200	-335.00

Table 4.7: *Optimized Arrhenius parameters for R17b*

4.6.1 R17a: Collected works

Theoretical papers:

Author	Method
85_COB_HIP [87]	Statistical adiabatic channel model
85_COB_TRO [88]	Statistical adiabatic channel model
88_COB [89]	Statistical adiabatic channel model
95_BAR_DAT [90]	Study on rovibrational states of HO2
95_DOB_STU [91]	Quantum mechanical calculations
95_KEN_PAC [92]	Quantum chemistry calculations
96_DUC_PET [93]	Conventional TST/ RRKM theory calculations
96_KEN_PAC [94]	Quantum chemistry calculations
96_KEN_PACb [95]	Quantum chemistry calculations
96_MAN_TAY [96]	Quantum chemical theory of recombination
97_GER_MIL [97]	Quantum chemistry calc. (flux correlation approach)
97_KEN_PAC [98]	Quantum chemistry calculations
98_SON_HAS [99]	RRKM theory calculations
99_HIM_ROD [100]	RRKM theory calculations

00_HAR_MAE [101]	Adiabatic channel + classical trajectory calculations
00_HAR_TRO [102]	Ab initio PES calculations + classical trajectory calc.
00_TRO [103]	Ab initio PES calculations + classical trajectory calc.
01_MAR_VAR [104]	DMBE IV + Ab initio PES
01_MAR_VARb [105]	DMBE IV + Ab initio PES
04_TEI_CAR [106]	DMBE IV PES + classical trajectory calculations
06_LIN_RAC [107]	Quantum mechanical calc. on DMBE IV model
06_TRO_USH [108]	Quantum chemistry calculations
08_SEL_GEO [58]	High-level quantum chemistry methods
08_TRO_USH [109]	Quantum capture calculations
13_PER_DAW [110]	Classical trajectory calculations
14_HAR_KLI [111]	Comparison between uncontracted and internally contracted MRCI PES

Table 4.8: *Theory works collection for R17a*

Experimental works:

Author	Reactor/Technique	T range [K]	P range [atm]	Bath gas
65_GET_SCH [112]	Shock tube	1164 - 1849	3.2	AR
67_GUT_HAR [113]	Shock tube	1000 - 1300	Not found	AR
69_GET_BLA [33]	Shock tube	1300 – 1600	1.1 – 3.7	N2,H2O,AR
70_BIS_DOR [114]	Pulse radiolysis	298	1.065	H2

70_BLA_GET [115]	Shock tube	1430 - 1650	2.15	AR
71_GAY_PRA [41]	Shock tube	1800 - 2250	2.64	AR
71_HIC_EYR [116]	Pulse radiolysis	298	1	AR
72_KUR [117]	Shock tube	200 - 434	0.05 – 0.5	N2,HE,CH4,AR
72_AHU_MIC [118]	Mercury resonance	298	0.543	H2,AR,NE,KR,HE
72_WES_DEH [119]	Esr spectroscopy	298	0.0026	AR
73_PEE_MAH [120]	Burner	1900	0.0526	O2
74_WON_DAV [121]	Flow tube	220 - 360	0.026 – 0.39	AR
74_HAC_HOY [122]	Electron beam	298 – 669	Not found	HE
77_SLA [123]	Shock tube	1070	2	N2
78_CAM_ROG [124]	Discharge tube	425	0.0035	N2
79_ISH_SUG [125]	Pulse radiolysis	298	0.98	H2
82_NIE_SIL [126]	Pulse radiolysis	298	0.98	H2
82_PAM_SKI [127]	Shock tube	1000 - 2500	2.47	AR
83_PRA_WOO [128]	Discharge tube	231 - 512	0.0079	AR
84_HOR [129]	Photooxidation of formaldehyde	373	0.543	CO2, CH2O

85_BOR_COB [130]	Flash photolysis	298	0.987	N2
85_COB_HIP [131]	Flash photolysis	298	0.986 – 197.38	AR,N2,CH4
85_HOR [132]	Flash photolysis	373	0.7895	MeOH
87_HSU_DUR [133]	Discharge tube	298	0.022	HE,N2
89_HSU_AND [134]	Discharge tube	298 - 639	0.0066 -0.092	HE,N2,H2O
89_PIR_MIC [135]	Shock tube	746 - 987	0.3	AR
91_HAN_PIL [136]	Flash photolysis	800 - 850	0.132 – 0.32	N2
93_CAR_KES [137]	Flow tube	298 - 580	0.066 – 0.658	N2,H2O,AR
95_BRO_BAR [138]	Flow tube	680 – 825	1	N2
96_DAV_PET [139]	Shock tube	1260 - 1375	48 - 120	AR,N2
96_DUC_PET [140]	Shock tube	298 – 500	0.0065 - 180	AR,N2
98_ASH_HAY [141]	Laminar flow react.	750 – 900	Not found	N2,CO2,AR,H2O
98_MUE_YET [142]	Flow tube	800 – 900	10 – 14	N2,AR
01_BAT_GOL [143]	Shock tube	1050 - 1350	7 – 150	AR,N2,H2O
02_MIC_SU [144]	Shock tube	300 – 700	0.033 – 0.3	HE,NE,AR,KR,O2,N2

04_HAH_KRA [145]	Flash photolysis	300 – 700	0.98 - 890	AR
05_HWA_RYU [146]	Shock tube	950 - 1200	Not found	AR
08_FER_LUT [147]	Flash photolysis	300 – 900	1.4 - 940	HE,AR,N2
09_MER_CAL [148]	Shock tube	900 – 1265	1 - 18	AR,N2,H2O
09_PAN_DAV [149]	Shock tube	870 - 1180	3.5	AR
11_VAS_DAV [150]	Shock tube	1170 - 1270	17 - 33	CO2
18_SHA_CHO [151]	Shock tube	1150 – 1270	17 - 33	AR,H2O,CO2,N2
19_CHO_GIR [152]	HP Shock tube	1450 - 2100	9 - 22	AR,N2,CO2

Table 4.9: *Experimental data collection for R17a*

4.6.2 R17a: Model optimization

The optimization in this case is done on the model used in the original mechanism, the original TROE formalism has been converted into a PLOG.

For the sake of simplicity, Figure 4.10 reports a series of plots for the optimization routine of this reaction, the bath gas and the operative condition (i.e. the "frozen" variable) for which the presented data are valid are reported in a header for every plot.

a)Bath CH4, 298 K

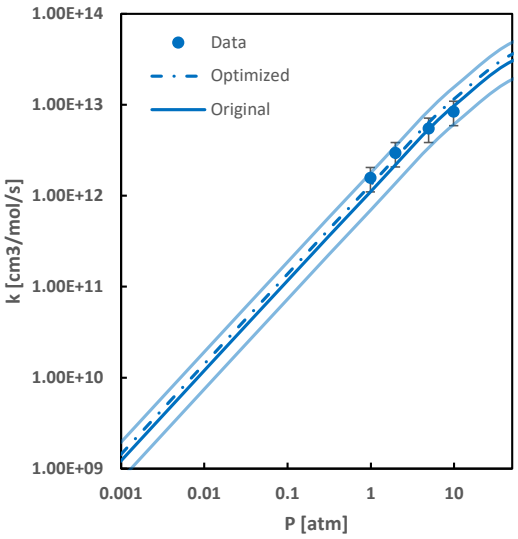

b) Bath H2O, 650 K

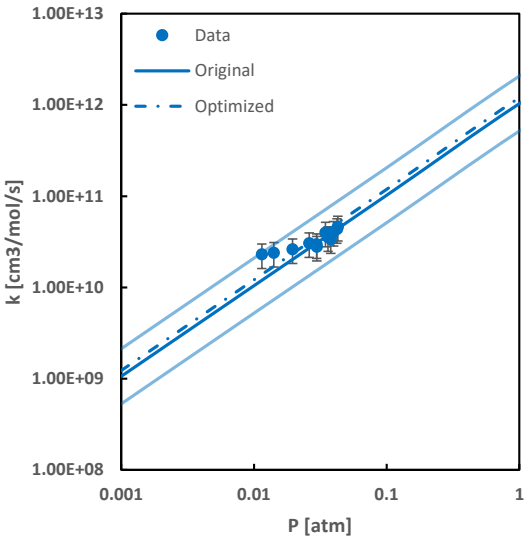

c) Bath CO2, 25atm:

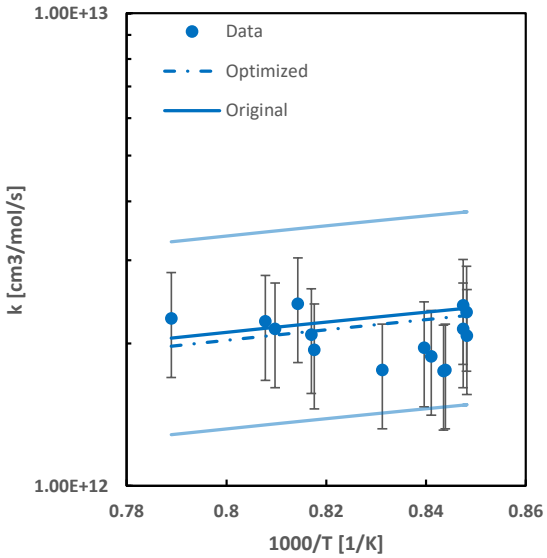

d)Bath HE, 300 K

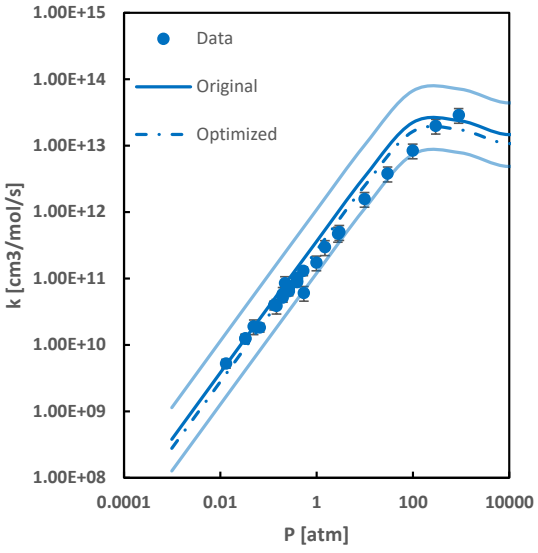

e) Bath HE, 500K

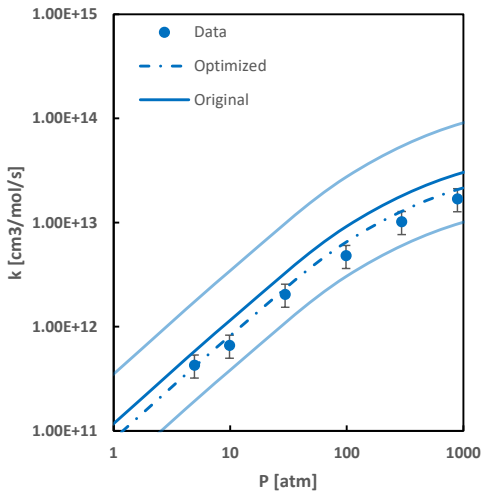

f) Bath H2, 298 K

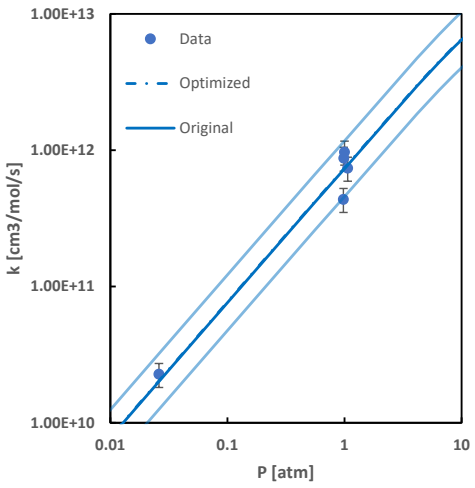

g) Bath N2, 298 K

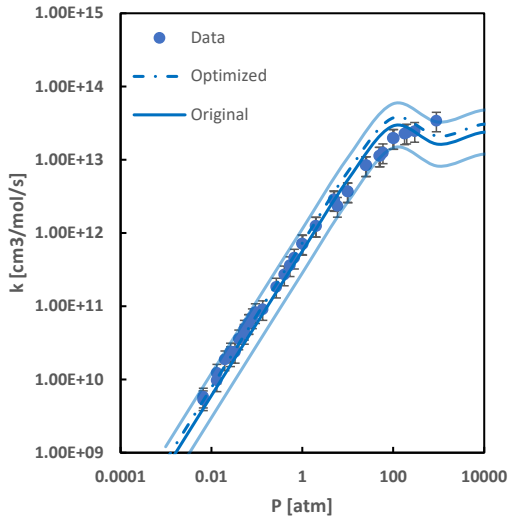

h) Bath N2, 500 K

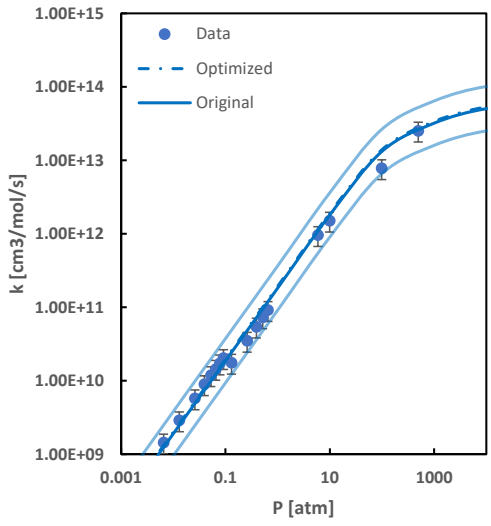

i)Bath AR, 300 K

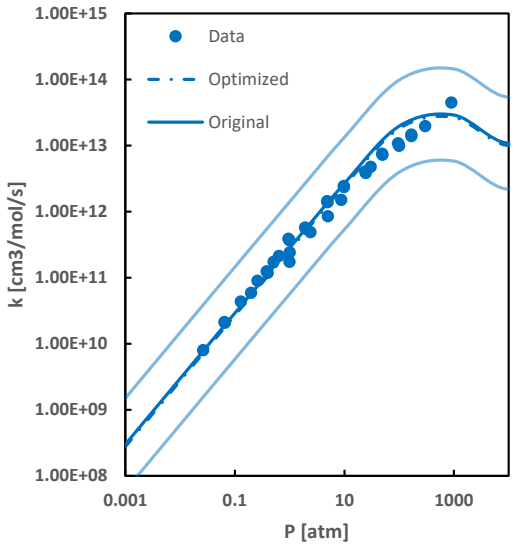

j)Bath AR, 700 K

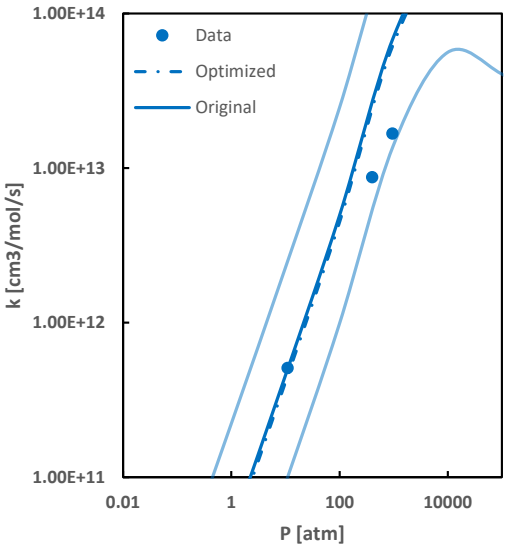

Figure 4.10: *R17a optimization routine for different bath gases, straight line represents theoretical calculations, dashed line is the optimized curve, light blue lines are the limits in which the optimizer works*

As it can be seen from those figures, there's already a good agreement between experimental data and the original model, therefore the optimization effect is minimal in most of the cases.

After the optimization, this is the PLOG expression for this reaction:

Reaction	A	n	Ea
H+O2=HO2	4.6500e+12	0.440	0.00 (dummy variables)
PLOGMX / 0.000986920	2.89802E+14	-2.31829	-220.503
PLOGMX / 0.00986920	2.87277E+15	-2.31829	-217.29
PLOGMX / 0.0986920	2.84230E+16	-2.31829	-210.355
PLOGMX / 0.986920	2.82785E+17	-2.31829	-191.214
PLOGMX / 9.86920	3.03780E+18	-2.31829	-111.496
PLOGMX / 98.6920	6.40939E+19	-2.40829	378.577
PLOGMX / 986.920	1.90953E+22	-2.78829	2810.59
PLOGMX / 9869.20	2.72529E+18	-1.43829	1897.03
PLOGMX / 98692.0	4.08561E+16	-0.78829	1657.81
PLOGMX / 986920.	5.08483E+13	0.088711	234.099
PLOGMX / 9.86920e+06	1.01529E+13	0.297711	-1.38E+02
PLOGMX / 2.46730e+07	8.54659E+12	0.320711	-1.76E+02
PLOGSP / AR 0.000986920	2.29599E+13	-2.02399	-123.296
PLOGSP / AR 0.00986920	2.27754E+14	-2.02399	-120.672
PLOGSP / AR 0.0986920	2.25428E+15	-2.02399	-115.274
PLOGSP / AR 0.986920	2.23425E+16	-2.02399	-101.674
PLOGSP / AR 9.86920	2.30020E+17	-2.02399	-52.2847
PLOGSP / AR 98.6920	3.39393E+18	-2.06399	225.058
PLOGSP / AR 986.920	4.65736E+20	-2.36399	1903.6
PLOGSP / AR 9869.20	7.70749E+19	-1.84399	3182.79
PLOGSP / AR 98692.0	1.87574E+16	-0.65999	1741.71
PLOGSP / AR 986920.	3.17653E+13	0.206007	652.232
PLOGSP / AR 9.86920e+06	2.02340E+12	0.562007	12.3824
PLOGSP / AR 2.46730e+07	1.52285E+12	0.599007	-51.7635
PLOGSP / N2 0.000986920	2.89802E+14	-2.31829	-220.503
PLOGSP / N2 0.00986920	2.87277E+15	-2.31829	-217.29
PLOGSP / N2 0.0986920	2.84230E+16	-2.31829	-210.355
PLOGSP / N2 0.986920	2.82785E+17	-2.31829	-191.214

PLOGSP / N2 9.86920	3.03780E+18	-2.31829	-111.496
PLOGSP / N2 98.6920	6.40939E+19	-2.40829	378.577
PLOGSP / N2 986.920	1.90953E+22	-2.78829	2810.59
PLOGSP / N2 9869.20	2.72529E+18	-1.43829	1897.03
PLOGSP / N2 98692.0	4.08561E+16	-0.78829	1657.81
PLOGSP / N2 986920.	5.08483E+13	0.088711	234.099
PLOGSP / N2 9.86920e+06	1.01529E+13	0.297711	-137.821
PLOGSP / N2 2.46730e+07	8.54659E+12	0.320711	-175.987
PLOGSP / CH4 0.000986920 3	3.06800E+12	-2.17475	-69.1998
PLOGSP / CH4 0.00986920	3.00220E+15	-2.17475	-65.2193
PLOGSP / CH4 0.0986920	2.97055E+16	-2.17475	-56.1143
PLOGSP / CH4 0.986920	2.98032E+17	-2.17475	-28.1155
PLOGSP / CH4 9.86920	3.47772E+18	-2.18475	105.619
PLOGSP / CH4 98.6920	1.35941E+20	-2.34475	964.897
PLOGSP / CH4 986.920	1.63195E+22	-2.61475	3721.76
PLOGSP / CH4 9869.20	7.56029E+16	-0.88975	1440.18
PLOGSP / CH4 98692.0	1.90829E+15	-0.32175	1352.38
PLOGSP / CH4 986920.	1.18901E+13	0.337246	196.898
PLOGSP / CH4 9.86920e+06	4.62736E+12	0.460246	-18.3223
PLOGSP / CH4 2.46730e+07	4.15571E+12	0.474246	-41.6736
PLOGSP / CO2 0.000986920 5	5.41180E+13	-2.20216	-171.931
PLOGSP / CO2 0.00986920	5.48583E+15	-2.20216	-167.018
PLOGSP / CO2 0.0986920	5.43281E+16	-2.20216	-155.025
PLOGSP / CO2 0.986920	5.53571E+17	-2.20216	-113.685
PLOGSP / CO2 9.86920	7.45179E+18	-2.23216	108.316
PLOGSP / CO2 98.6920	6.78378E+20	-2.49216	1502.14
PLOGSP / CO2 986.920	1.54265E+21	-2.27216	3483.77
PLOGSP / CO2 9869.20	5.84052E+16	-0.85116	1549.86
PLOGSP / CO2 98692.0	2.10689E+14	-0.06666	767.83
PLOGSP / CO2 986920.	7.37587E+12	0.366842	-8.52238
PLOGSP / CO2 9.86920e+06	4.11327E+12	0.442842	-139.708
PLOGSP / CO2 2.46730e+07	3.82986E+12	0.452842	-154.919

PLOGSP / H2 0.000986920 2	8.11360E+13	-2.1754	229.895
PLOGSP / H2 0.00986920	2.78613E+15	-2.1754	233.374
PLOGSP / H2 0.0986920	2.75645E+16	-2.1754	241.041
PLOGSP / H2 0.986920	2.74920E+17	-2.1754	263.04
PLOGSP / H2 9.86920	3.02844E+18	-2.1854	359.595
PLOGSP / H2 98.6920	7.78721E+19	-2.2954	967.185
PLOGSP / H2 986.920	2.24464E+22	-2.6654	3616.5
PLOGSP / H2 9869.20	4.46778E+17	-1.0954	1998.71
PLOGSP / H2 98692.0	1.31999E+16	-0.5314	1968.88
PLOGSP / H2 986920.	2.65547E+13	0.278598	600.891
PLOGSP / H2 9.86920e+06	7.13364E+12	0.448598	298.665
PLOGSP / H2 2.46730e+07	6.17956E+12	0.467598	267.084
PLOGSP / H2O 0.000986920	1.05049E+15	-2.14171	-264.118
PLOGSP / H2O 0.00986920	1.03934E+16	-2.14171	-257.182
PLOGSP / H2O 0.0986920	1.03406E+17	-2.14171	-238.041
PLOGSP / H2O 0.986920	1.11083E+18	-2.14171	-158.324
PLOGSP / H2O 9.86920	2.34372E+19	-2.23171	331.75
PLOGSP / H2O 98.6920	6.98257E+21	-2.61171	2763.76
PLOGSP / H2O 986.920	9.96558E+17	-1.26171	1850.2
PLOGSP / H2O 9869.20	1.49399E+16	-0.61171	1610.98
PLOGSP / H2O 98692.0	1.85937E+13	0.265289	187.272
PLOGSP / H2O 986920.	3.71261E+12	0.474289	-184.648
PLOGSP / H2O 9.86920e+06	2.76182E+12	0.513289	-249.345
PLOGSP / H2O 2.46730e+07	2.65253E+12	0.519289	-257.7
PLOGSP / HE 0.000986920	2.41991E+14	-2.37715	69.9913
PLOGSP / HE 0.00986920	2.39988E+15	-2.37715	72.8078
PLOGSP / HE 0.0986920	2.37496E+16	-2.37715	78.6969
PLOGSP / HE 0.986920	2.35624E+17	-2.37715	93.9939
PLOGSP / HE 9.86920	2.45505E+18	-2.37715	152.287
PLOGSP / HE 98.6920	4.01928E+19	-2.43715	491.75
PLOGSP / HE 986.920	7.84552E+21	-2.77715	2444.08
PLOGSP / HE 9869.20	9.67360E+19	-1.93715	2962.3

PLOGSP / HE 98692.0	1.31534E+17	-0.98015	2008.25
PLOGSP / HE 986920.	1.47183E+14	-0.07285	710.793
PLOGSP / HE 9.86920e+06	1.51399E+13	0.221852	183.528
PLOGSP / HE 2.46730e+07	1.19453E+13	0.252852	130.37
PLOGSP / O2 0.000986920	1.71216E+14	-2.14171	416.449
PLOGSP / O2 0.00986920	1.69724E+15	-2.14171	419.662
PLOGSP / O2 0.0986920	1.67924E+16	-2.14171	426.598
PLOGSP / O2 0.986920	1.67070E+17	-2.14171	445.738
PLOGSP / O2 9.86920	1.79474E+18	-2.14171	525.456
PLOGSP / O2 98.6920	3.78669E+19	-2.23171	1015.53
PLOGSP / O2 986.920	1.12815E+22	-2.61171	3447.54
PLOGSP / O2 9869.20	1.61011E+18	-1.26171	2533.98
PLOGSP / O2 98692.0	2.41379E+16	-0.61171	2294.76
PLOGSP / O2 986920.	3.00414E+13	0.265289	871.051
PLOGSP / O2 9.86920e+06	5.99836E+12	0.474289	499.131
PLOGSP / O2 2.46730e+07	5.04935E+12	0.497289	460.965
PLOGSP / CO 0.000986920	3.78121E+14	-2.23	5.36747
PLOGSP / CO 0.00986920	3.74587E+15	-2.23	9.28368
PLOGSP / CO 0.0986920	3.70626E+16	-2.23	18.1996
PLOGSP / CO 0.986920	3.71529E+17	-2.23	45.383
PLOGSP / CO 9.86920	4.30016E+18	-2.24	173.943
PLOGSP / CO 98.6920	1.58871E+20	-2.39	998.999
PLOGSP / CO 986.920	2.26416E+22	-2.68	3765.11
PLOGSP / CO 9869.20	1.09628E+17	-0.961	1524.22
PLOGSP / CO 98692.0	3.03180E+15	-0.402	1467.37
PLOGSP / CO 986920.	1.63451E+13	0.276	282.158
PLOGSP / CO 9.86920e+06	6.12595E+12	0.403	58.1058
PLOGSP / CO 2.46730e+07	5.48124E+12	0.418	33.9142
PLOGSP / C2H6 0.000986920	5.96032E+14	-2.23	5.94077
PLOGSP / C2H6 0.00986920	5.90203E+15	-2.23	10.4807
PLOGSP / C2H6 0.0986920	5.84232E+16	-2.23	21.2851
PLOGSP / C2H6 0.986920	5.91209E+17	-2.23	56.9447

PLOGSP / C2H6	9.86920	7.47503E+18	-2.25	240.675
PLOGSP / C2H6	98.6920	4.85178E+20	-2.47	1414.63
PLOGSP / C2H6	986.920	7.04877E+21	-2.48	3830.52
PLOGSP / C2H6	9869.20	7.49269E+16	-0.886	1601.35
PLOGSP / C2H6	98692.0	5.98474E+14	-0.19	1112.75
PLOGSP / C2H6	986920.	1.15196E+13	0.321	201.26
PLOGSP / C2H6	9.86920e+06	5.74752E+12	0.412	44.1537
PLOGSP / C2H6	2.46730e+07	5.29101E+12	0.423	26.3941

Table 4.10: *Optimized PLOG for R17a*

4.6.3: R17 Impact on the model

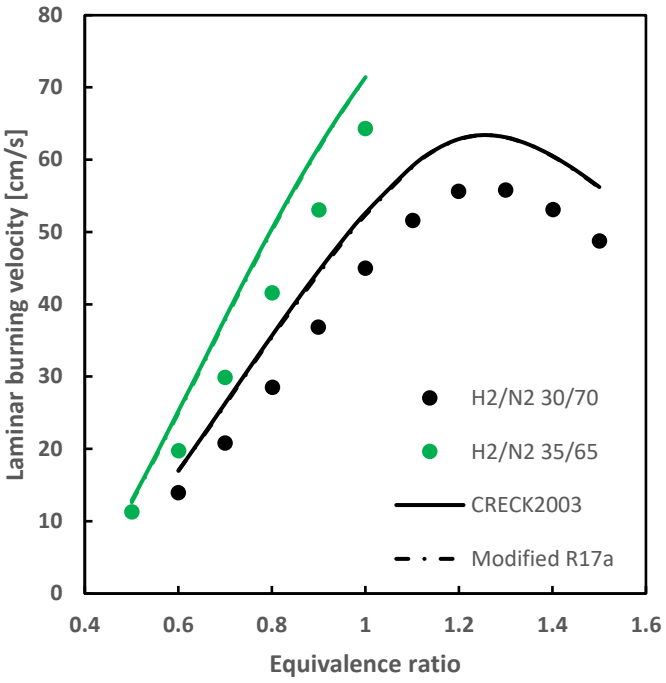

Figure 4.11: *Effect of the R17a reaction modify on flame velocities at atmospheric pressures, data are taken from a work by Voss et al. [153]*

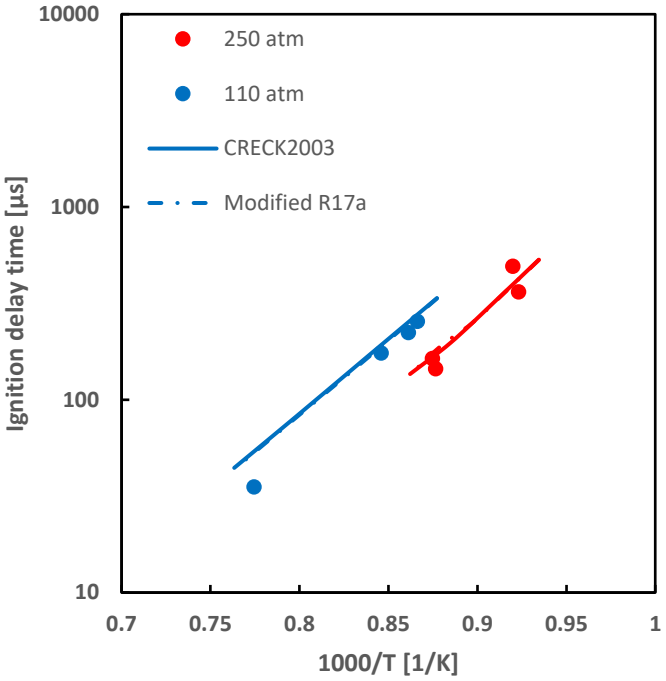

Figure 4.12: *Effect of the R17a reaction modify in a Shock tube experiment, data are taken from a work by Shao et al. [73]*

Very low effects can be seen, this was expectable since also the mechanism modifications after the optimization step are not so relevant.

Let's also see the effect of the full PES correction, i.e. reaction R17a and R17b put together:

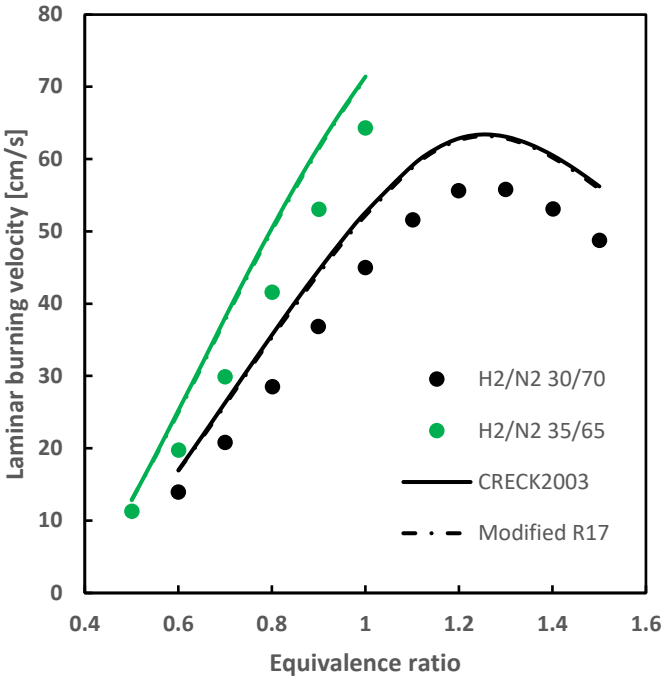

Figure 4.13: *Effect of the R17 full PES modify on flame velocities at atmospheric pressures, data are taken from a work by Voss et al.*

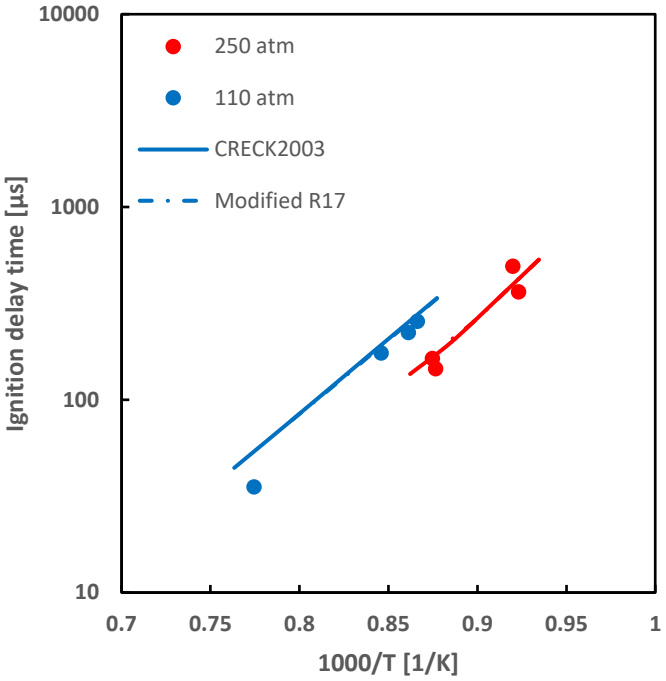

Figure 4.14: *Effect of the R17 full PES modify in a Shock Tube, data are taken from a work by Shao et al.*

Also in this case, there are no relevant changes between the models, once again this was expectable, since also for reaction R17b the optimization step made few changes on the mechanism.

4.7 R18 PES

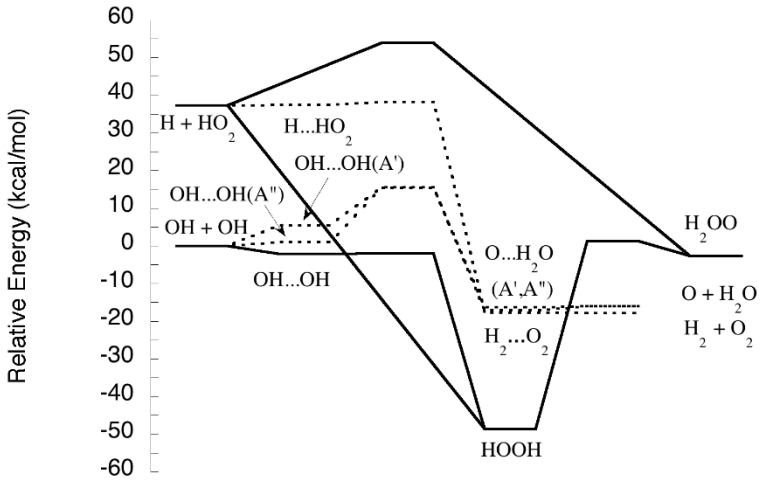

Figure 4.15: *Energy level representation for R18 PES*

In this PES, two hydrogen atoms and two oxygen atoms are involved.

As can be seen from this figure, many reaction paths are possible:

$$R18a: OH\cdot + OH\cdot + M \rightarrow H_2O_2 + M$$

A third body reaction that is a recombination of two hydroxyl radicals into a more stable product.

Other possible reactions (all written in the exothermic direction) are:

$$R18b: OH\cdot + OH\cdot \rightarrow O: + H_2O$$
$$R18c: H\cdot + HO_2\cdot \rightarrow H_2 + O_2$$
$$R18d: H\cdot + HO_2\cdot \rightarrow OH\cdot + OH\cdot$$

The second, in particular, is a chain terminating reaction, while the others are propagation reactions.

Furthermore, two other reactions belong to this PES:

$$R18e: H\cdot + H\cdot + O_2 \rightarrow H_2 + O_2$$
$$R18f: H\cdot + H\cdot + O_2 \rightarrow OH\cdot + OH\cdot$$

That are termolecular reactions, respectively a termination and a propagation reaction.

In this work, only R18a,R18c and R18d have been studied, the other reactions have already been investigated and optimized in previous works.

For this PES, in particular for R18c and even more in R18d reaction, a lack in experimental data has to be outlined, surely a deeper investigation should be needed to refine the model.

4.7.1 R18: Collected works

- **R18a:**

Theoretical papers:

Author	Method
08_TRO_USH [154]	Ab initio potential energy surface calculations
09_SEL_GEO [155]	Ab initio potential energy surface calculations
11_TRO [156]	Ab initio potential energy surface calculations
12_BUR_KLI [157]	Ab initio calculations integrated with experimental data analysis

Table 4.11: *Theory works collection for R18a*

Experimental papers:

Author	Reactor/Technique	T range [K]	P range [atm]	Bath gas
88_ZEL_EWI [158]	Flash photolysis	253 - 353	0.025 – 1.07	N2
02_KAP_LUT [159]	Shock tube	950 - 1250	0.986 – 14.8	AR
07_JAN_BAR [160]	Pulse radiolysis	423.15 – 623.15	247	N2O
09_HON_FAR [161]	Shock tube	1000 - 1200	0.9 – 3.2	AR,N2
10_HON_COO [162]	Shock tube	1000 - 1460	1 – 2.25	AR
12_SAN_CHE [163]	Flash photolysis	298 - 835	1 - 100	HE
13_SAJ_SEB [164]	Shock tube	930 - 1235	1 – 10.2	AR

Table 4.12: *Experimental data collection for R18a*

- **R18c:**

Theoretical papers:

Author	Method
72_WES_DEH [165]	Steady-state approximation
77_SHA [166]	Transition state theory
86_BOU_CAR [167]	Ab initio calculations
99_KAR_OSH [168]	Ab initio PES calculations
00_FIL_REC [169]	Complete active space self-consistent field (CASSCF) method
00_MIC_SUT [170]	Ab initio PES determination

07_MOU_SAH [171]	Ab initio calculations + Transition state theory + RRKM theory
09_MOU_YOU [172]	Quasi-classical trajectory simulations
11_STA_SHA [173]	Ab initio PES determination

Table 4.13: *Theory works collection for R18c*

Experimental papers:

Author	Reactor/Technique	T range [K]
74_BAL_FUL [174]	Burner	300 – 773.15
82_SRI_QUI [175]	Flow tube	296
86_KEY [176]	Flow tube	273
89_KOI [177]	Shock tube	1200
00_MIC_SUT [170]	Shock tube	1820 – 2100

Table 4.14: *Experimental data collection for R18c*

- **R18d:**

Theoretical papers:

Author	Method
07_MOU_SAH [178]	Ab initio calculations + Transition state theory + RRKM theory
09_MOU_YOU [179]	Quasi-classical trajectory simulations

Table 4.15: *Theory works collection for R18d*

Experimental papers:

Author	Reactor/Technique	T range [K]
82_SRI_QUI [175]	Flow tube	296
83_PRA_WOO [128]	Flow tube	370
86_KEY [176]	Flow tube	245 - 300

Table 4.16: *Experimental data collection for R18d*

4.7.2 R18: Model optimization

Optimization for this PES occurs starting on the coefficients used in the original model.

- **R18a:**

As in Figure 4.10, also Figure 4.16 comprehends the optimization step for a series of different bath gases and operative conditions for reaction R18a, these conditions are reported in a header:

a) N2 bath, 298K

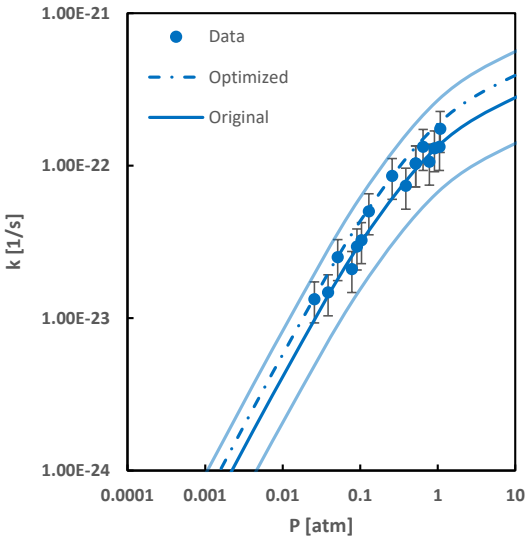

b) N2 bath, 1.44 atm

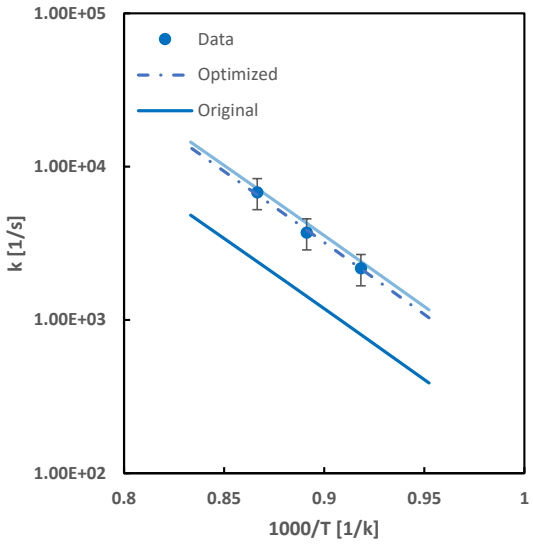

c)AR bath, 0.98 atm

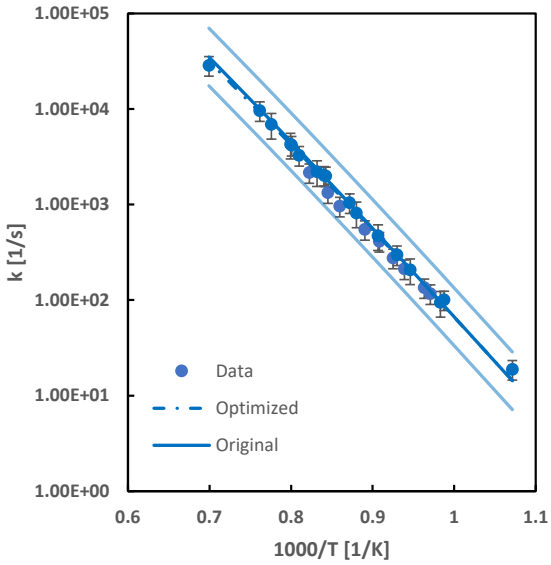

d)AR bath, 1.73 atm

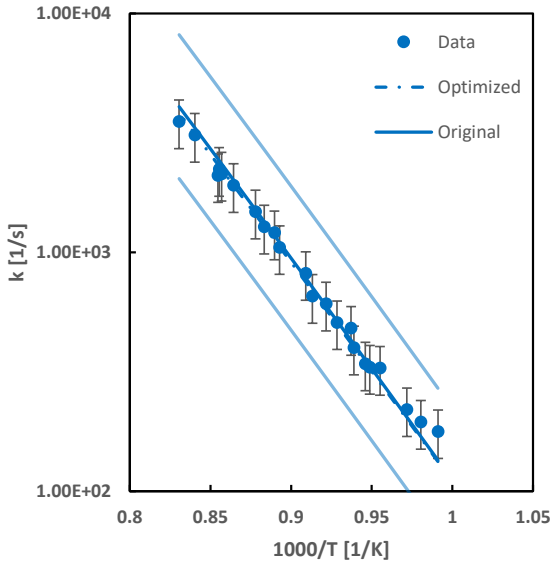

e)HE bath, 9.7 atm

f)N2O bath, 246 atm

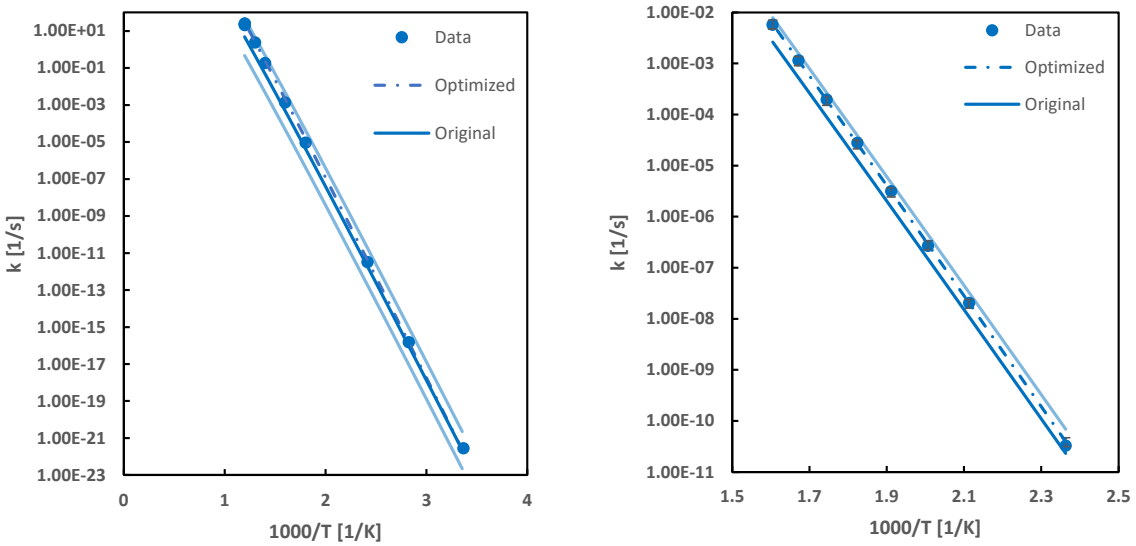

Figure 4.16: *R18a optimization routine for different bath gases, straight line represents theoretical calculations, dashed line is the optimized curve, light blue lines are the limits in which the optimizer works*

The effect of the optimization routine is not negligible in this case, this is particularly true when nitrogen is the bath gas, here is outlined a factor of ~1.4 ratio between optimized and original model.

Revised PLOG coefficients:

Reaction	A	n	Ea
H2O2=2OH	2.0000e+12	0.900	48749.00
PLOGMX / 0.000986920	3.97318E+19	-3.37829	48392.9
PLOGMX / 0.00986920	4.31747E+20	-3.38829	48457.1
PLOGMX / 0.0986920	6.90672E+21	-3.44829	48671.5
PLOGMX / 0.986920	5.79649E+23	-3.70829	49484.2
PLOGMX / 9.86920	3.98453E+25	-3.92829	50757.2
PLOGMX / 98.6920	4.17186E+24	-3.32829	51163.1
PLOGMX / 986.920	1.67724E+21	-2.07829	50637.6
PLOGMX / 9869.20	2.05760E+18	-1.05929	50097.3
PLOGMX / 98692.0	2.22746E+15	-0.08829	49309.1
PLOGMX / 986920.	1.51968E+13	0.585711	48559.3
PLOGMX / 9.86920e+06	5.07435E+12	0.736711	48407.8
PLOGMX / 2.46730e+07	4.26369E+12	0.760711	48384.5
PLOGSP / AR 0.000986920	3.97318E+19	-3.37829	48392.9
PLOGSP / AR 0.00986920	4.31747E+20	-3.38829	48457.1
PLOGSP / AR 0.0986920	6.90672E+21	-3.44829	48671.5
PLOGSP / AR 0.986920	5.79649E+23	-3.70829	49484.2
PLOGSP / AR 9.86920	3.98453E+25	-3.92829	50757.2
PLOGSP / AR 98.6920	4.17186E+24	-3.32829	51163.1
PLOGSP / AR 986.920	1.67724E+21	-2.07829	50637.6
PLOGSP / AR 9869.20	2.05760E+18	-1.05929	50097.3
PLOGSP / AR 98692.0	2.22746E+15	-0.08829	49309.1
PLOGSP / AR 986920.	1.51968E+13	0.585711	48559.3
PLOGSP / AR 9.86920e+06	5.07435E+12	0.736711	48407.8
PLOGSP / AR 2.46730e+07	4.26369E+12	0.760711	48384.5
PLOGSP / N2 0.000986920	1.27982E+20	-3.27844	49334.2
PLOGSP / N2 0.00986920	1.43380E+21	-3.29844	49411.8
PLOGSP / N2 0.0986920	2.69848E+22	-3.37844	49684.7
PLOGSP / N2 0.986920	3.35389E+24	-3.67844	50657.6
PLOGSP / N2 9.86920	9.66118E+25	-3.78844	51838.3

PLOGSP / N2 98.6920	2.91451E+24	-3.03844	52056.9
PLOGSP / N2 986.920	8.80226E+20	-1.76844	51455.4
PLOGSP / N2 9869.20	1.33925E+18	-0.78644	50911.3
PLOGSP / N2 98692.0	5.18999E+15	0.011558	50321.4
PLOGSP / N2 986920.	2.37840E+13	0.728558	49450.1
PLOGSP / N2 9.86920e+06	9.93146E+12	0.848558	49330.3
PLOGSP / N2 2.46730e+07	8.61021E+12	0.868558	49311.3
PLOGSP / CO2 0.000986920	4.32193E+19	-3.29	48813.1
PLOGSP / CO2 0.00986920	4.86976E+20	-3.31	48893.1
PLOGSP / CO2 0.0986920	9.44718E+21	-3.39	49176.9
PLOGSP / CO2 0.986920	1.24187E+24	-3.7	50174.8
PLOGSP / CO2 9.86920	3.05431E+25	-3.79	51336.5
PLOGSP / CO2 98.6920	7.58812E+23	-3.02	51525.3
PLOGSP / CO2 986.920	2.24927E+20	-1.74	50915.7
PLOGSP / CO2 9869.20	3.45897E+17	-0.768	50366.9
PLOGSP / CO2 98692.0	1.66164E+15	0	49810.1
PLOGSP / CO2 986920.	7.20530E+12	0.722	48921.8
PLOGSP / CO2 9.86920e+06	3.10233E+12	0.839	48806.3
PLOGSP / CO2 2.46730e+07	2.70134E+12	0.858	48787.9
PLOGSP / H2O 0.000986920	2.18840E+20	-3.3	48857.4
PLOGSP / H2O 0.00986920	3.21730E+21	-3.35	49040.9
PLOGSP / H2O 0.0986920	2.05582E+23	-3.57	49750.6
PLOGSP / H2O 0.986920	2.19044E+25	-3.85	51055.1
PLOGSP / H2O 9.86920	5.28777E+24	-3.36	51583.3
PLOGSP / H2O 98.6920	2.99923E+21	-2.14	51130.2
PLOGSP / H2O 986.920	2.85247E+18	-1.08	50573.3
PLOGSP / H2O 9869.20	1.45465E+15	-0.00438	49667.3
PLOGSP / H2O 98692.0	1.31765E+13	0.64	49006.2
PLOGSP / H2O 986920.	3.66699E+12	0.816	48828.8
PLOGSP / H2O 9.86920e+06	2.52411E+12	0.867	48779
PLOGSP / H2O 2.46730e+07	2.35717E+12	0.877	48770.2
PLOGSP / H2 0.000986920	1.02186E+20	-3.3	48833

PLOGSP / H2	0.00986920	1.27887E+21	-3.33	48955.5
PLOGSP / H2	0.0986920	4.20652E+22	-3.47	49426
PLOGSP / H2	0.986920	7.86613E+24	-3.82	50682.5
PLOGSP / H2	9.86920	1.81222E+25	-3.61	51530.5
PLOGSP / H2	98.6920	4.42672E+22	-2.56	51343.7
PLOGSP / H2	986.920	1.87793E+19	-1.36	50720.9
PLOGSP / H2	9869.20	1.88232E+16	-0.358	50012.2
PLOGSP / H2	98692.0	3.30327E+13	0.514	49135.9
PLOGSP / H2	986920.	4.67112E+12	0.782	48861.8
PLOGSP / H2	9.86920e+06	2.72735E+12	0.857	48789.2
PLOGSP / H2	2.46730e+07	2.48291E+12	0.87	48776.9
PLOGSP / CO	0.000986920	7.66312E+19	-3.3	48825.6
PLOGSP / CO	0.00986920	9.19363E+20	-3.32	48931.4
PLOGSP / CO	0.0986920	2.46360E+22	-3.44	49329.5
PLOGSP / CO	0.986920	4.51864E+24	-3.79	50518.7
PLOGSP / CO	9.86920	2.39996E+25	-3.68	51481.4
PLOGSP / CO	98.6920	1.20132E+23	-2.72	51415
PLOGSP / CO	986.920	4.05340E+19	-1.48	50779.5
PLOGSP / CO	9869.20	5.17102E+16	-0.499	50141.6
PLOGSP / CO	98692.0	1.82040E+15	0	49891.6
PLOGSP / CO	986920.	5.27606E+12	0.765	48878.6
PLOGSP / CO	9.86920e+06	2.83088E+12	0.851	48794.1
PLOGSP / CO	2.46730e+07	2.54483E+12	0.866	48780.1
PLOGSP / HE	0.000986920	3.46303E+19	-2.9957	50171
PLOGSP / HE	0.00986920	3.67620E+20	-3.0057	50224.3
PLOGSP / HE	0.0986920	5.19265E+21	-3.0457	50392.9
PLOGSP / HE	0.986920	2.86425E+23	-3.2557	51048.6
PLOGSP / HE	9.86920	3.68886E+25	-3.5557	52359.3
PLOGSP / HE	98.6920	1.41305E+25	-3.1257	52954.1
PLOGSP / HE	986.920	1.01754E+22	-1.9357	52547.7
PLOGSP / HE	9869.20	8.21974E+18	-0.8457	51977.7
PLOGSP / HE	98692.0	4.68336E+15	0.221996	51107.8

PLOGSP / HE 986920.	3.02548E+13	0.912296	50400.8
PLOGSP / HE 9.86920e+06	7.51086E+12	1.1043	50207.1
PLOGSP / HE 2.46730e+07	6.05923E+12	1.1343	50178.1
PLOGSP / O2 0.000986920	3.22632E+19	-3.29	48807.8
PLOGSP / O2 0.00986920	3.55046E+20	-3.31	48877.6
PLOGSP / O2 0.0986920	6.07595E+21	-3.37	49116.4
PLOGSP / O2 0.986920	6.12212E+23	-3.65	50001.3
PLOGSP / O2 9.86920	2.92769E+25	-3.82	51238.8
PLOGSP / O2 98.6920	1.74427E+24	-3.16	51560.8
PLOGSP / O2 986.920	5.94879E+20	-1.89	50995.8
PLOGSP / O2 9869.20	8.28329E+17	-0.895	50458.9
PLOGSP / O2 98692.0	1.56741E+15	0	49757.9
PLOGSP / O2 986920.	8.84006E+12	0.694	48950.3
PLOGSP / O2 9.86920e+06	3.28706E+12	0.831	48814
PLOGSP / O2 2.46730e+07	2.80361E+12	0.853	48792.8
PLOGSP / H2O2 0.000986920	2.20361E+20	-3.3	48857.7
PLOGSP / H2O2 0.00986920	3.24571E+21	-3.35	49041.8
PLOGSP / H2O2 0.0986920	2.08765E+23	-3.58	49754
PLOGSP / H2O2 0.986920	2.20390E+25	-3.85	51058
PLOGSP / H2O2 9.86920	5.21301E+24	-3.35	51583.3
PLOGSP / H2O2 98.6920	2.92812E+21	-2.14	51128.2
PLOGSP / H2O2 986.920	2.80418E+18	-1.08	50571.9
PLOGSP / H2O2 9869.20	1.42392E+15	-0.00145	49664.3
PLOGSP / H2O2 98692.0	1.30901E+13	0.64	49005.3
PLOGSP / H2O2 986920.	3.66050E+12	0.816	48828.6
PLOGSP / H2O2 9.86920e+06	2.52263E+12	0.868	48779
PLOGSP / H2O2 2.46730e+07	2.35623E+12	0.877	48770.2

Table 4.17: *Optimized PLOG for R18a*

- **R18c:**

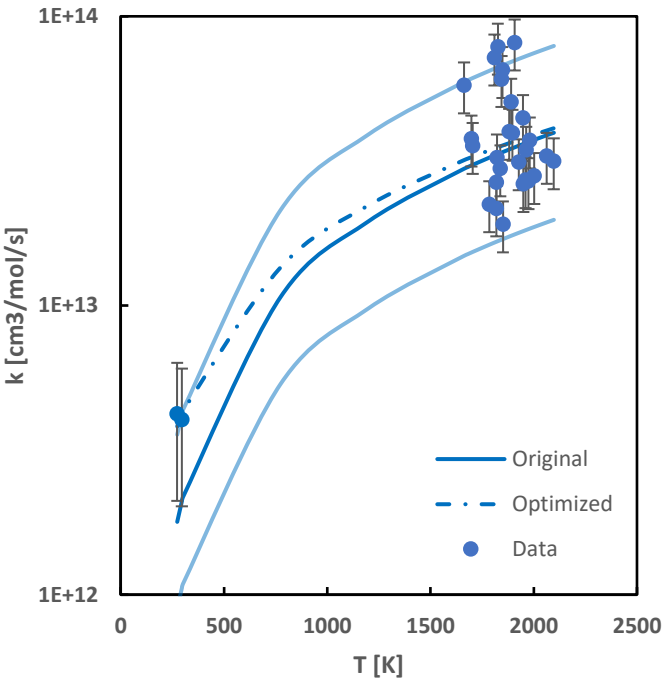

Figure 4.17: *R18c optimization routine, straight line represents theoretical calculations, dashed line is the optimized curve, light blue lines are the limits in which the optimizer works*

While for high temperature cases the optimized mechanism is in good agreement with the original one, an interesting difference (around a factor 2) is evidenced at low temperatures, however, only two datapoints are responsible of this change, more experimental investigation appears to be necessary at low temperature cases to clarify reaction behaviour at these conditions.

The following Arrhenius coefficients are obtained after the optimization:

Reaction	A	n	Ea
H+HO2=H2+O2	1.3600e+10	1.052	142.01

Table 4.18: *Optimized Arrhenius parameters for R18c*

- **R18d:**

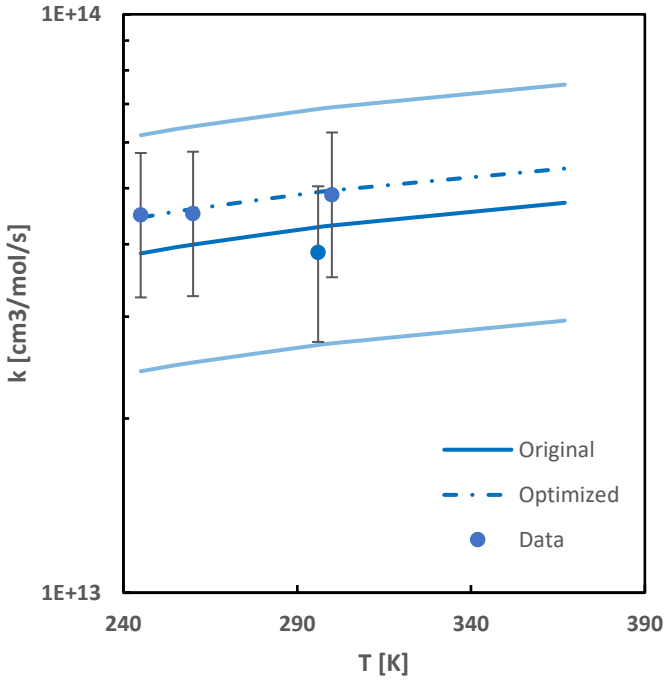

Figure 4.18: *R18d optimization routine, straight line represents theoretical calculations, dashed line is the optimized curve, light blue lines are the limits in which the optimizer works*

Also in this case very few datapoints are present from experimental side, and the temperature range investigated is very restricted, even though data are in very good agreement (factor 1.15) with the original mechanism.

These appear to be the Arrhenius coefficients for this reaction after optimization:

Reaction	A	n	Ea
H+HO2=2OH	8.5900e+13	-0.010	292.13

Table 4.19: *Optimized Arrhenius parameters for R18d*

4.7.3 R18: Impact on the model

- **R18a:**

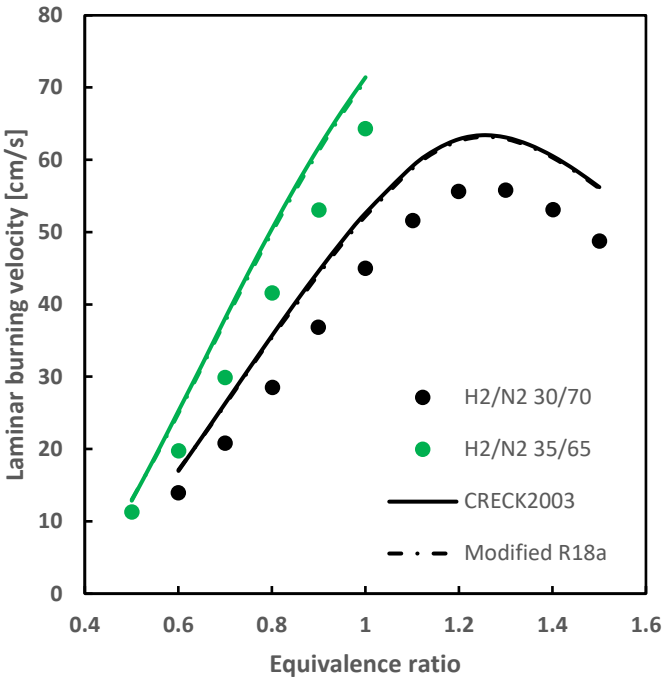

Figure 4.19: *Effect of R18a reaction modify on flame velocities at atmospheric pressures, data are taken from a work by Voss et al.*

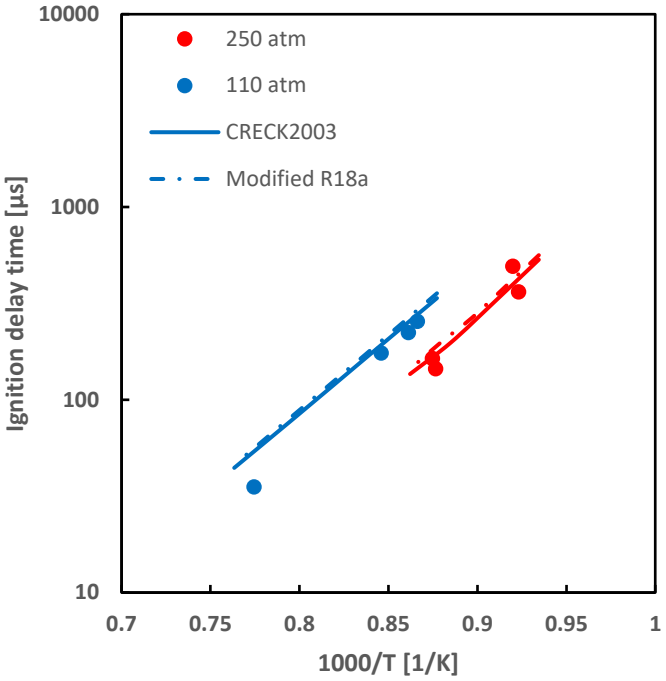

Figure 4.20: *Effect of R18a reaction modify in a Shock Tube, data are taken from a work by Shao et al.*

The most evident effects are at high pressures and high temperature, while for flames at atmospheric pressure, despite the non-negligible effect of the optimization step for N_2 seen in Figure 4.16, its consequences on the whole mechanism seem to be almost neglectable.

- **R18c:**

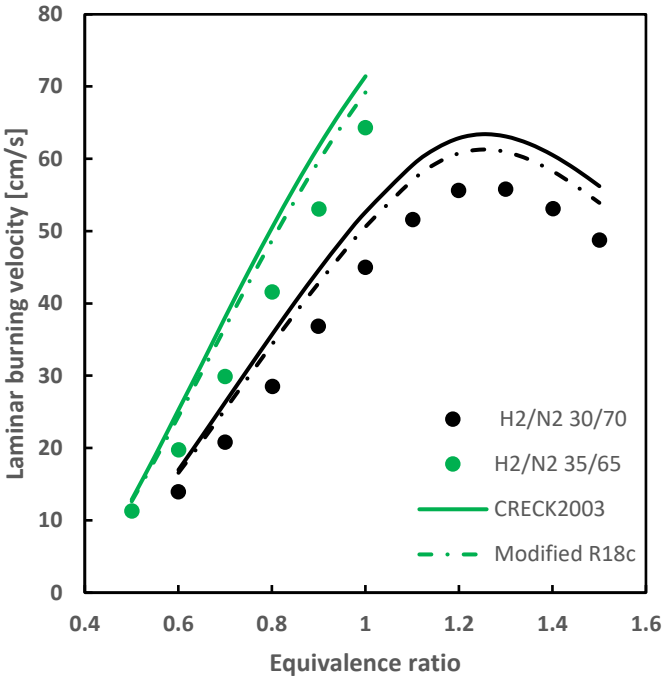

Figure 4.21: *Effect of R18c reaction modify on flame velocities at atmospheric pressures, data are taken from a work by Voss et al.*

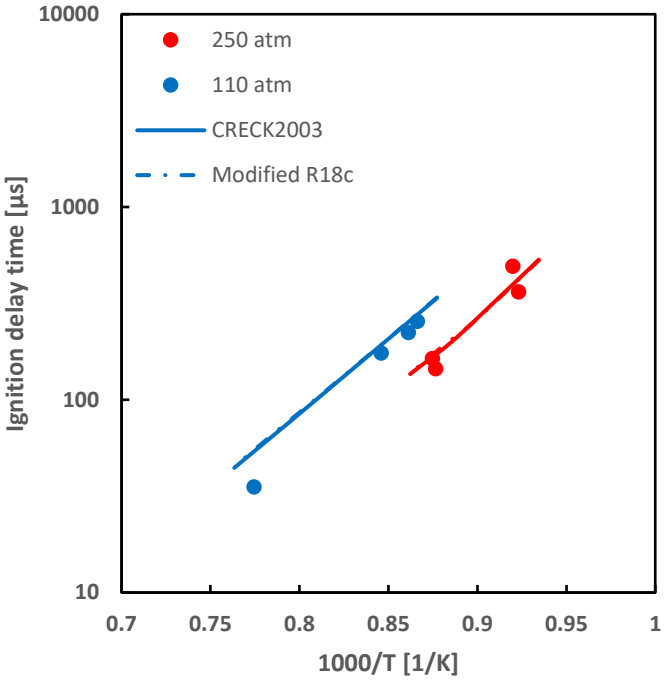

Figure 4.22: *Effect of R18c reaction modify in a Shock Tube, data are taken from a work by Shao et al.*

In this case, there's a clear effect on the low temperature and pressure flames, while for the shock tubes the impact of the modified reaction is poor, this is coherent with the results outlined in Figure 4.17, i.e. relevant changes is low temperature regime and similar behavior with respect to the original model at high temperatures.

- **R18d:**

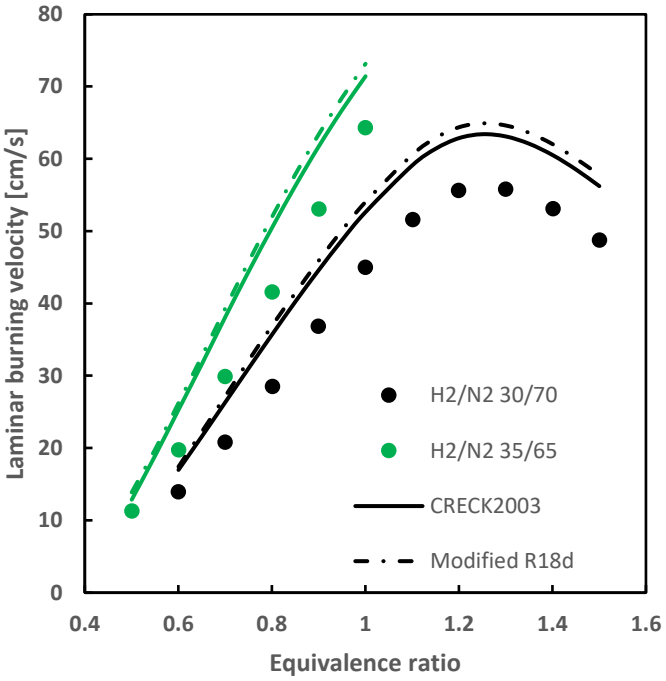

Figure 4.23: *Effect of R18d reaction modify on flame velocities at atmospheric pressures, data are taken from a work by Voss et al.*

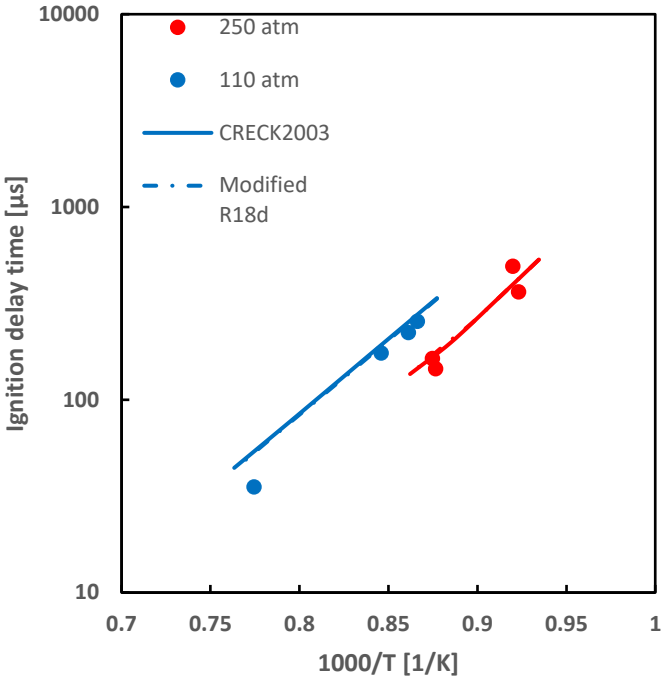

Figure 4.24: *Effect of R18d reaction modify in a Shock Tube, data are taken from a work by Shao et al.*

Similarly to R18c, the most evident effect is on low T and P cases, even if in the opposite direction, i.e. modified R18c reaction underestimated flame velocity with respect to the original model while R18d reaction overestimates it.

No relevant changes are outlined in the shock tube cases.

Let's now see the effect of the full PES correction:

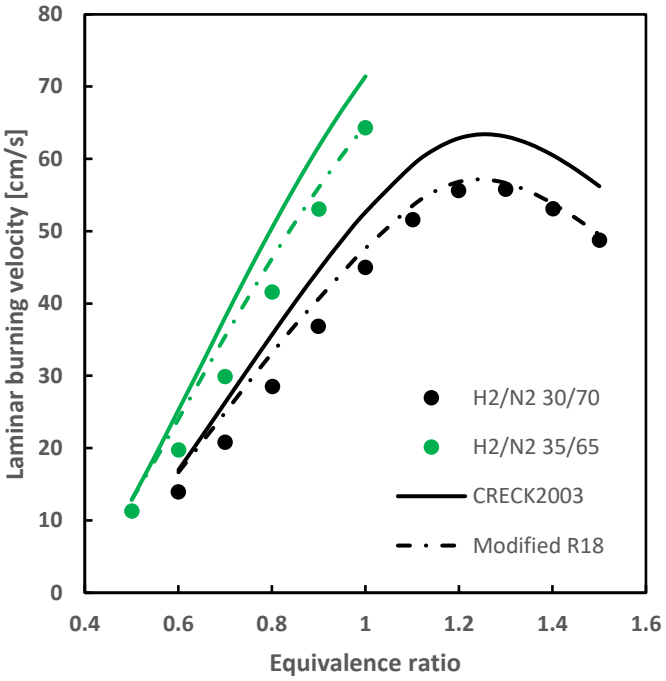

Figure 4.25: *Effect of R18 full PES modify on flame velocities at atmospheric pressures, data are taken from a work by Voss et al.*

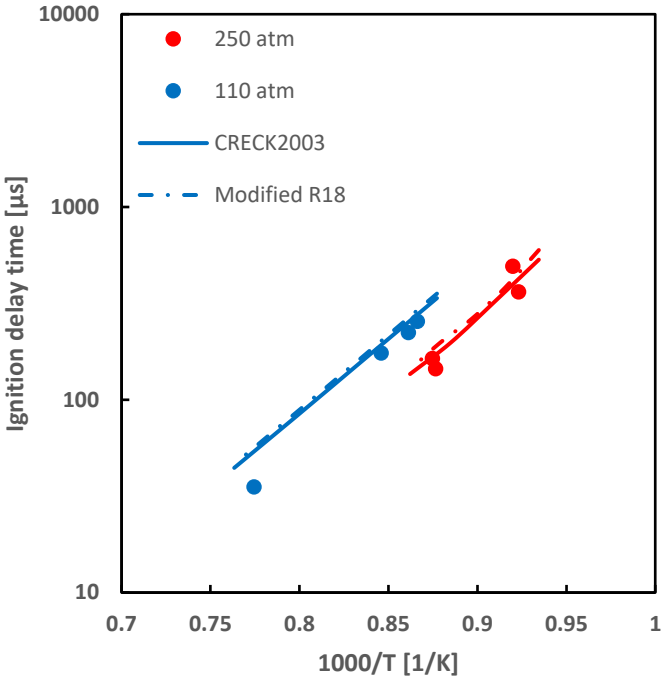

Figure 4.26: *Effect of the R18 full PES modify in a Shock Tube, data are taken from a work by Shao et al.*

The effect is very clear in the flame cases, and results in a better representation of the experimental data, a certain impact can be seen also for the shock tubes.

It must be said that a huge effect is related to the introduction of reaction R18e (that is $H\cdot + H\cdot + O_2 \rightarrow H_2 + O_2$), this reaction, that was not present in Polimi model CRECK2003 and has been studied and introduced in the previous project, has a large impact on the whole mechanism:

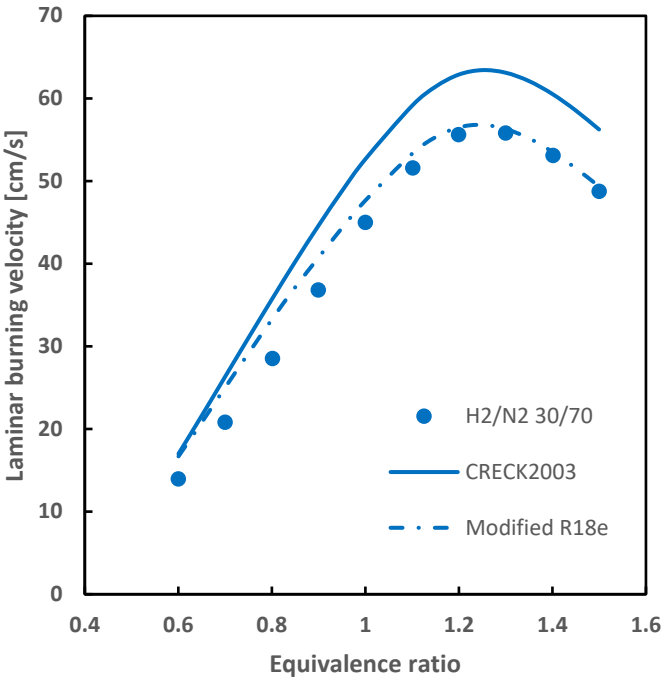

Figure 4.27: *Effect of R18e reaction modify on flame velocities at atmospheric pressures, data are taken from a work by Voss et al.*

4.8 R24 PES

This is the PES for 3 oxygen atoms reaction, in particular the involved reaction is a recombination between molecular and atomic oxygen to give ozone:

$$R24: O_2 + O: + M \rightarrow O_3 + M$$

A reaction made possible by a collisional stabilization of the instable O3 intermediate with a third body.

This reaction does not have a potential barrier, but a saddle point is present in the O3 formation pathway, this creates a bottleneck in the reaction.

4.8.1 R24: Collected works

Theoretical papers: 11_DAV_LOL [180], 13_AYO_BAB [181],13_DAV_LOL [182], all these works use ab initio quantum chemistry calculations.

Experimental papers:

Author	Reactor/Technique	T range [K]	P range [atm]	Bath gas
27_WUL_TOL [183]	Flow tube	420 - 450	1	O3
57_BEN_AXW [184]	Flow tube	340 - 385	0.0722	O3
58_KAU [185]	Electron beam	296	0.0017	O2
59_ELI_OGR [186]	Flow tube	213	0.00365	O2
60_KRE_PET [22]	Electron beam	350	0.0026	O2

60_ZAS_URB [187]	Pyrex vessel	390 - 405	0.015 – 0.069	O2
61_HAC_MAR [188]	Flow tube	1123	0.00185	O2
62_WES_DAV [189]	Shock tube	680 - 910	1.71	AR
64_KAU_KEL [190]	Flow tube	300	0.0059	O2
65_CLY_MCK [191]	Flow tube	188 - 373	0.0015 – 0.0093	AR
65_SAU_DOR [192]	High pressure vessel	296	12 - 98	AR
67_KAU_KEL [193]	Flow tube	300	0.0033 – 0.0047	HE,AR,O2,N2,CO2,H2O, N2O,CF4,SF6
67_MUL_WIL [194]	Flow tube	213 - 386	0.006	O2,HE,AR,CO2
68_MEA_PER [195]	Pulsed radiolysis	295	0.6 – 0.92	CO2,N2O,O2,CO
70_DON_HUS [196]	Flash photolysis	298	0.19 – 0.71	HE,AR,KR
70_HIP_TRO [197]	Photolysis	298	1 - 200	N2
70_SLA_BLA [198]	Photolysis	300	0.021 - 0.0365	AR,N2
71_STU_NIK [199]	Photolysis	300	0.016 – 0.068	O2,N2,CO
72_BEV_JOH [200]	Pulse radiolysis	295	0.07 – 4	O2,C2H4,CO2,AR

72_HUI_HER [201]	Flash photolysis	200 - 346	0.068 – 0.66	HE,N2,AR
73_BAL_LAR [202]	Flow tube	295	0.0013 – 0.013	O2,N2,AR
74_SNE [203]	Flash photolysis	295	0.0236 – 0.0487	O2
76_HOG_BUR [204]	Flow tube	300	0.0003 – 0.0014	O2
79_ARN_COM [205]	Flash photolysis	218 - 301	0.00426 – 0.066	O2,N2,AR
79_END_GLA [206]	Shock tube	800	0.165 – 0.98	HE,NE,AR,KR,XE,N2,O2, CO2,CF4,SF6
80_SUG_ISH [207]	Electron beam	296	0.065 – 1.25	HE
80_KLA_AND [208]	Flash photolysis	219 - 368	0.066 – 0.27	O2,N2,AR
82_LIN_LEU [209]	Flash photolysis	219 - 353	0.0103 – 0.326	HE,N2,AR,O2
84_CRO_TRO [210]	Flash photolysis	293 - 295	1 - 200	AR,N2,CO2,SF6
85_BOR_COB [130]	Flash photolysis	298	3 – 200	N2
97_AND_HUL [211]	Photolysis	296	0.263	N2,O2
98_SEH_NIE [212]	Pulse radiolysis	295	0.986	AR

Table 4.20: *Experimental data collection for R24*

4.9 R26 PES

In this PES, 3 oxygen atoms and 2 hydrogen atoms are involved, these are the outlined reactions:

$$R26a: HO_2\cdot + OH\cdot \rightarrow H_2O + O_2$$
$$R26b: H_2O_2 + O(^3P) \rightarrow OH\cdot + HO_2\cdot$$
$$R26c: H\cdot + OH\cdot + O_2 \rightarrow H_2O + O_2$$

So, there are two termination reactions (a and c) and a propagation reaction, reaction c is termolecular.

Reaction b) is the one studied in this work.

4.9.1 R26b: Collected works

Theoretical papers:

Author	Method
03_TAR_BAH [213]	Ab initio calculations
08_KOU_BAH [214]	Ab initio calculations Transition state theory method

Table 4.21: *Theory works collection for R26b*

Experimental papers:

Author	Reactor/Technique	T range [K]
71_ALB_HOY [215]	Flow tube	325 - 800
73_DAV_WON [216]	Flash photolysis	283 – 368
83_WIN_NIC [217]	Flash photolysis	298 – 386

Table 4.22: *Experimental data collection for R26b*

4.9.2 R26b: Model optimization

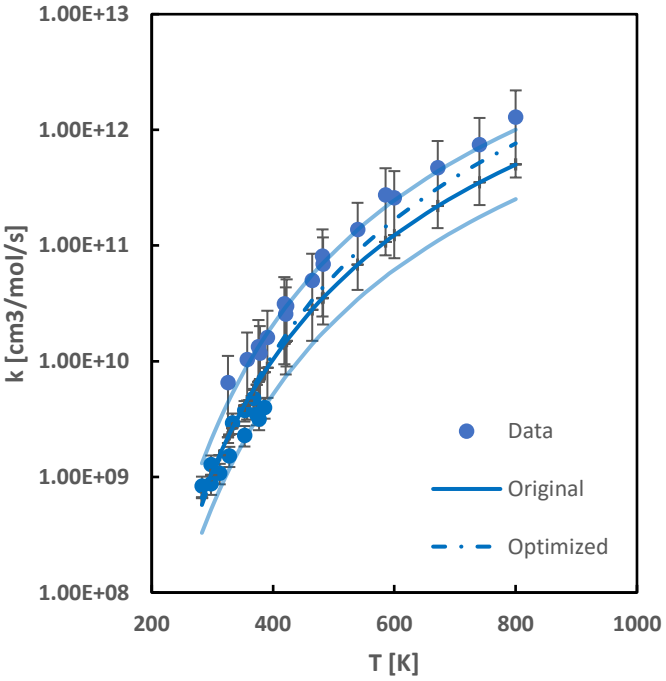

Figure 4.28: *R26b optimization routine, straight line represents theoretical calculations, dashed line is the optimized curve, light blue lines are the limits in which the optimizer works*

As it can be seen, the original model was already in good agreement with the experimental data, (the f factor in this case is 0.3, which corresponds to a factor 2) however, a non-negligible optimization effect is visible at high temperatures.

These are the new Arrhenius coefficients found:

Reaction	A	n	Ea
O+H2O2=OH+HO2	1.0800e+07	2.083	4381.77

Table 4.23: *Optimized Arrhenius parameters for R26b*

4.9.3 R26: Impact on the model

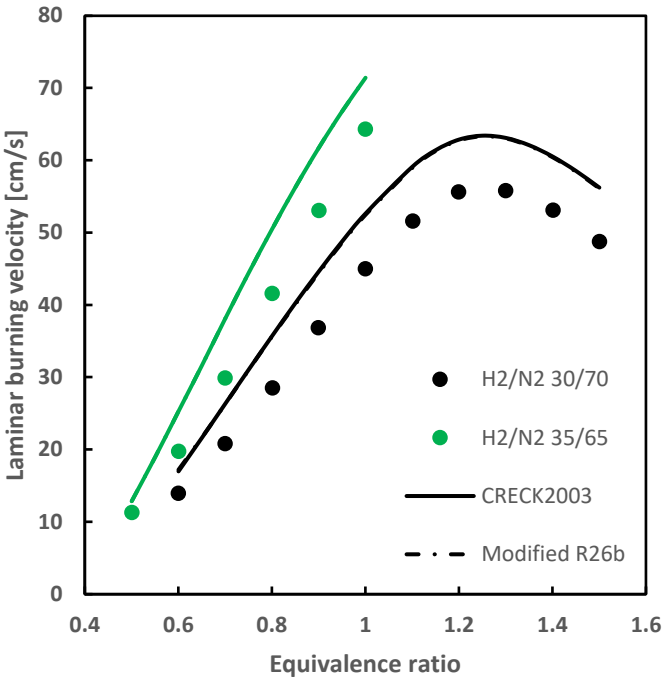

Figure 4.29: *Effect of R26b reaction modify on flame velocities at atmospheric pressures, data are taken from a work by Voss et al.*

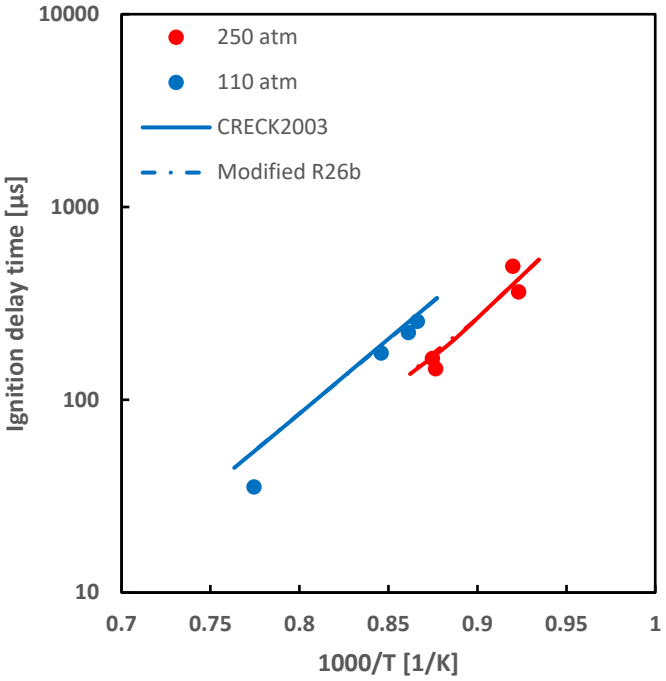

Figure 4.30: *Effect of R26b reaction modify in a Shock Tube, data are taken from a work by Shao et al.*

No relevant changes can be outlined, this is coherent with the fact that the optimization effect is not really impacting.

Let's see the changes due to the full PES modification:

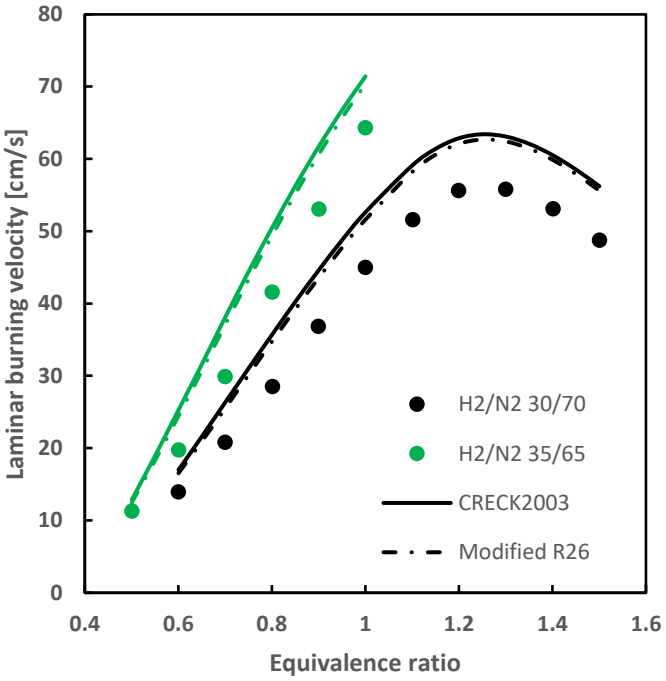

Figure 4.31: *Effect of the R26 full PES modify on flame velocities at atmospheric pressures, data are taken from a work by Voss et al.*

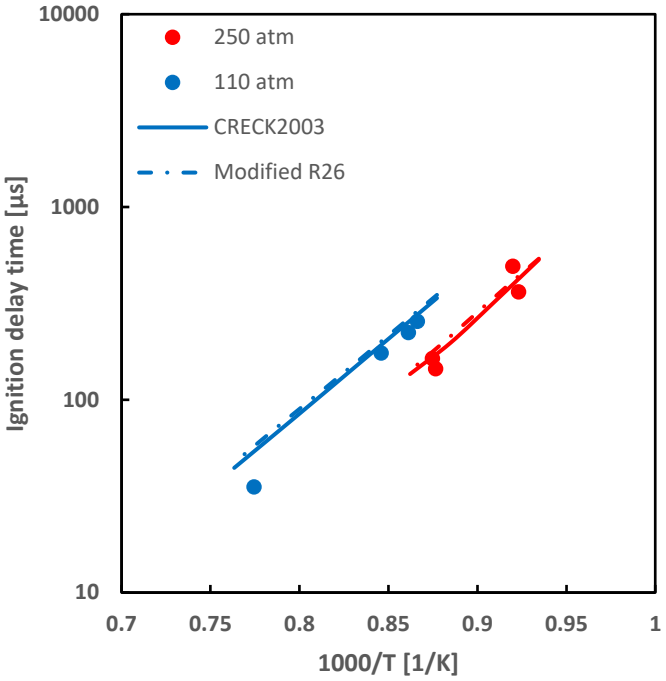

Figure 4.32: *Effect of the R26 full PES modify in a Shock Tube, data are taken from a work by Shao et al.*

Some differences between the two models are more evident in this case, this is clear for shock tubes in particular, even if they are still narrow.

4.10 R34 PES

This PES has been recently studied in a work by Klippenstein et al. [218]

In particular, the Arrhenius parameters for the termination reaction:

$$R34a: HO_2 \cdot + HO_2 \cdot \rightarrow H_2O_2 + O_2$$

Have been revised, and a new reaction pathway, that was not included in previous Polimi model, is defined:

$$R34b: HO_2 \cdot + HO_2 \cdot \rightarrow OH \cdot + OH \cdot + O_2$$

These appear to be the modified coefficients for those two reactions:

Reaction	A	n	Ea
2HO2=O2+H2O2	1.9300e-02	4.120	-4960.00
2HO2=O2+2OH	6.4100e+17	-1.540	8540.00

Table 4.24: *Arrhenius parameters for R34a and R34b*

4.10.1 R34: Impact on the model

The most evident effects of these implemented reactions are at high pressures, as can be seen from the following shock tube experiments:

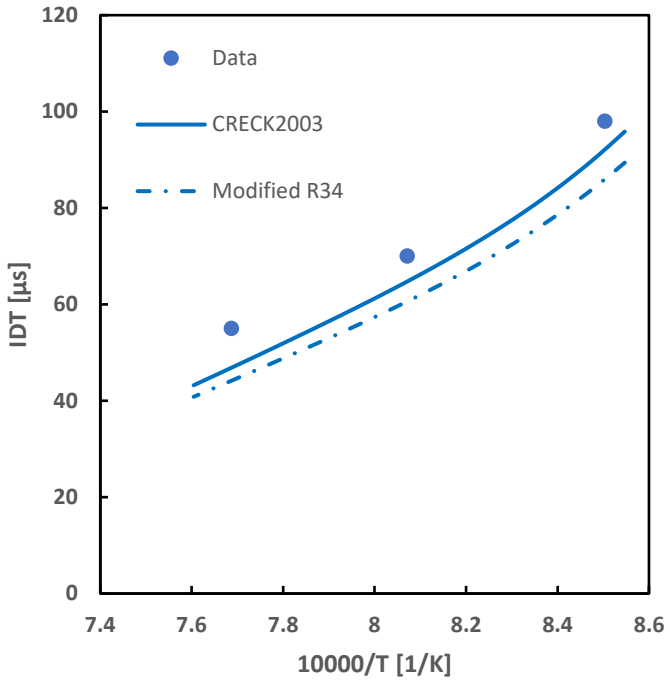

Figure 4.33: *Effect of the R26 full PES modify in a Shock Tube at very high pressures (260 atm), data are taken from a work by Petersen et al. [219]*

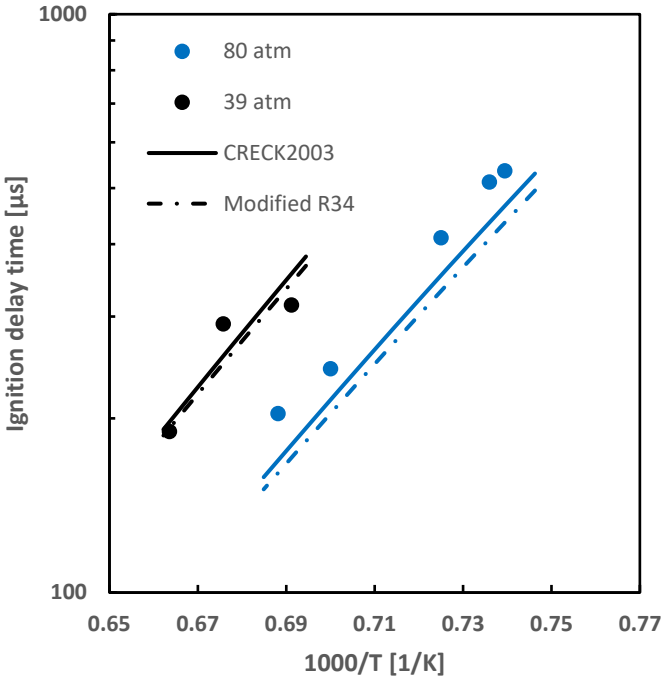

Figure 4.34: *Effect of the R34 full PES modify in a Shock Tube, data are taken from a work by Shao et al.*

What can be also seen is that the revised reaction effect grows in importance as pressure rises.

5. Model validation

5.1 Introduction

Given the results obtained from Chapter 4, it is now possible to realize a revised model, in this chapter the new model is tested and compared with the Aramco mech 2.0.

As already said, the validation process is carried out in OpenSMOKE++, the tests were performed on a large database of macroscopic experiments, that are summarized and reported in the following tables:

1D Premixed laminar flames:

Author	Temperature conditions	Pressure conditions	Mixture
Wang et al. [220]	300 K	0.1 – 0.2 MPa	CO-H2-CO2-O2
Voss et al. [152]	298 K	1 atm	H2-CO-N2-O2
Sabard et al. [221]	303 – 343 K	0.05 - 0.1 MPa	H2-N2-O2
Grosseuvres et al. [222]	296 – 413 K	0.1 MPa	H2-N2-O2-H2O
Krejci et al. [223]	298 - 443 K	1 - 10 atm	H2-N2-O2-HE
Wang, Costa et al. [74]	298 K	0.1 – 0.5 MPa	CH4-O2-N2-CO2
Zhang et al. [224]	300 K	1 atm	H2-CO-CH4-CO2-N2
Konnov et al. [225]	298 K	1 atm	CO-H2-CO2
Sun et al. [226]	298 K	1 – 40 atm	CO-H2-N2-O2
Hu et al. [227]	300 – 543 K	1 atm	CH4-O2-CO2

Han et al. [228]	298 K	1 atm	CH4-N2-O2
Oh et al. [229]	300 K	1 atm	CH4-N2-O2
De Persis et al. [230]	300 K	1 atm	CH4-CO2-N2-O2
Xie et al. [231]	300 K	0.1 – 0.3 MPa	CH4-CO2-O2
Cai et al. [232]	353 K	0.1 – 0.5 MPa	CH4-N2-O2
Gu et al. [233]	300 - 402 K	0.1 – 1 MPa	CH4-N2-O2
Lowry et al. [234]	298 K	1 – 10 atm	CH4-N2-O2
Rozenchan et al. [235]	298 K	1 – 40 atm	CH4-O2-HE-N2
Mevel et al. [236]	303 K	0.1 MPa	H2-N2-O2
Mazas et al. [237]	373 – 473 K	1 atm	CH4-O2-N2-H2O
Khan et al. [238]	300 K	1 atm	CH4-N2-O2-CO2
Alfe et al. [239]	300 K	1 atm	CH4-O2
Berg et al. [240]	450 – 2000 K	0.03 atm	CH4-O2-N2

Table 5.1: *1D Premixed laminar flames database and operative conditions*

Shock Tubes:

Author	Temperature conditions	Pressure conditions	Mixture
Mevel et al. [236]	920 – 1628 K	230 – 648 kPa	H2-N2-O2-Ar
Karimi et al. [241]	1139 – 1297 K	100 – 200 bar	CH4-O2-CO2-Ar
Shao et al. [73]	1040 – 1270 K	33 – 260 atm	CH4-H2-O2-CO2
Dean et al. [242]	2000 – 2800 K	1.2 – 1.4 atm	CO-H2-N2
Eubank et al. [243]	1300 – 1850 K	4 atm	CH4-O2-N2-AR

Kalitan et al. (2005) [244]	850 – 1250 K	1.15 atm	H2-CO-N2-O2
Kalitan et al. (2006) [244]	930 – 1270 K	1.12 – 15.44 atm	H2-CO-N2-O2
Petersen et al. [219]	1000 – 1600 K	15 – 260 atm	CH4-O2-AR-N2-HE
Seery et al. [245]	1400 – 1800 K	1.8 – 3.9 atm	CH4-O2-AR
Spadaccini et al. [246]	1300 – 1950 K	5.7 – 9.3 atm	CH4-O2-AR
Xia et al. [247]	900 – 1500 K	10 atm	CO-H2-O2-AR
Krejci et al. [223]	950 – 2000 K	1.6 – 32 atm	H2-O2-CO

Table 5.2: *Shock tubes database and operative conditions*

PFR:

Author	Temperature conditions	Pressure conditions	Mixture
Alzueta et al. [248]	900 K	1.05 atm	CO-O2-H2O-N2
Kim et al. [249]	1040 K	1 – 9.6 atm	CO-O2-H2O-N2
Rasmussen et al. [250,251]	600 – 1800 K	1 – 100 bar	CH4-O2-N2-H2O
Sabia et al. [252]	1200 – 1500 K	1 atm	CH4-O2-N2
Sen et al. [253]	600 – 1000 K	6 atm	CH4-O2-AR
Sivaramakrishnan et al. [254]	1000 – 1450 K	24 - 450 atm	CO-O2-H2-AR

Table 5.3: *Plug Flow Reactors database and operative conditions*

PSR:

Author	Temperature conditions	Pressure conditions	Mixture
Bakali et al. [255]	1100 – 1500 K	1 atm	CH4-C2H6-O2-N2
Cong et al. (2008) [256,257]	900 – 1500 K	1 - 10 atm	CH4-H2-CO-CO2-O2-N2
Cong et al. (2009) [258,259]	900 – 1250 K	1 - 10 atm	CH4-O2-H2O-CO2-N2
Dagaut et al. (1991) [260]	900 – 1250 K	1 – 10 atm	CH4-O2-N2
Dagaut et al. (2003) [261]	800 – 1400 K	1 atm	CO-H2-O2-N2
Dagaut et al. (2006) [262]	900 – 1250 K	10 atm	CH4-C2H6-H2-O2-N2

Table 5.4: *Perfectly Stirred Reactors database and operative conditions*

As can be seen from the tables, not all the experiments considered deal with hydrogen, there are also data for methane combustion or for mixed fuels, but, as said in Chapter2, the model used for OpenSMOKE++ is hierarchical, thus the effects of hydrogen model revision will be evident also for these cases.

This whole database is also available in SciExpeM framework, developed by Ramalli et al. [263], it is also possible to plot the operative conditions of the experiments contained in SciExpeM database in a 3D plot (axes are T, p and equivalence ratio) as follows:

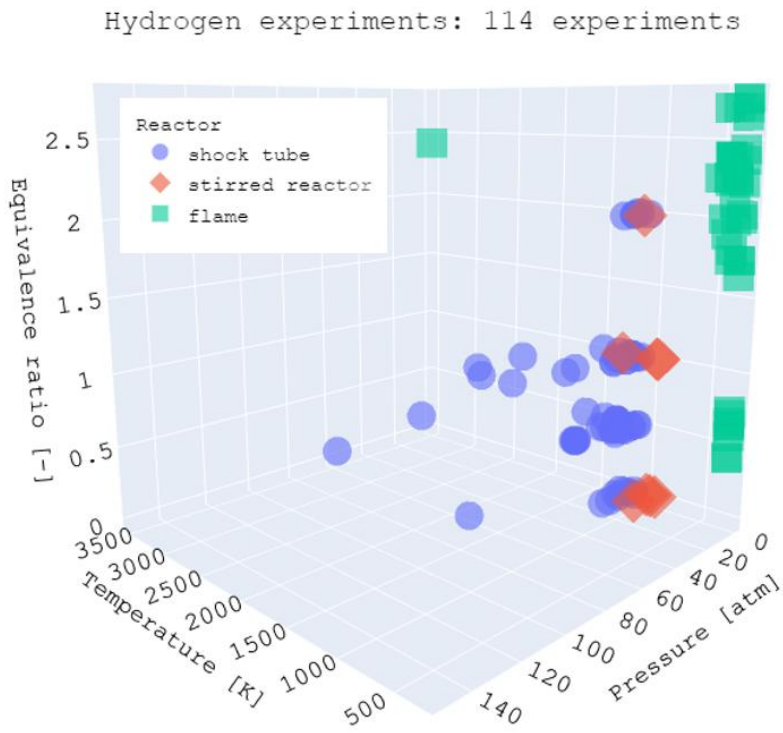

Figure 5.1: *Experimental conditions for hydrogen database, courtesy of Timoteo Dinelli*

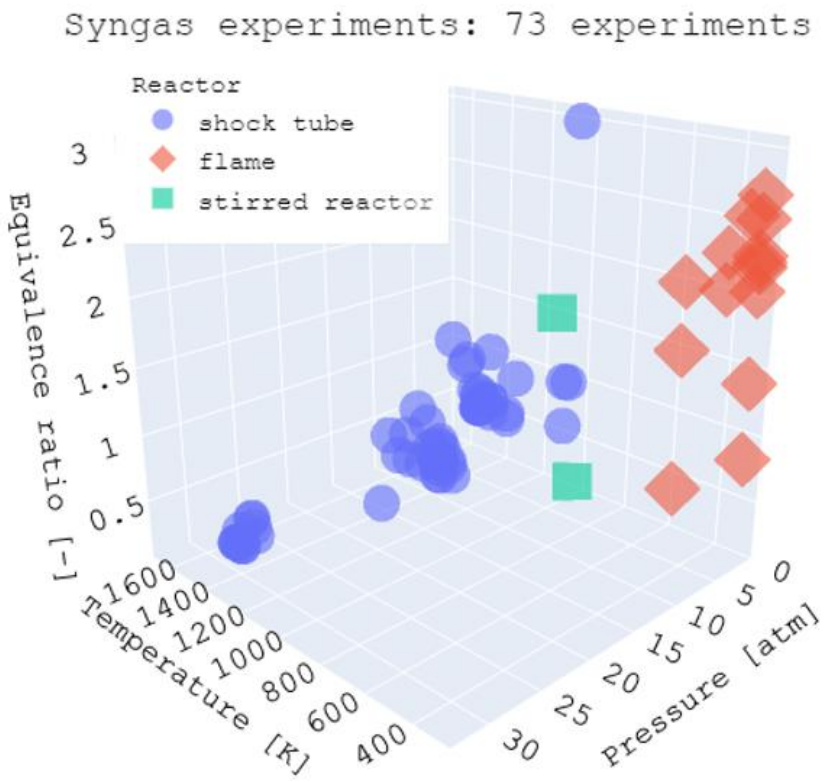

Figure 5.2: *Experimental conditions for syngas database, courtesy of Timoteo Dinelli*

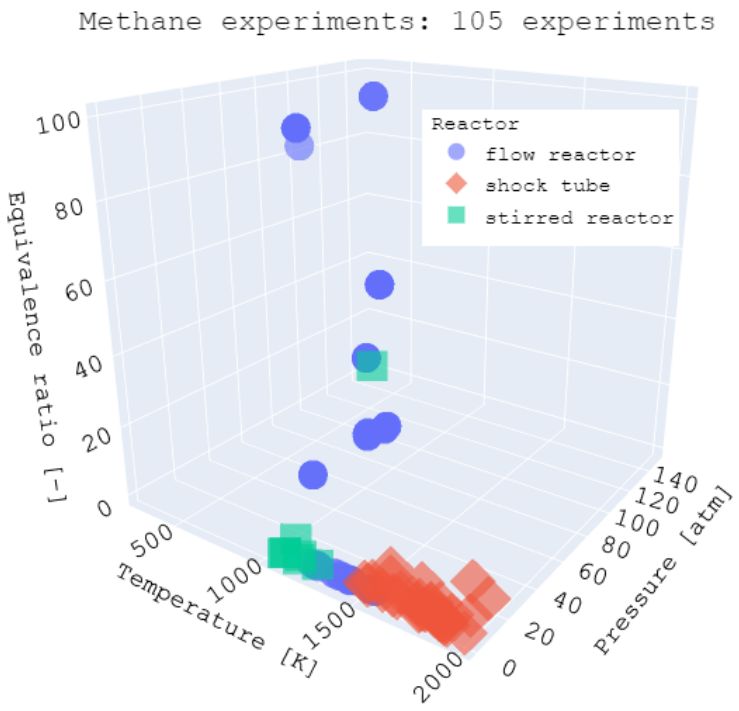

Figure 5.3: *Experimental conditions for methane database, courtesy of Timoteo Dinelli*

5.2 Model testing

The whole database has been tested, here just a sample with some interesting cases is reported:

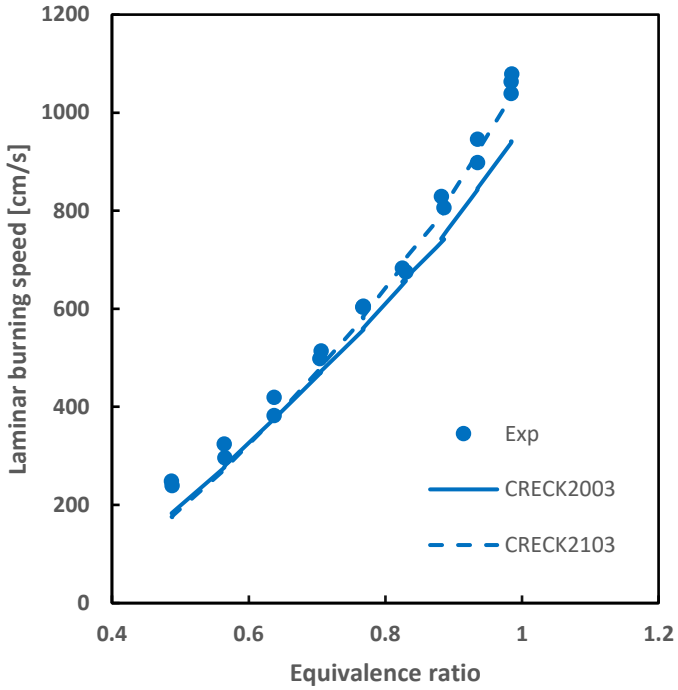

Figure 5.4: *Model comparison, data are taken from a work by Mevel et al., temperature is 303K, pressure at 1 atm, the mixture is H_2-N_2-O_2 at different compositions*

A better behaviour in fitting experimental data is evident in this case for an equivalence ratio> 0.7, while the models are overlapped below this value, an unequivocal improvement is introduced by the revised model for this case.

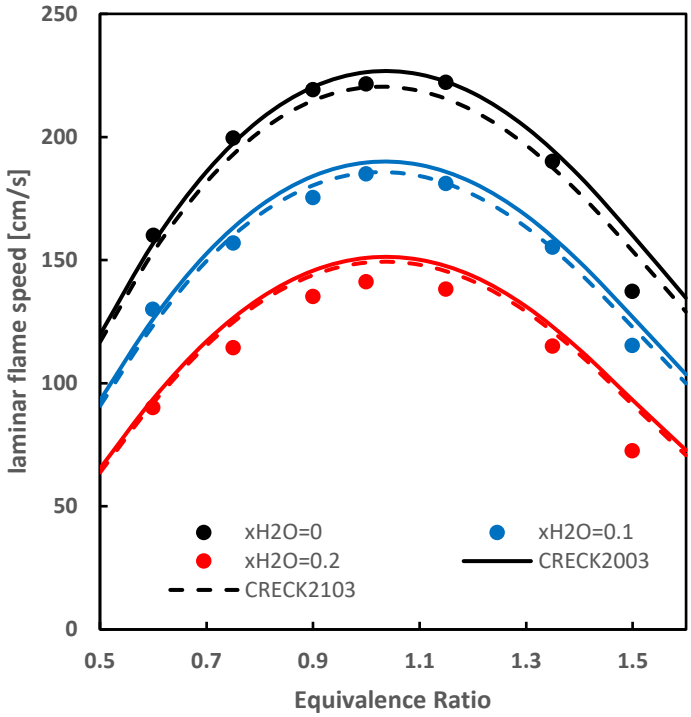

Figure 5.5: *Model comparison, data are taken from a work by Mazas et al., temperature is at 343K, pressure at 1 atm, mixture is CH_4-N_2-O_2-H_2O*

CRECK2103 model in this case shows results that are below the original one, the difference becomes more evident when water dilution is lower, the bigger differences between the models can be seen for equivalent ratio ~ 1.

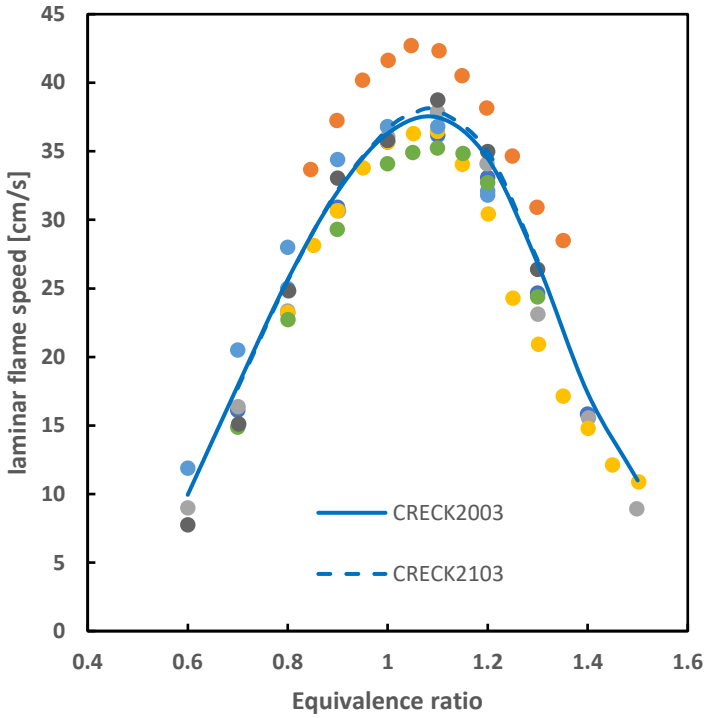

Figure 5.6: *Model comparison, eexperimental data are from all works dealing with CH_4-air mixtures at 298K, 1atm*

Not so evident changes are outlined in general, just in stoichiometric and quasi-stoichiometric conditions new model slightly overestimates the flame velocity if compared with CRECK2003, while most of the data are below the predicted flame speeds.

a) CH_4-O_2-HE mixture

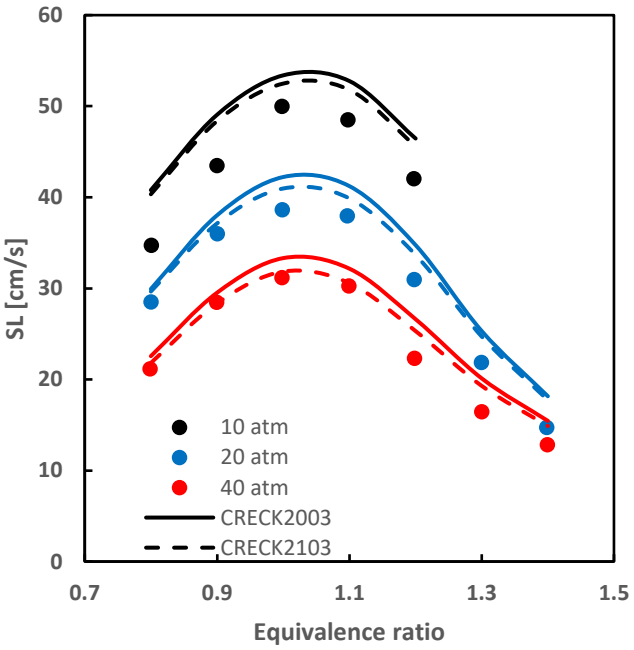

b) CH4-Air mixture

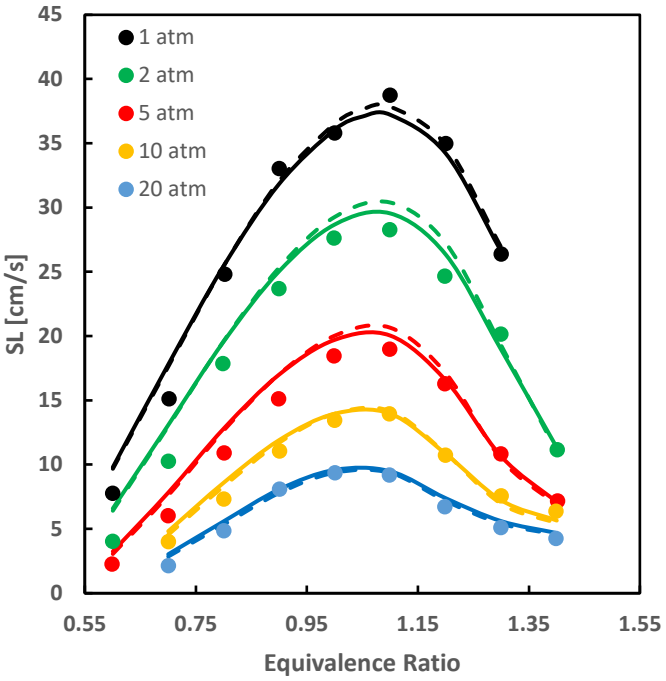

Figure 5.7: *Model comparison, data are taken from a work by Rozenchan et al., at room temperature and different pressures*

Once again, the main differences between the models are in quasi-stoichiometric conditions, it is interesting to outline that in Figure 5.7a), i.e. with Helium as a diluent, CRECK2103 flame speeds are below the original model, while for Figure 5.7b), with N_2 as a diluent, the trend is inverse, this happens since bath gases are treated separately in PLOG optimization.

Furthermore, when pressure increases, there's an improvement in fitting experimental data for CRECK2103 model.

a) CH_4-N_2-O_2 mixture, 1atm

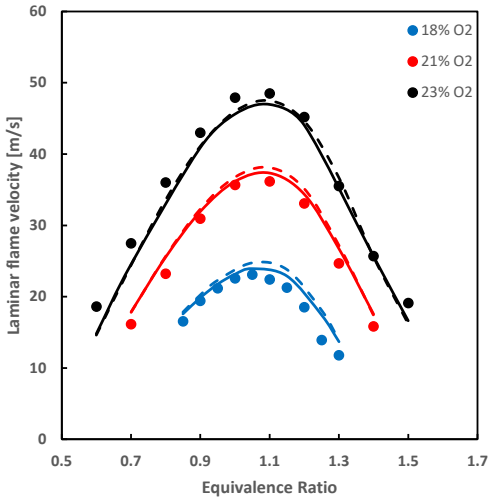

b) CH_4-N_2-O_2 mixture, 3atm

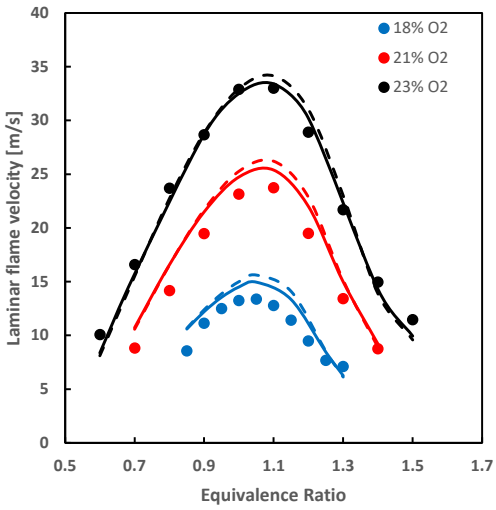

d) CH_4-N_2-O_2 mixture, 5atm

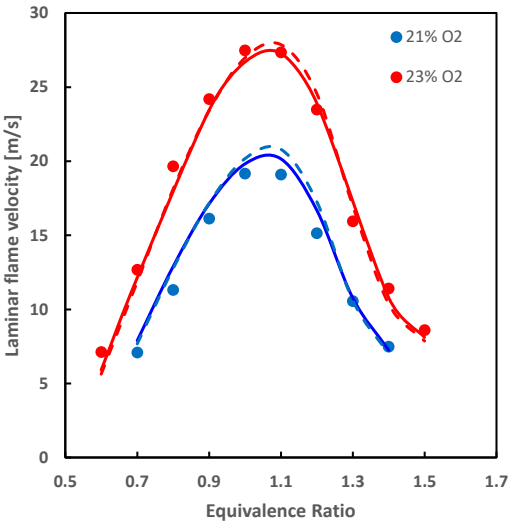

e) CH_4-CO_2-O_2 mixture, 1atm

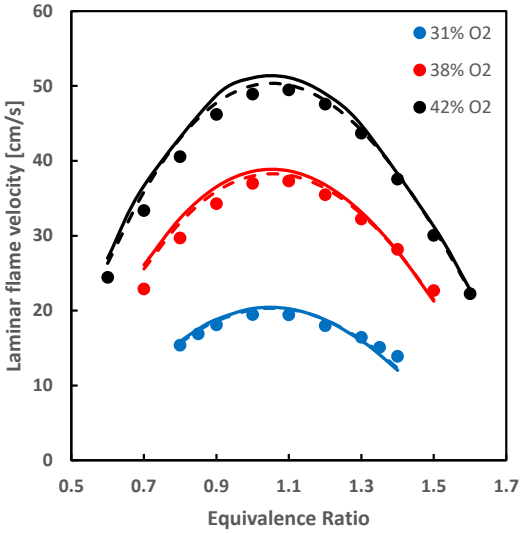

f) CH_4-CO_2-O_2 mixture, 2atm

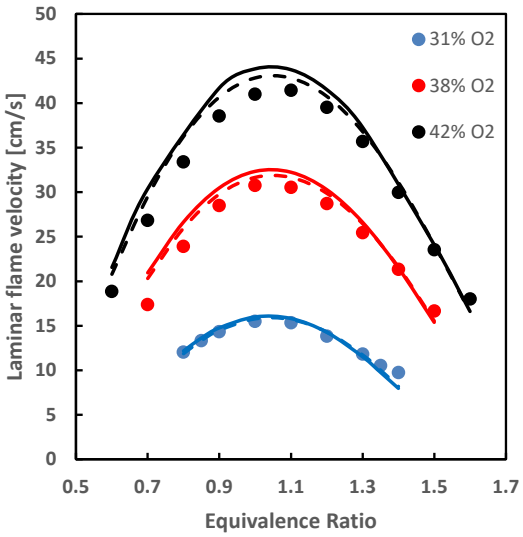

g) CH_4-CO_2-O_2 mixture, 3atm

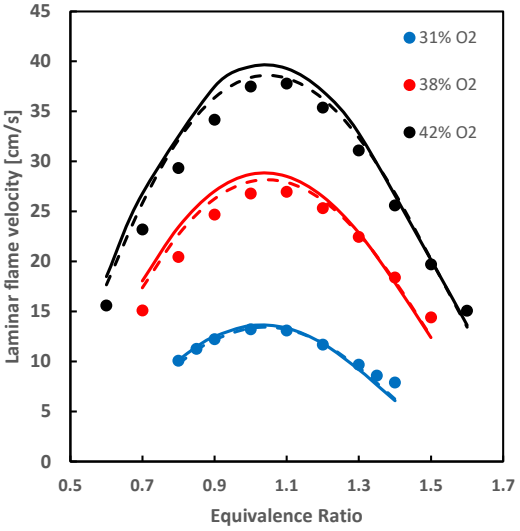

Figure 5.8: *Model comparison, data are taken from a work by Wang-Costa et al., at room temperature*

Also in this case, an inverse trend is seen when diluent is CO_2 or N_2 instead, then the same conditions already outlined for other cases seem to be true also in this case.

a) CH_4-O_2-He mixture, 15 atm

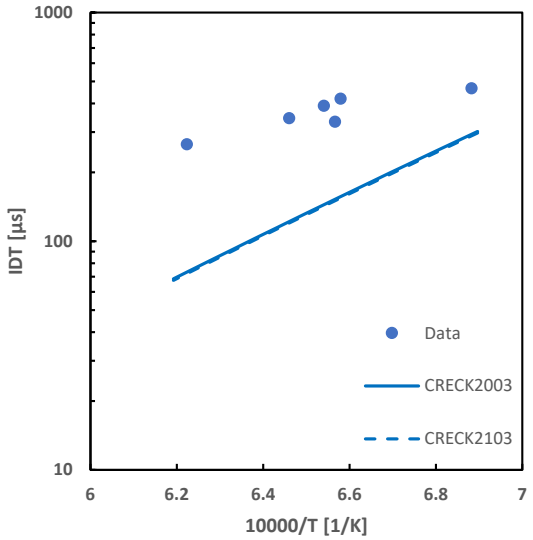

b) CH_4-O_2-AR mixture, 40 atm

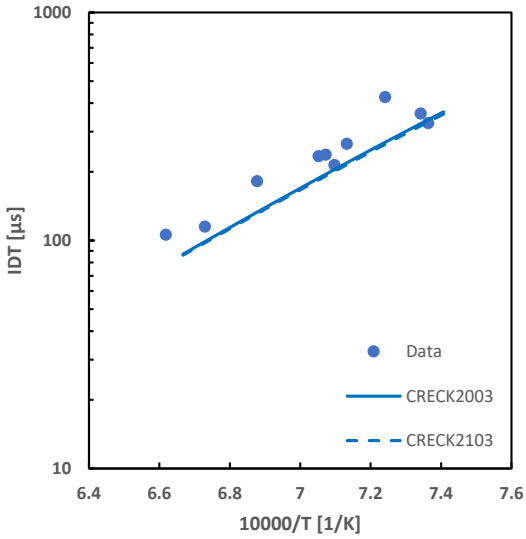

c) CH_4-O_2-N_2 mixture, 260 atm

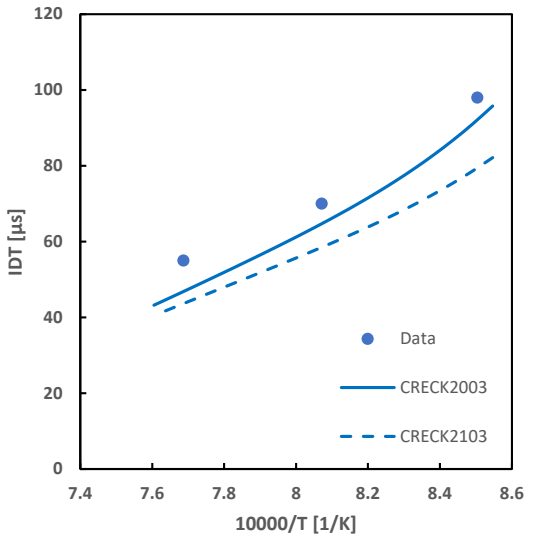

Figure 5.9: *Model comparison, data are taken from a work by Petersen et a*l.

While no significative differences can be outlined for Figure 5.9a) and b), great differences arise in case c), it is not clear whether it has to be attributable to the high pressure involved or to the bath gas involved (nitrogen for this case), still, this result is coherent with what shown in Figure 4.33, probably R34 PES modify is the main responsible of ignition delay time underestimation for this case, even if here this effect is more evident.

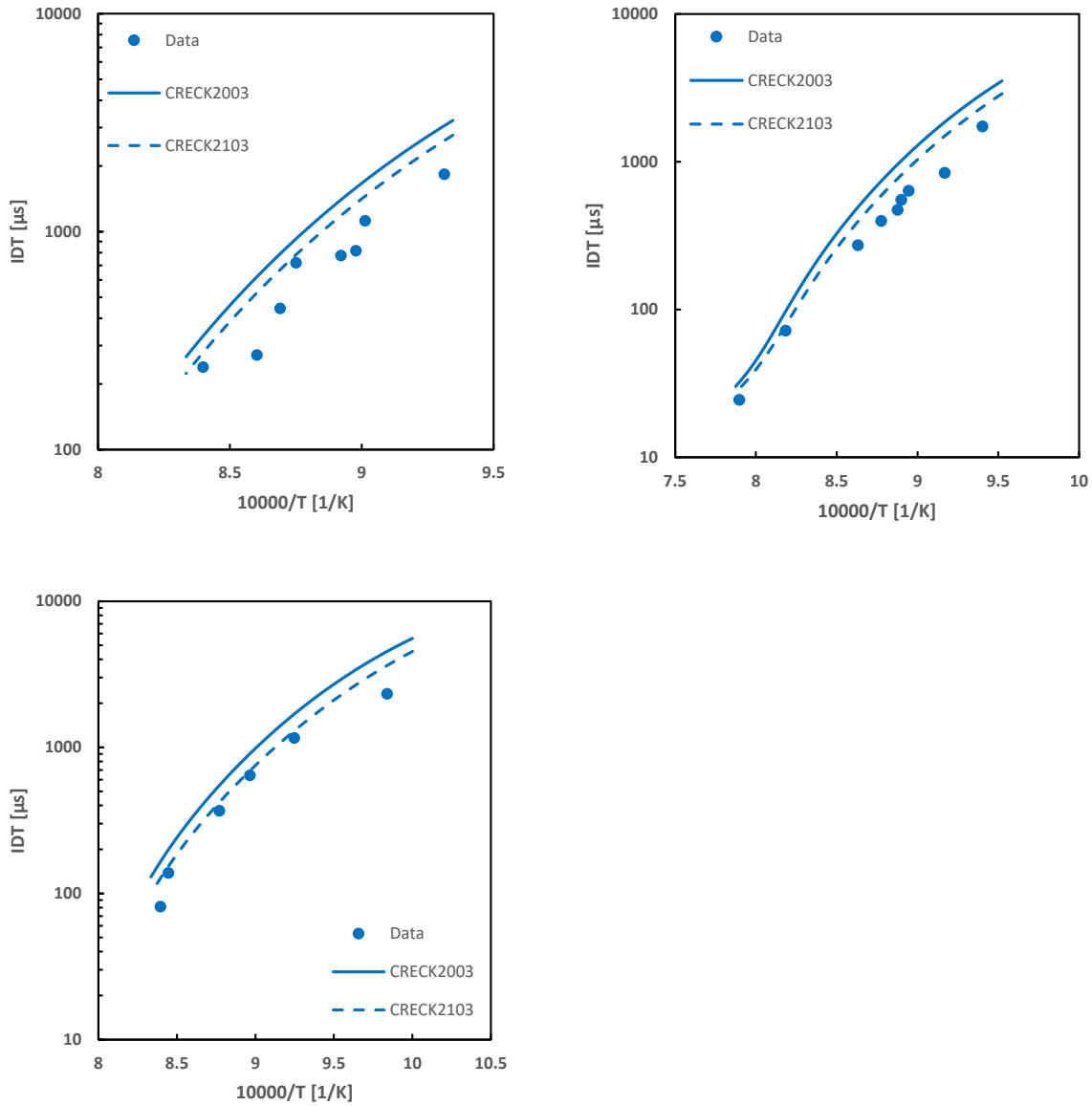

Figure 5.10: *Model comparison, data are taken from a work by Kalitan et al., p ranges between 13-15 atm, CO-H_2-O_2-N_2 mixture at different compositions*

What can be seen in general is a better behavior of the new model especially in cases at high pressures (except for Petersen at 260 atm, Figure 5.9c), this can be justified with the introduction of PLOG expression for pressure dependent reactions, that results in an improved representation of experimental data when pressure dependence is studied.

However, not in every case analyzed the solution proposed by the new model is better if compared to Aramco mech 2.0, this is actually reasonable, since that model is "well-trained", i.e. validated and tested on a large scale of experiments, therefore it can provide very accurate results, even though it doesn't rely on accurate theoretical bases.

Furthermore, new model still needs some work, first of all in completing the revision for missing reactions; in addition to this, some reactions, as already seen in Chapter 4, show a lack of trustable data, so, if new works on microscopical experiments will be published, it would improve the accuracy of the optimization step, also more investigation on different bath gases would be helpful for the completeness of the model.

6. Conclusions and future developments

Summarizing, this work proposes a method to define a state of the art model for hydrogen oxidation kinetics starting from theoretical bases and reconciling experimental data in an optimization routine.

All the available data have been collected, even though in this step a very evident inhomogeneity in data distribution has been outlined, this results in reactions that have a solid and coherent database to rely on, and others that show poor data, this arises some doubts also on their reliability.

Still, some work on the theoretical step has to be done, to determine all the reactions on a theoretical basis, and complete the revision for all the reactions, however, the method for the following steps is already defined.

Then an optimization routine has been performed in OptiSMOKE++, here the reconciliation between theory and experimental data takes place, an optimized model is given as a result, for pressure dependent reactions, written using a PLOG formalism, this step has to be repeated for every bath gas for which both theoretical and experimental inputs are provided.

Lastly, from the results obtained with optimization step, the new model is built (based on Aramco mech 2.0), and this has been compared with Aramco mech 2.0 on a large database on ideal reactors, some interesting results are outlined, i.e. PLOG formalism introduces a better agreement in medium-high pressure cases.

As previously said, this model can still be improved, deepening both theoretical and experimental knowledge on each elementary reaction, in this way a fully validated state of the art model can be achieved.

Some future development can arise from this work, first of all this new model can be used in simulations for the design of new facilities working with hydrogen as a fuel, furthermore, the same method used in this work can be applied also on kinetic modeling on bigger molecules, to improve the effectiveness of these models and give better previsions in efficiency or in determination of pollutant emissions (CO,CO2 or soot formation).

Bibliography

[1] https://climate.nasa.gov/

[2] Alexander Mahler, The colors of hydrogen, International PtX Hub Berlin, 2021

[3] J. Dwyer, J.G. Hansel, T. Phillips, Temperature influence on the flammability limits of heat treating atmospheres, Semantic scholar, 2003

[4] Wenguo Liu, Haibin Zuo, Jingsong Wang, Qingguo Xue, Binglang Ren, Fan Yang, The production and application of hydrogen in steel industry, international journal of hydrogen energy, 2021, volume 46, pp. 10548-10569

[5] https://www.airbus.com/en/innovation/zero-emission/hydrogen/zeroe

[6] Stephen J. Klippenstein, Carlo Cavallotti, Ab initio kinetics for pyrolysis and combustion systems, Computer Aided Chemical Engineering, 2019, Volume 49, pp 115-167.

[7] Magnus Fürst, Andrea Bertolino, Alberto Cuoci, Tiziano Faravelli, Alessio Frassoldati, and Alessandro Parente. Optismoke++: A toolbox for optimization of chemical kinetic mechanisms. Computer Physics Communications, 264:107940, 2021.

[8] Alberto Cuoci, Alessio Frassoldati, Tiziano Faravelli, Eliseo Ranzi, OpenSMOKE++: An object-oriented framework for the numerical modeling of reactive systems with detailed kinetic mechanisms, Computer Physics Communications, 2015. 192: p. 237-264.

[9] International Journal of Chemical Kinetics 45.10 (2013): 638-675.

[10] Brian M Adams, W J TBohnhoff, K R Dalbey, J P Eddy, M S Eldred, D M Gay, K Haskell, Patricia D Hough, and Laura P Swiler. DAKOTA, a multilevel parallel object-oriented framework for design optimization, parameter estimation, uncertainty quantification, and sensitivity analysis: version 5.0 user's manual. Sandia National Laboratories, Tech. Rep. SAND2010-2183, 2009.

[11] Lionel Elliott, Derek B. Ingham, Adrian G. Kyne, Nicolae S. Mera, Mohamed Pourkashanian, and Christopher W. Wilson. Multiobjective genetic algorithm optimization for calculating the reaction rate coefficients for hydrogen

combustion. Industrial and Engineering Chemistry Research, 42(6):1215– 1224, 2003

[12] Steiner, W., The recombination of hydrogen atoms, Trans. Faraday Soc., Volume 35, pp 623-636, 1935

[13] Cooley, S.D.; Anderson, R.C., Flame propagation studies using the hydrogen-bromine reaction, J. Ind. Eng. Chem., Volume 44, 1952

[14] Ge, Y.B.; Gordon, M.S.; Battaglia, F.; Fox, R.O., Theoretical Study of the Pyrolysis of Methyltrichlorosilane in the Gas Phase. 3. Reaction Rate Constant Calculations, J. Phys. Chem. A, Volume 114, pp 2384 – 2392, 2010

[15] Bulewicz, E.M.; Sugden, T.M., The recombination of hydrogen atoms and hydroxyl radicals in hydrogen flame gases, Trans. Faraday Soc., Volume 54, pp 1855 – 1860, 1958

[16] Padley, P.J.; Sugden, T.M., Photometric investigations of alkali metals in hydrogen flame gases. IV. Thermal and chemiluminescent effects produced by free radicals, Proc. R. Soc. London A, Volume 248, pp 248 – 265, 1958

[17] Avramenko, L.I.; Kolesnikova, R.V., The determination of the rate constants of the simple reactions of hydrogen atoms, Bull. Acad. Sci. USSR Div. Chem. Sci. (Engl. Transl.), pp 1839 – 1843, 1961

[18] Dixon, G.; Sutton, M.M.; Williams, A., The kinetics of hydrogen atom recombination, Discuss. Faraday Soc., Volume 33, 1962

[19] Marshall, T.C., Studies of atomic recombination of nitrogen, hydrogen, and oxygen by paramagnetic resonance, Phys. Fluids, Volume 5, pp 743 – 753, 1962

[20] Patch, R.W., Shock-tube measurement of dissociation rates of hydrogen, J. Chem. Phys., Volume 36, pp 1919 – 1924, 1962

[21] Rink, J.P., Shock tube determination of dissociation rates of hydrogen, J. Chem. Phys., Volume 36, pp 262 – 265, 1962

[22] Kretschmer, C.B.; Petersen, H.L., Kinetics of three-body atom recombination, J. Chem. Phys., Volume 39, pp 1772 – 1778, 1963

[23] Larkin, F.S.; Thrush, B.A., Recombination of hydrogen atoms in the presence of atmospheric gases, Discuss. Faraday Soc., Volume 37, pp 112 – 117, 1964

[24] Rosenfeld, J.L.J.; Sugden, T.M., Burning velocity and free radical recombination rates in low temperature hydrogen flames. II. Rate constants for recombination reactions, Combust. Flame, Volume 8, pp 44-50, 1964

[25] Schott, G.L.; Bird, P.F., Kinetic studies of hydroxyl radicals in shock waves. IV. Recombination rates in rich hydrogen-oxygen mixtures, J. Chem. Phys., Volume 41, pp 2869 – 2876, 1964

[26] T. A. Jacobs, R. R. Giedt, and Norman Cohen, Kinetics of Decomposition of HF in Shock Waves, J. Chem. Phys, Volume 43, 1965

[27] Larkin, F.S.; Thrush, B.A., The kinetics of hydrogen-atom recombination, Symp. Int. Combust. Proc., Volume 10, pp 397-402, 1965

[28] Jacobs, T.A.; Giedt, R.R.; Cohen, N, Kinetics of hydrogen halides in shock waves. II. A new measurement of the hydrogen dissociation rate, J. Chem. Phys., Volume 47, pp 54-57, 1967

[29] Azatyan, V.V.; Romanovich, L.B.; Filippov, S.B., Study of the kinetics of the recombination of atomic hydrogen by the EPR method, Kinet. Catal., Volume 9, pp 986-987, 1968

[30] Bennett, J.E.; Blackmore, D.R., Masurement by electron spin resonance of the decay of hydrogen atoms in flow systems at high pressures, J. Chem. Soc. Chem. Commun., pp 1521 – 1522, 1968

[31] Myerson, A.L.; Watt, W.S., Atom-formation rates behind shock waves in hydrogen and the effect of added oxygen, J. Chem. Phys., Volume 49, 1968

[32] Eberius, H.; Hoyermann, K.; Wagner, H.Gg., Zur reaktion H + H + H2O →H2 + H2O, Ber. Bunsenges. Phys. Chem., Volume 73, 1969

[33] Getzinger, R.W.; Blair, L.S., Recombination in the hydrogen-oxygen reaction: a shock tube study with nitrogen and water vapour as third bodies, Combust. Flame, Volume 13, pp 271-284, 1969

[34] Halstead, C.J.; Jenkins, D.R., Radical recombination in rich premixed hydrogen/oxygen flames, Symp. Int. Combust. Proc., Volume 12, pp 979-987, 1969

[35] Hurle, I.R.; Jones, A.; Rosenfeld, J.L.J., Shock-wave observations of rate constants for atomic hydrogen recombination from 2500 to 7000 °K: collisional stabilization by exchange of hydrogen atoms, Proc. R. Soc. London A, Volume 310, pp 253-276, 1969

[36] Bennett, J.E.; Blackmore, D.R., Gas-phase recombination rates of hydrogen and deuterium atoms, J. Chem. Phys., Volume 53, pp 4400-4401, 1970

[37] Dixon-Lewis, G, Flame structure and flame reaction kinetics. V. Investigation of reaction mechanism in a rich hydrogen+nitrogen+oxygen flame by solution of conservation equations, Proc. R. Soc. London A, Volume 317, pp 235-263, 1970

[38] Halstead, C.J.; Jenkins, D.R., Rates of H + H + M → H2 + M and H + OH + M → H2O + M reactions in flames, Combust. Flame, Volume 14, pp 321-324, 1970

[39] Ham, D.O.; Trainor, D.W.; Kaufman, F., Letters to the Editor: Gas phase kinetics of H+H+H2→2H2, J. Chem. Phys., Volume 53, pp 4395-4396, 1970

[40] Bennett, J.E.; Blackmore, D.R., Rates of Gas-Phase Hydrogen-Atom Recombination at Room Temperature in the Presence of Added Gases, Symp. Int. Combust. Proc., Volume 13, 1971

[41] Gay, A.; Pratt, N.H., Hydrogen-Oxygen Recombination Measurements in a Shock Tube Steady Expansion, Proc. Int. Symp. Shock Tubes Waves, Volume 8, 1971

[42] Azatyan, V.V.; Borodulin, R.R.; Intezarova, E.I., Kinetics of Recombination of Atomic Hydrogen and Deuterium, Dokl. Phys. Chem. (Engl. Transl.), Volume 213, 1973

[43] W. D. Breshears and P. F. Bird, Precise Measurements of Diatomic Dissociation Rates in Shock Waves*, 1973

[44] Teng, L.; Winkler, C.A., The Rate of Recombination of H Atoms in the Presence of NH3, Can. J. Chem., Volume 51, 1973

[45] Trainor, D.W.; Ham, D.O.; Kaufman, F., Gas Phase Recombination of Hydrogen and Deuterium Atoms, J. Chem. Phys., Volume 58, 1973

[46] Mallard, W.G.; Owen, J.H., Rate Constant for H + H + Ar = H2 + Ar from 1300 to 1700K, Int. J. Chem. Kinet., Volume 6, 1974

[47] Walkauskas, L.P.; Kaufman, F., Gas Phase Hydrogen Atom Recombination, Symp. Int. Combust. Proc., Volume 15, 1975

[48] Lynch, K.P.; Schwab, T.C.; Michael, J.V., Lyman-α Absorption Photometry at High Pressure and Atom Density Kinetic Results for H Recombination, Int. J. Chem. Kinet., Volume 8, 1976

[49] Mitchell, D.N.; Le Roy, D.J., An Experimental Test of the Orbiting Resonance Theory of Hydrogen Atom Recombination at Room Temperature, J. Chem. Phys., Volume 67, 1977

[50] Hong Du and Jan P. Hessler, Rate coefficient for the reaction H+O2→OH+O: Results at high temperatures, 2000 to 5300 K, J. Chem. Phys., Volume 96, 1992

[51] Kenji Maeda, Hyperfine structure of the hydroxyl free radical (OH) in electric and magnetic fields, New Journal of Physics 17, 2015, https://iopscience.iop.org/article/10.1088/1367-2630/17/4/045014/ampdf

[52] Y. Hldaka, S. Takaharhl, H. Kawano, M. Suga, W. C. Gardiner, Jr., Shock-Tube Measurement of the Rate Constant for Excited OH(A2z+) Formation in the Hydrogen-Oxygen Reaction, J. Phys. Chem., Volume 86, pp 1429-1433, 1982

[53] Tohru Koike, Kihei Morinaga, Further studies of the Rate Constant for Chemical Excitation of OH in shock waves, Bull. Chem. Soc. Jpn., 55, pp 52-54, 1982

[54] VALÉRIE NAUDET, SANDRA JAVOY & CLAUDE-ETIENNE PAILLARD (2001) A High Temperature Chemical Kinetics Study of the Reaction: OH+Ar = H+O+Ar by Atomic Resonance Absorption Spectrophotometry, COMBUSTION SCIENCE AND TECHNOLOGY, 164:1, 113-128, DOI: 10.1080/00102200108952164, 2001

[55] Javoy, S.; Naudet, V.; Abid, S.; Paillard, C.E., Elementary reaction kinetics studies of interest in H2 supersonic combustion chemistry, Expt. Thermal Fluid Sci., Volume 27, pp 371-377, 2003

[56] Joel M. Hall, Eric L. Petersen, An Optimized Kinetics Model for OH Chemiluminescence at High Temperatures and Atmospheric Pressures, Wiley InterScience (www.interscience.wiley.com), 2005

[57] Kathrotia, T.; Fikri, M.; Bozkurt, M.; Hartmann, M.; Riedel, U.; Schulz, C., Study of the H plus O plus M reaction forming OH *: Kinetics of OH * chemiluminescence in hydrogen combustion systems, Combust. Flame, Volume 157, pp 1261-1273, 2010

[58] Sellevag, S.R.; Georgievskii, Y.; Miller, J.A., The temperature and pressure dependence of the reactions H+O2(+M)-> HO2(+M) and H+OH(+M)-> H2O(+M), J. Phys. Chem. A, Volume 112, pp 5085-5095, 2008

[59] N. Balakrishnan, Quantum calculations of the O (3P)+ H2 --> OH+ OH reaction, The Journal of Chemical Physics, Volume 121, 2004

[60] J. Troe, Predictive Possibilities of Unimolecular Rate Theory, The Journal of Physical Chemistry, Volume 83, 1979

[61] Oldenberg, O.; Rieke, F.F., Kinetics of OH radicals as determined by their absorption spectrum. V. A spectroscopic determination of a rate constant, J. Chem. Phys., Volume 7, pp 485-492, 1939

[62] Black, G.; Porter, G., Vacuum ultra-violet flash photolysis of water vapour, Proc. R. Soc. London A, Volume 266, pp 185-197, 1961

[63] Dixon, G.; Sutton, M.M.; Williams, A., The kinetics of hydrogen atom recombination, Discuss. Faraday Soc., Volume 33, 1962

[64] Rosenfeld, J.L.J.; Sugden, T.M., Burning velocity and free radical recombination rates in low temperature hydrogen flames. II. Rate constants for recombination reactions, Combust. Flame, Volume 8, pp 44-50, 1964

[65] Schott, G.L.; Bird, P.F., Kinetic studies of hydroxyl radicals in shock waves. IV. Recombination rates in rich hydrogen-oxygen mixtures, J. Chem. Phys., Volume 41, pp 2869-2876, 1964

[66] Getzinger, R.W., A shock-wave study of recombination in near-stoichiometric hydrogen-oxygen mixtures, Symp. Int. Combust. Proc., Volume 11, pp 117-124, 1967

[67] Homer, J.B.; Hurle, I.R., The dissociation of water vapour behind shock waves, Proc. R. Soc. London A, Volume 314, pp 585-598, 1970

[68] Friswell, N.J.; Sutton, M.M., Radical Recombination Reactions in H2/O2/N2 Flames: Participation of the HO2 Radical, Chem. Phys. Lett., Volume 15, 1972

[69] Davis, M.G.; McGregor, W.K.; Mason, A.A., OH Chemiluminescent Radiation from Lean Hydrogen-Oxygen Flames, J. Chem. Phys., Volume 61, 1974

[70] Zellner, R.; Erler, K.; Field, D., Kinetics of the Recombination Reaction OH + H + M H2O + M at Low Temperatures, Symp. Int. Combust. Proc., Volume 16, 1977

[71] Goodings, J.M.; Hayhurst, A.N., Heat release and radical recombination in premixed fuel-lean flames of H2 + O2 + N2. Rate constants for H + OH + M → H2O + M and HO2 + OH → H2O + O2, J. Chem. Soc. Faraday Trans. 2, Volume 84, 1988

[72] N.K. Srinivasan, J.V. Michael, The Thermal Decomposition of Water, Wiley InterScience (www.interscience.wiley.com), 2006

[73] Jiankun Shao, Rishav Choudhary, David F. Davidson, Ronald K. Hanson, Samuel Barak, Subith Vasu, Ignition delay times of methane and hydrogen highly diluted in carbon dioxide at high pressures up to 300 atm, Proceedings of the Combustion Institute, 37, 4555-4562, 2019

[74] Shixing Wang, Zhihua Wang, Yong He, Xinlu Han, Zhiwei Sun, Yanqun Zhu, Mario Costa, Laminar burning velocities of Ch4/O2/N2 and oxygen-enriched CH4/O2/CO2 flames at elevated pressures measured using the heat flux method, Fuel, 259, 2020

[75] Matthews, D.L., Interferometric measurement in the shock tube of the dissociation rate of oxygen, Phys. Fluids, Volume 2, pp 170 – 178, 1959

[76] Kretschmer, C.B.; Petersen, H.L., Recombination kinetics of atomic oxygen at room temperature, J. Chem. Phys., Volume 33, pp 948-949, 1960

[77] Morgan, J.E.; Elias, L.; Schiff, H.I., Recombination of oxygen atoms in the absence of O2, J. Chem. Phys., Volume 33, pp 930-931, 1960

[78] Reeves, R.R.; Mannella, G.; Harteck, P., Rate of recombination of oxygen atoms, J. Chem. Phys., Volume 32, pp 632-633, 1960

[79] Rink, J.P.; Knight, H.T.; Duff, R.E., Shock tube determination of dissociation rates of oxygen, J. Chem. Phys., Volume 34, pp 1942 – 1947, 1961

[80] Wray, K.L., Shock-tube study of the recombination of O atoms by Ar catalysts at high temperatures, J. Chem. Phys., Volume 38, pp 1518-1524, 1963

[81] Wray, K.L., Kinetics of O2 dissociation and recombination, Symp. Int. Combust. Proc., Volume 10, pp 523-537,1965

[82] Kiefer, J.H.; Lutz, R.W., Recombination of oxygen atoms at high temperatures as measured by shock-tube densitometry, J. Chem. Phys., Volume 42, pp 1709-1714, 1965

[83] Kondratiev, V.N.; Nikitin, E.E., Letters to the Editor: Rate constants for the process O2+Ar=O+O+Ar, J. Chem. Phys., Volume 45, pp 1078-1079, 1966

[84] Campbell, I.M.; Thrush, B.A., The association of oxygen atoms and their combination with nitrogen atoms, Proc. R. Soc. London, Volume 296, pp 222-232, 1967

[85] Campbell, I.M.; Thrush, B.A., Reactivity of hydrogen to atomic nitrogen and atomic oxygen, Trans. Faraday Soc., Volume 64, 1968

[86] Campbell, I.M.; Gray, C.N., Rate Constants for O(3P) Recombination and Association with N(4S), Chem. Phys. Lett., Volume 18, 1973

[87] C.J. Cobos, H. Hippler, J. Troe, High-Pressure Falloff Curves and Specific Rate Constants for the Reactions H+O2 ⇌ HO2⇌ HO+O, J. Phys. Chem., Volume 89, pp 342-349, 1985

[88] C.J. Cobos, J. Troe, Theory of thermal unimolecular reactions at high pressures. II. Analysis of experimental results, The Journal of Chemical Physics, 83, 1010, 1985

[89] C.J. Cobos, Statistical adiabatic channel model study of the H+O2→ HO2 reaction on the Lemon and Hase Potential Energy Surface, Chemical Physics letters, Volume 152, 1988

[90] V.J. Barclay, Christopher E. Dateo, I.P. Hamilton, Brian Kendrick, Russel T. Pack, David W. Schwenke, Anomalous symmetries of the rovibrational states of HO2: Consequences on a conical intersection, J. Chem. Phys., 103, 1995

[91] Abigail J. Dobbyn, Michael Stumpf, Hans-Martin Keller, William L. Hase, and Reinhard Schinke, Quantum mechanical study of the unimolecular dissociation of HO2: A rigorous test of RRKM theory, J. Chem. Phys. 102, 1995

[92] Brian Kendrick, Russell T Pack, Recombination resonances in thermal H + 0 2 scattering, Chemical Physics Letters, 235, 291-296, 1995

[93] Ronald J. Duchovic, J. David Pettigrew, Beth Welling, and Taha Shipchandler, Conventional transition state theory/Rice–Ramsperger–Kassel–Marcus theory calculations of thermal termolecular rate coefficients for H(D)+O2+M, The Journal of Chemical Physics, 105, 1996

[94] Brian Kendrick, and Russell T Pack, Geometric phase effects in H+O2 scattering. I. Surface function solutions in the presence of a conical intersection, J. Chem. Phys., 104, 1996

[95] Brian Kendrick, and Russell T Pack, Geometric phase effects in H+O2 scattering. II. Recombination resonances and stateto-state transition probabilities at thermal energies, J. Chem. Phys., 104, 1996

[96] Vladimir A. Mandelshtam, Howard S. Taylor, and William H. Miller, Collisional recombination reaction H+O2+M→HO2+M: Quantum mechanical study using filter diagonalization, J. Chem. Phys., 105, 1996

[97] Timothy C. Germann and William H. Miller, Quantum Mechanical Pressure-Dependent Reaction and Recombination Rates for O + OH f H + O2, HO2, J. Phys. Chem. A 1997, 101, 6358-6367

[98] Brian Kendrick, and Russell T Pack, Geometric phase effects in the resonance spectrum, state-to-state transition probabilities and bound state spectrum of HO2, J. Chem. Phys. 106, 1997

[99] Kihyung Song† and William L. Hase, Role of State Specificity in the Temperature- and Pressure-Dependent Unimolecular Rate Constants for HO2 f H + O2 Dissociation, J. Phys. Chem. A 1998, 102, 1292-1296

[100] Ulrich Himmer and Emil Roduner, The addition reaction of X to (X O = Mu, H, D) : isotope effects in 2 intra- and intermolecular energy transfer, Phys. Chem. Chem. Phys., 2000, 2, 339-347

[101] L. B. Harding, A. I. Maergoiz, J. Troe, and V. G. Ushakov, Statistical rate theory for the reaction system: SACM/CT calculations between 0 and 5000 K, J. Chem. Phys. 113, 2000

[102] L. B. Harding, J. Troe and V. G. Ushakov, Classical trajectory calculations of the high pressure limiting rate constants and of specific rate constants for the reaction H + O dynamic isotope effects between tritium + O2 and muonium + O2, Phys. Chem. Chem. Phys., 2000, 2, 631-642

[103] JURGEN TROE, DETAILED MODELING OF THE TEMPERATURE AND PRESSURE DEPENDENCE OF THE REACTION H + O2 (+M) → HO2 (+M), Proceedings of the Combustion Institute, Volume 28, 2000/pp. 1463–1469

[104] J. M. C. Marques and A. J. C. Varandas, On the high pressure rate constants for the addition H/Mu+ O2 reactions, Phys. Chem. Chem. Phys., 2001, 3, 505-507

[105] J. M. C. Marques and A. J. C. Varandas, Reply to the "Comment on ""On the high pressure rate constants for the addition reactionsÏÏÏ by L. B. Harding, J. Troe and H/Mu + O2 V. G. Ushakov, Phys. Chem. Chem. Phys., 2001, 3, 2630, Phys. Chem. Chem. Phys., 2001, 3, 2632È2633

[106] Heshel Teitelbaum, Pedro J. S. B. Caridade, and António J. C. Varandas, Calculation of the rate constant for state-selected recombination of H+O2(v) as a function of temperature and pressure, The Journal of Chemical Physics 120, 10483 (2004)

[107] Shi Ying Lin, Edward J. Rackham, and Hua Guo, Quantum Mechanical Rate Constants for H + O2 →O + OH and H + O2 →HO2 Reactions, J. Phys. Chem. A 2006, 110, 1534-1540

[108] J. Troe, and V. G. Ushakov, A Simple Method Relating Specific Rate Constants k(E,J) and Thermally Averaged Rate Constants k∞(T) of Unimolecular Bond Fission and the Reverse Barrierless Association Reactions, J. Phys. Chem. A 2006, 110, 6732-6741

[109] J. Troe, and V. G. Ushakov, Quantum capture, adiabatic channel, and classical trajectory study of the high pressure rate constant of the reaction between 0 and 5000 K, The Journal of Chemical Physics 128, 204307 (2008)

[110] Jamin W. Perry, Richard Dawes, Albert F. Wagner, and Donald L. Thompson, A classical trajectory study of the intramolecular dynamics, isomerization, and unimolecular dissociation of HO2, J. Chem. Phys. 139, 084319 (2013)

[111] Lawrence B. Harding • Stephen J. Klippenstein • Hans Lischka • Ron Shepard, Comparison of multireference configuration interaction potential energy surfaces for H + O2 →HO2: the effect of internal contraction, Theor Chem Acc (2014) 133:1429

[112] R. w. GETZINGER AND G. L. SCHOTT, Kinetic Studies of Hydroxyl Radicals in Shock Waves. V. Recombination via the H +02 +M~H02 +M Reaction in Lean Hydrogen-Oxygen Mixtures, THE JOURNAL OF CHEMICAL PHYSICS VOLUME 43, NUMBER 9, 1965

[113] David Gutman, Edward A. Hardwidge, Frank A. Dougherty, and Robert W. Lutz, ShockTube Study of the Recombination Rate of Hydrogen Atoms with Oxygen Molecules, The Journal of Chemical Physics, 47, 1967

[114] W. P. Bishop, and Leon M. Dorfman, Pulse Radiolysis Studies. XVI. Kinetics of the Reaction of Gaseous Hydrogen Atoms with Molecular Oxygen by Fast Lyman-α Absorption Spectrophotometry, The Journal of Chemical Physics, 52, 1970

[115] L. S. Blair and R. W. Getzinger, A Shock Tube Study of Recombination in the Hydrogen-Oxygen Reaction Using Infrared Emiission from Water Vapor, Combustion and Flame, 5, 1970

[116] T. Hikida, J. A. Eyre, and Leon M. Dorfman, Pulse Radiolysis Studies. XX. Kinetics of Some Addition Reactions of Gaseous Hydrogen Atoms by Fast Lyman-α Absorption Spectrophotometry, The Journal of Chemical Physics, 54, 1971

[117] Michael J. Kurylo, Absolute Rate Constants for the Reaction + 02 + M — H02 + M over the Temperature Range 203-404 K, The Journal of Physical Chemistry, Vol. 78, No. 84, 1972

[118] J. J. Ahumada, J. V. Michael, and D. T. Osborne, Pressure Dependence and Third Body Effects on the Rate Constants for H+O2, H+NO, and H+CO, The Journal of Chemical Physics, 57, 3736, 1972

[119] A. A. Westenberg* and N. deHaas, Steady-State Intermediate Concentrations and Rate Constants. Some H02 Results, The Journal of Physical Chemistry, Vol. 76, No. 11, 1972

[120] Peeters, J.; Mahnen, G., Reaction Mechanisms and Rate Constants of Elementary Steps in Methane-Oxygen Flames, Symp. Int. Combust. Proc., vol. 14, 1973

[121] Wong, W.; Davis, D.D., A Flash Photolysis-Resonance Fluorescence Study of the Reaction of Atomic Hydrogen with Molecular Oxygen H + O2 + M → HO2 + M, Int. J. Chem. Kinet., vol 6, 1974

[122] Hack W., Hoyermann K., Wagner H. Gg., Ueber einige Radikalreaktionen im H-O-N-System, Z. Naturforsh. A, 29, 1974

[123] M. W. SLACK, Rate Coefficient for H + 02 + M = HO 2 + M Evaluated from Shock Tube Measurements of Induction Times, COMBUSTION AND FLAME 28,241-249 1977

[124] Campbell, I.M.; Rogerson, J.S.; Handy, B.J., Studies of Reactions of Atoms in a Discharge Flow Stirred Reactor Part 3. - The O + H2 + O2 System, J. Chem. Soc. Faraday Trans. 1, Vol 74, 1978

[125] Ishikawa, Y.; Sugawara, K.; Sato, S., The Rate Constants for H and D-Atom Additions to O2, NO, Acetylene, and 1,3-Butadiene, Bull. Chem. Soc. Jpn., Volume 52, 1979

[126] Nielsen, O.J.; Sillesen, A.; Luther, K.; Troe, J., H atom yields in the pulse radiolysis of H2: Reactions with O2, ClNO, and HI, J. Phys. Chem., Volume 86, 1982

[127] Pamidimukkala, K.R.; Skinner, G.B., Resonance Absorption Measurements of Atom Concentrations in Reacting Gas Mixtures. 9. Measurements of O Atoms in Oxidationof H2 and D2, Proc. Int. Symp. Shock Tubes Waves, volume 13, 1982

[128] Pratt, G.L.; Wood, S.W., Stoichiometry and rate of reaction of hydrogen atoms with oxygen, J. Chem. Soc. Faraday Trans. 1, Volume 79, 1983

[129] Horowitz, A., Photooxidation of formaldehyde in oxygen-lean atmospheres, J. Phys. Chem., Volume 88, 1984

[130] Borrell, P.; Cobos, C.J.; Croce de Cobos, A.E.; Hippler, H.; Luther, K.; Ravishankara, A.R.; Troe, J., Radical association reactions in gases at high pressures, Ber. Bunsenges. Phys. Chem., Volume 89, 1985

[131] C. J. Cobos, H. Hippier, and J. Troe, High-Pressure Falloff Curves and Specific Rate Constants for the Reactions H+O2 ⇌ HO2⇌ HO+O, J. Phys. Chem. 1985, 89, 342-349

[132] Abraham Horowitz, Photolytlc and Dark Reactions in Gaseous Mixtures of CH20, 02, and MeOH at 373 K, J. Phys. Chem., 1985, 89, 1764-1766

[133] Hsu, K.-J.; Durant, J.L.; Kaufman, F., Rate constants for H + O2 + M at 298 K for M = He, N2, and H2O, J. Phys. Chem., vol 91, 1987

[134] K.-J. Hsu, S. M. Anderson, J. L. Durant, and F. Kaufman, Rate Constants for + 02 + M from 298 to 639 K for M = He, N2, and H20, J. Phys. Chem. 1989, 93, 1018-1021

[135] Pirraglia, A.N.; Michael, J.V.; Sutherland, J.W.; Klemm, R.B., A flash photolysis-shock tube kinetic study of the H atom reaction with O2: H + O2 = OH + O (962 K T 1705 K) and H + O2 + Ar →HO2 + Ar (746 K T 987 K), J. Phys. Chem., vol 93, 1989

[136] Mark A. Hanning-Lee, Michael J. Pilling' and Jonathan F. Warr, Time-resolved Study of Hydrogen Atoms in the H,-0, System under Conditions close to Criticality, J. CHEM. SOC. FARADAY TRANS., 1991, 87(18), 2907-2912

[137] Carleton, K.L.; Kessler, W.J.; Marinelli, W.J., H + O2 + M (=N2, H2O, Ar) three-body rate coefficients at 298-750 K, J. Phys. Chem., vol. 97, 6412 – 6417, 1993

[138] J.H. BROMLY and F. J. BARNES, P.F. NELSON , B.S. HAYNES, Kinetics and Modeling of the H2-O2-NOx System, International Journal of Chemical Kinetics, Vol. 27, 1165- 1178, 1995

[139] Davidson, D.F.; Petersen, E.L.; Rohrig, M.; Hanson, R.K.; Bowman, C.T., Measurement of the rate coefficient of H + O2 + M →' HO2 + M for M = Ar and N2 at high pressures, Symp. Int. Combust. Proc., Volume 26, 481-488, 1996

[140] Ronald J. Duchovic, J. David Pettigrew, Beth Welling, and Taha Shipchandler, Conventional transition state theory/Rice–Ramsperger–Kassel–Marcus theory calculations of thermal termolecular rate coefficients for H(D)+O2+M, J. Chem. Phys. 105 (23), 15 December 1996

[141] PETER J. ASHMAN and BRIAN S. HAYNES, RATE COEFFICIENT OF H ~ O2 ~ M → HO2 ~ M (M $ H2O, N2, Ar, CO2), Twenty-Seventh Symposium (International) on Combustion/The Combustion Institute, 1998/pp. 185–191

[142] MARK A. MUELLER, RICHARD A. YETTER, and FREDERICK L. DRYER, MEASUREMENT OF THE RATE CONSTANT FOR H ~ O2 ~ M → HO2 ~ M (M $ N2, Ar) USING KINETIC MODELING OF THE HIGH-PRESSURE H2/O2/NOx REACTION, Twenty-Seventh Symposium (International) on Combustion/The Combustion Institute, 1998/pp. 177–184

[143] Ronald W. Bates, David M. Golden, Ronald K. Hanson and Craig T. Bowman, Experimental study and modeling of the reaction H + O2+ M→ HO2

+M(M=Ar,N2,H2O), at elevated pressures and temperatures between 1050 and 1250 K., Phys. Chem. Chem. Phys., 2001, 3, 2337-2342

[144] J. V. Michael, M.-C. Su, J. W. Sutherland, J. J. Carroll, and A. F. Wagner, Rate Constants For H + O2 + M f HO2 + M in Seven Bath Gases, J. Phys. Chem. A 2002, 106, 5297-5313

[145] Hahn, J.; Krasnoperov, L.; Luther, K.; Troe, J., Pressure dependence of the reaction H+O2 (+Ar) -> HO2 (+Ar) in the range 1-900 bar and 300-700 K, Phys. Chem. Chem. Phys., vol 6, 1997 – 1999, 2004

[146] S.M. Hwang, Si-Ok Ryu, K.J. De Witt, M.J. Rabinowitz, High temperature rate coefficient measurements of H + O2 chain-branching and chain-terminating reaction, Chemical Physics Letters 408 (2005) 107–111

[147] R. X. Fernandes, K. Luther, J. Troe and V. G. Ushakov, Experimental and modelling study of the recombination reaction H+O2 (+M) - HO2 (+M) between 300 and 900 K, 1.5 and 950 bar, and in the bath gases M = He, Ar, and N2, Phys. Chem. Chem. Phys., 2008, 10, 4313–4321

[148] John D. Mertens, Danielle M. Kalitan, Alexander B. Barrett, Eric L. Petersen, Determination of the rate of H + O2 + M →HO2 + M (M = N2, Ar, H2O) from ignition of syngas at practical conditions, Proceedings of the Combustion Institute 32 (2009) 295–303

[149] G.A. Pang, D.F. Davidson, R.K. Hanson, Experimental study and modeling of shock tube ignition delay times for hydrogen–oxygen–argon mixtures at low temperatures, Proceedings of the Combustion Institute 32 (2009) 181–188

[150] Subith S. Vasu, David F. Davidson, and Ronald K. Hanson, Shock Tube Study of Syngas Ignition in Rich CO2 Mixtures and Determination of the Rate of H+O2+CO2→ HO2 +CO2, Energy Fuels 2011, 25, 990–997

[151] Jiankun Shao, Rishav Choudhary, Adam Susa, David F. Davidson, Ronald K. Hanson, Shock tube study of the rate constants for H + O2+ M→HO2+ M (M = Ar, H2O, CO2, N2) at elevated pressures, Proceedings of the Combustion Institute 000 (2018) 1–8

[152] Rishav Choudhary, Julian J. Girard, Yuzhe Peng, Jiankun Shao, David F. Davidson, Ronald K. Hanson, Measurement of the reaction rate of H + O2 + M→HO2

+ M, for M= Ar, N2, CO2, at high temperature with a sensitive OH absorption diagnostic, Combustion and Flame 203 (2019) 265-278

[153] S. Voss, S. Hartl, C. Hasse, Determination of laminar burning velocities for lean low calorific H2/N2 and H2/CO/N2 gas mixtures. International journal of hydrogen energy 39, 2014, pp.19810-19817.

[154] J. Troe and V. G. Ushakov, SACM/CT Study of the dissociation/recombination dynamics of hydrogen peroxide on an ab initio potential energy surface Part II. Specific rate constants k(E,J), thermal rate constants kN(T), and lifetime distributions, Phys. Chem. Chem. Phys., 2008, 10, 3915–3924

[155] Stig R. Sellevåg, Yuri Georgievskii, and James A. Miller, Kinetics of the Gas-Phase Recombination Reaction of Hydroxyl Radicals to Form Hydrogen Peroxide, J. Phys. Chem. A 2009, 113, 4457–4467

[156] J. Troe, The thermal dissociation/recombination reaction of hydrogen peroxide H2O2+M <-> 2OH+M III. Analysis and representation of the temperature and pressure dependence over wide ranges

[157] Michael P. Burke, Stephen J. Klippenstein, Lawrence B. Harding, A quantitative explanation for the apparent anomalous temperature dependence of OH + HO2 = H2O+O2 through multi-scale modelling, Proceedings of the Combustion Institute 34 (2013) 547–555

[158] R. Zellner, F. Ewig, R. Paschke, and G. Wagner, Pressure and Temperature Dependence of the Gas-Phase Recombination of Hydroxyl Radicals, J. Phys. Chem. 1988, 92, 4184-4190

[159] Ch. Kappel, K. Luther and J. Troe, Shock wave study of the unimolecular dissociation of H2O2 in its falloff range and of its secondary reactions, Phys. Chem. Chem. Phys., 2002, 4, 4392–4398

[160] Ireneusz Janik and David M. Bartels, Charles D. Jonah, Hydroxyl Radical Self-Recombination Reaction and Absorption Spectrum in Water Up to 350 °C, J. Phys. Chem. A 2007, 111, 1835-1843

[161] Hong, Z.K.; Farooq, A.; Barbour, E.A.; Davidson, D.F.; Hanson, R.K., Hydrogen Peroxide Decomposition Rate: A Shock Tube Study Using Tunable Laser Absorption of H_2O near 2.5 mu m, J. Phys. Chem. A, 113, 12919-12925, 2009

[162] Hong, Z.K.; Cook, R.D.; Davidson, D.F.; Hanson, R.K., A Shock Tube Study of OH + H_2O_2 -> H_2O + HO_2 and H_2O_2 + M -> 2OH+M using Laser Absorption of H_2O and OH, J. Phys. Chem. A, 114, 5718 – 5727, 2010

[163] Manuvesh Sangwan, Evgeni N. Chesnokov, and Lev N. Krasnoperov, Reaction OH + OH Studied over the 298−834 K Temperature and 1 - 100 bar Pressure Ranges, J. Phys. Chem. A 2012, 116, 6282−6294

[164] M. B. SAJID,ET. ES-SEBBAR, T. JAVED, C. FITTSCHEN, A. FAROOQ, Measurement of the Rate of Hydrogen Peroxide Thermal Decomposition in a Shock Tube Using Quantum Cascade Laser Absorption Near 7.7 μm, International Journal of Chemical Kinetics DOI 10.1002/kin.20827, 2013

[165] A. A. Westenberg and N. deHaas, Steady-State Intermediate Concentrations and Rate Constants. Some H02 Results, The Journal of Physical Chemistry, Vol. 76, No. 11, 1972

[166] ROBERT SHAW, Estimation of Rate Constants as a Function of Temperature for the Reactions W + XYZ = WX + YZ, Where W, X, Y, and Z are H or 0 Atoms, INTERNATIONAL JOURNAL OF CHEMICAL KINETICS, VOL. IX, 929-941 (1977)

[167] A. Boutalib, H. Cardy, C. Chevaldonnet, M. Chaillet, Ab initio study of the two competitive channels HO2+H→H2+O2 and HO2+H→ H2O+O, Chemical Physics, 110 (1986), 295-302

[168] Sergei P. Karkach, and Vladimir I. Osherov, Ab initio analysis of the transition states on the lowest triplet H2O2 potential surface, The Journal of Chemical Physics 110, 11918 (1999)

[169] Michael Filatov, Werner Reckien, Sigrid D. Peyerimhoff, and Sason Shaik, What Are the Reasons for the Kinetic Stability of a Mixture of H2 and O2?, J. Phys. Chem. A 2000, 104, 12014-12020

[170] J. V. MICHAEL, J. W. SUTHERLAND, L. B. HARDING and A. F. WAGNER, INITIATION IN H2/O2: RATE CONSTANTS FOR H2+ O2 → H + HO2 AT HIGH TEMPERATURE, Proceedings of the Combustion Institute, Volume 28, 2000/pp. 1471–1478

[171] Seyed Hosein Mousavipour and Vahid Saheb, Theoretical Study on the Kinetic and Mechanism of H +HO2 Reaction, Bull. Chem. Soc. Jpn. Vol. 80, No. 10, 1901–1913 (2007)

[172] Seyed Hosein Mousavipour and Issa Yousefiasl, Quasi-Classical Trajectory Dynamics Study on the Reaction of H with HO2, Bull. Chem. Soc. Jpn. Vol. 82, No. 8, 953–962 (2009)

[173] Alexander Starik and Alexander Sharipov, Theoretical analysis of reaction kinetics with singlet oxygen molecules, Phys. Chem. Chem. Phys., 2011, 13, 16424–16436

[174] Baldwin, R.R.; Fuller, M.E.; Hillman, J.S.; Jackson, D.; Walker, R.W., Second Limit of Hydrogen + Oxygen Mixtures: the Reaction H + HO2, J. Chem. Soc. Faraday Trans. 1, vol 70, 1974

[175] Sridharan, U.C.; Qiu, L.X.; Kaufman, F., Kinetics and Product Channels of the Reactions of HO2 with O and H Atoms at 296 K, J. Phys. Chem., vol 86, 1982

[176] Keyser, L.F., Absolute rate constant and branching fractions for the H + HO2 reaction from 245 to 300 K, J. Phys. Chem., 90, 1986

[177] Tohru Koike, Shock Tube studies of the H2-O2 Reaction by Atomic Resonance Absorption Spectroscopy, Bull.Chem.Soc.JPn., 62, 2480-2484, 1989

[178] Seyed Hosein Mousavipour and Vahid Saheb, Theoretical Study on the Kinetic and Mechanism of H þ HO2 Reaction, Bull. Chem. Soc. Jpn. Vol. 80, No. 10, 1901–1913 (2007)

[179] Seyed Hosein Mousavipour* and Issa Yousefiasl, Quasi-Classical Trajectory Dynamics Study on the Reaction of H with HO2, Bull. Chem. Soc. Jpn. Vol. 82, No. 8, 953–962 (2009)

[180] Richard Dawes, Phalgun Lolur, Jianyi Ma, Hua Guo, Communication: Highly accurate ozone formation potential and implications for kinetics, The journal of chemical physics, 135, 2011

[181] Mehdi Ayouz, Dimitri Babikov, Global permutationally invariant potential energy surface for ozone forming reaction, The Journal of Chemical Physics, 138, 2013

[182] Richard Dawes, Phalgun Lolur, Anyang Li, Bin Hiang, Hua Guo, Communication: an accurate global potential energy surface for the ground electronic state of ozone, The Journal of Chemical Physics, 139, 2013

[183] OLIVER R. WULF' AND RICHARD C. TOLMAN, THE THERMAL DECOMPOSITION OF OZONE. 111. THE TEMPERATURE COEFFICIENT OF REACTION RATE, CONTRIBUTION FROM THE GATES CHEMICALABORATORY, CALIFORNIA INSTITUTE OF TECHNOLOGY, NO. 137, 1927

[184] Benson, S.W.; Axwworthy, A.E., Jr., Mechanism of the gas phase, thermal decomposition of ozone, J. Chem. Phys., 26, 1718 – 1726, 1957

[185] Kaufman, F., Air afterglow and kinetics of some reactions of atomic oxygen, J. Chem. Phys., 28, 352-353, 1958

[186] Elias, L.; Ogryzlo, E.A.; Schiff, H.I., The study of electrically discharged O2 by means of an isothermal calorimetric detector, Can. J. Chem., 37, 1680-1689, 1959

[187] Zaslowsky, J.A.; Urbach, H.B.; Leighton, F.; Wnuk, R.J.; Wojtowicz, J.A., The kinetics of the homogeneous gas phase thermal decomposition of ozone, J. Am. Chem. Soc., 82, 2682-2686, 1960

[188] D. S. Hacker, S. A. Marshall, and M. Steinberg, Recombination of Atomic Oxygen on Surfaces, The Journal of Chemical Physics 35, 1788 (1961)

[189] Wesley M. Jones and Norman Davidson, The Thermal Decomposition of Ozone in a Shock Tube, CONTRIBUTION FROM THE GATES AND CRELLIN LABORATORIES OF CHEMISTRY, CALIFORNIA INSTITUTE OF TECHSOLOGY, AND THE Los ALAMOS SCIENTIFIC LABORATORY, UNIVERSITY OF CALIFORNIA, Los ALAMOS NEW MEXICO, 1962

[190] Kaufman, F.; Kelso, J.R., Rate constant of the reaction O + 202 → O3 + O2, J. Chem. Phys., 40, 1162-1163, 1964

[191] Clyne, M.A.A.; McKenney, D.J.; Thrush, B.A., Rate of combination of oxygen atoms with oxygen molecules, Trans. Faraday Soc., 61, 2701-2709, 1965

[192] Myran C. Sauer, Jr., and Leon M. Dorfman, Pulse Radiolysis of Gaseous Argon-Oxygen Solutions. Rate Constant for the Ozone Formation Reaction, Journal of !he American Chemica/ Sociefy 1 8737 1 Sepfember 5, 1965

[193] Kaufman, F.; Kelso, J.R., M effect in the gas-phase recombination of O with O2, J. Chem. Phys., 46, 4541-4543, 1967

[194] Mulcahy, M.F.R.; Williams, D.J., Kinetics of combination of oxygen atoms with oxygen molecules, Trans. Faraday Soc., 64, 59-70, 1968

[195] Meaburn, G.M.; Perner, D.; LeCalve, J.; Bourene, M., A pulsed-radiolysis study of atomic oxygen reactions in the gas phase, J. Phys. Chem., 72, 3920-3925, 1968

[196] Donovan, R.J.; Husain, D.; Kirsch, L.J., Reactions of atomic oxygen. Part 1 - The rate of the reaction O+O2+M→O3+M (M = He, Ar and Kr), J. Chem. Soc. Faraday Trans. 1, 66, 2551-2559, 1970

[197] Hippler, H.; Troe, J., Hochdruckbereich der Rekombination O + O2 → O3, Ber. Bunsenges. Phys. Chem., 75, 1971

[198] Slanger, T.G.; Black, G., Reaction rate measurements of O(3P) atoms by resonance fluorescence. I. O(4P)+O2+M→O3+M and O(3P)+NO+M→NO2+M, J. Chem. Phys., 53, 3717-3721, 1970

[199] Stuhl, F.; Niki, H., Measurements of Rate Constants for Termolecular Reactions of O(3P) with NO, O2, CO, N2, and CO2 Using a Pulsed Vacuum-uv Photolysis-Chemiluminescent Method, J. Chem. Phys., 55, 1971

[200] Bevan, P.L.T.; Johnson, G.R.A., Kinetics of Ozone Formation in the Pulse Radiolysis of Oxygen Gas, J. Chem. Soc. Faraday Trans. 1, 69, 1973

[201] Huie, R.E.; Herron, J.T.; Davis, D.D., Absolute Rate Constants for the Reaction O + O2 + M →O3 + M over the Temperature Range 200-346K, J. Phys. Chem., 76, 1972

[202] Ball, M.J.; Larkin, F.S., Determination of the Rates of Atomic Reactions by the Discharge-flow Method, Nature (London) Phys. Sci., 245, 1973

[203] Snelling, D.R., The Ultraviolet Flash Photolysis of Ozone and the Reactions of O(1D) and O2(1Σg+), Can. J. Chem., 52, 1974

[204] Hogan, L.G.; Burch, D.S., A Measurement of the Rate Constant for the Reaction O + O2 + O2 → O3 + O2, J. Chem. Phys., 65, 1976

[205] Arnold, I.; Comes, F.J., Temperature Dependence of the Reactions O(3P) + O3 → 2O2 and O(3P) + O2 + M → O3 + M, Chem.Phys., 42, 1979

[206] H. Endo, K. Glanrer, and J. Troe, Shock Wave Study of Collisional Energy Transfer in the Dissociation of NO2, CINO, O3, and N20, The Journal of Physical Chemistry, Vol. 83, No. 16, 1979

[207] Sugawara, K.; Ishikawa, Y.; Sato, S., Absolute Rate Constants for the Reactions of O(3P) with Several Molecules, Bull. Chem. Soc. Jpn., 53, 1980

[208] Klais, O.; Anderson, P.C.; Kurylo, M.J., A Reinvestigation of the Temperature Dependence of the Rate Constant for the Reaction O + O2 + M → O3 + M (for M = O2,

N2, and Ar) by the Flash Photolysis Resonance Fluorescence Technique, Int. J. Chem. Kinet., 12, 1980

[209] Lin, C.L.; Leu, M.T., Temperature and Third-Body Dependence of the Rate Constant for the Reaction O + O2 + M → O3 + M, Int. J. Chem. Kinet., 14, 1982

[210] Croce de Cobos, A.E.; Troe, J., High-pressure range of the recombination O + O2 → O3, Int. J. Chem. Kinet., 16, 1984

[211] Anderson, S.M.; Hulsebusch, D.; Mauersberger, K., Surprising rate coefficients for four isotopic variants of O+O2+M, J. Chem. Phys., 107, 5385-5392, 1997

[212] Sehested, J.; Nielsen, O.J.; Egsgaard, H.; Larsen, N.W.; Andersen, T.S.; Pedersen, T., Kinetic study of the formation of isotopically substituted ozone in argon, J. Geophys. Res., 103, 3545-3552, 1998

[213] Y. Tarchouna, M. Bahri, N. Jaidane, Z. Ben Lakhdar, J.P. Flament, Theoretical study of the kinetics of the hydrogen abstraction reaction H2O2+O(3P) → OH+ HO2, Journal of Molecular Structure (Theochem) 664-665 (2003) 189-196

[214] H. Koussa, M. Bahri, Theoretical kinetics study of two competing path in the H2O2+O(3P) → HO2 + OH reaction, Journal of Molecular Structure: THEOCHEM 850 (2008) 17-20

[215] E. A. ALBERS, K. HOYERMANN, H. GG. WAGNER, AND J. WOLFRUM, ABSOLUTE MEASUREMENTS OF RATE COEFFICIENTS FOR THE REACTIONS OF H AND O ATOMS WITH H20~ AND H20, Institut fiir Physikalische Chemie der Universitdt, Bochum und GSttingen, GSttingen, Germany, 1971

[216] D. Davis W. Wong R. Schiff, A Dye Laser Flash Photolysis Kinetics Study of the Reaction of Ground-State Atomic Oxygen with Hydrogen Peroxide, The Journai of Physical Chemistry. Vol. 78, No. 4., 1974

[217] P. H. Wine, J. M. Nlcovlch, R. J. Thompson, and A. R. Ravlshankara, Kinetics of O(3PJ) Reactions with H202 and O3, The Journal of Physical Chemistry, Vol. 87, No. 20, 1983

[218] Stephen J. Klippenstein, Raghu Sivaramakrishnan, Ultan Burke, Kieran P. Somers, Henry J. Curran, Liming Cai, Heinz Pitsch, Matteo Pelucchi, Tiziano Faravelli, Peter Glarborg, HȮ2 + HȮ2: High Level Theory and the Role of Singlet Channels

[219] E.L. Petersen, D.F. Davidson, R.K. Hanson, Kinetics Modeling of Shock-Induced Ignition in Low-Dilution CH4/O2 Mixtures at High Pressures and Intermediate Temperatures, Combustion and Flame, Volume 117, Pages 272-290, 1999

[220] Jinhua Wang , Zuohua Huang, Hideaki Kobayashi, Yasuhiro Ogami, Laminar burning velocities and flame characteristics of CO-H2-CO2-O2 mixtures, International Journal of Hydrogen Energy 37 (2012), 19158-19167

[221] Jérémy Sabard, Nabiha Chaumeix, Ahmed Bentaib, Hydrogen explosion in ITER: Effect of oxygen content on flame propagation of H2/O2/N2 mixtures, Fusion Engineering and Design, 88 (2013) 2669-2673

[222] R. Grosseuvres, A. Comandini, A. Bentaib, N. Chaumeix, Combustion properties of H2/N2/O2/steam mixtures, Proceedings of the Combustion Institute 37 (2019) 1537–1546

[223] Michael C. Krejci, Olivier Mathieu, Andrew J. Vissotski, Sankaranarayanan Ravi, Travis G. Sikes, Eric L. Petersen, Alan Ke´rmone`s, Wayne Metcalfe, Henry J. Curran, Laminar Flame Speed and Ignition Delay Time Data for the Kinetic Modeling of Hydrogen and Syngas Fuel Blends, Journal of Engineering for Gas Turbines and Power FEBRUARY 2013, Vol. 135

[224] Qiaosheng Zhang, Guoyan Chen, Haoxin Deng, Xiaoping Wen, Fahui Wang, Anchao Zhang, Wei Sheng, Experimental and numerical study of the effects of oxygen-enriched air on the laminar burning characteristics of biomass-derived syngas, Fuel 285 (2021) 119183

[225] ALEXANDER A. KONNOV, IGOR V. DYAKOV and JACQUES DE RUYCK, NITRIC OXIDE FORMATION IN PREMIXED FLAMES OF H2 + CO + CO2 AND AIR, Proceedings of the Combustion Institute, Volume 29, 2002/pp. 2171–2177

[226] Hongyan Sun, S.I. Yang, G. Jomaas, C.K. Law, High-pressure laminar flame speeds and kinetic modeling of carbon monoxide/hydrogen combustion, Proceedings of the Combustion Institute 31 (2007) 439–446

[227] Xianzhong Hu, Qingbo Yu, Effect of the elevated initial temperature on the laminar flame speeds of oxy-methane mixtures, Energy 147 (2018) 876-883

[228] Ji-Woong Han, Chang-Eon Lee, Sung-Min Kum, and Yong-Soo Hwang, Study on the Improvement of Chemical Reaction Mechanism of Methane Based on the Laminar Burning Velocities in OEC, Energy & Fuels 2007, 21, 3202–3207

[229] Jeongseog Oh, Dongsoon Noh, Laminar burning velocity of oxy-methane flames in atmospheric condition, Energy 45 (2012) 669-675

[230] Stéphanie de Persis, Fabrice Foucher, Laure Pillier, Vladimiro Osorio, Iskender Gökalp, Effects of O2 enrichment and CO2 dilution on laminar methane flames, Energy 55 (2013) 1055-1066

[231] Yongliang Xie, Jinhua Wang, Meng Zhang, Jing Gong, Wu Jin, and Zuohua Huang, Experimental and Numerical Study on Laminar Flame Characteristics of Methane Oxy-fuel Mixtures Highly Diluted with CO2, Energy Fuels 2013, 27, 6231−6237

[232] Xiao Cai, Jinhua Wang , Weijie Zhang, Yongliang Xie, Meng Zhang, Zuohua Huang, Effects of oxygen enrichment on laminar burning velocities and Markstein lengths of CH4/O2/N2 flames at elevated pressures, Fuel 184 (2016) 466-473

[233] X. J. GU, M. Z. HAQ, M. LAWES, and R. WOOLLEY, Laminar Burning Velocity and Markstein Lengths of Methane–Air Mixtures, COMBUSTION AND FLAME 121:41–58 (2000)

[234] William Lowry, Jaap de Vries, Michael Krejci, Eric Petersen, Zeynep Serinyel, Wayne Metcalfe, Henry Curran, Gilles Bourque, Laminar Flame Speed Measurements and Modeling of Pure Alkanes and Alkane Blends at Elevated Pressures, Journal of Engineering for Gas Turbines and Power SEPTEMBER 2011, Vol. 133

[235] G. ROZENCHAN, D. L. ZHU, C. K. LAW and S. D. TSE, OUTWARD PROPAGATION, BURNING VELOCITIES, AND CHEMICAL EFFECTS OF METHANE FLAMES UP TO 60 atm, Proceedings of the Combustion Institute, Volume 29, 2002/pp. 1461–1469

[236] R. Mevel, J. Sabard, J. Lei, N. Chaumeix, Fundamental combustion properties of oxygen enriched hydrogen/air mixtures relevant to safety analysis: Experimental and simulation study, International Journal of Hydrogen Energy 41 (2016), 6905-6916

[237] A.N. Mazas, B. Fiorina, D.A. Lacoste, T. Schuller, Effects of water vapor addition on the laminar burning velocity of oxygen-enriched methane flames, Combustion and Flame 158 (2011) 2428-2440

[238] A.R. Khan, S. Anbusaravanan, Lokesh Kalathi, Ratnakishore Velamati, C. Prathap, Investigation of dilution effect with N2/CO2 on laminar burning velocity of premixed methane/oxygen mixtures using freely expanding spherical flames, Fuel 196 (2017) 225-232

[239] M. Alfè, B. Apicella, J.-N. Rouzaud, A. Tregrossi, A. Ciajolo, The effect of temperature on soot properties in premixed methane flames, Combustion and Flame 157 (2010) 1959–1965

[240] PAMELA A. BERG, DEBORAH A. HILL, ALISON R. NOBLE, GREGORY P. SMITH, JAY B. JEFFRIES, and DAVID R. CROSLEY, Absolute CH Concentration

Measurements in Low-Pressure Methane Flames: Comparisons with Model Results, COMBUSTION AND FLAME 121:223–235 (2000)

[241] Miad Karimi, Bradley Ochs, Zefang Liu, Devesh Ranjana, Wenting Sun, Measurement of methane autoignition delays in carbon dioxide and argon diluents at high pressure conditions, Combustion and Flame 204 (2019) 304-319

[242] A. M. DEAN, D. C. STEINER, E. E. WANG, A Shock Tube Study of the H2/O /CO/Ar and H2/N2O/CO/Ar Systems: Measurement of the Rate Constant for H + N2O = + OH*, Combustion and Flame 32, 73-83 (1978)

[243] C. S. EUBANK, M. J. RABINOWITZ, W. C. GARDINER, JR., AND R. E. ZELLNER, SHOCK-INITIATED IGNITION OF NATURAL GAS-AIR MIXTURES, Eighteenth Symposium (International) on Combustion, The Combustion Institute, 1981

[244] Danielle M. Kalitan, Eric L. Petersen, John D. Mertens, Mark W. Crofton, IGNITION OF LEAN CO/H2/AIR MIXTURES AT ELEVATED PRESSURES, Proceedings of GT2006 ASME Turbo Expo 2006: Power for Land, Sea and Air May 8-11, 2006, Barcelona, Spain

[245] Daniel J. Seery and Craig T. Bowman, An Experimental and Analytical Study of Methane Oxidation Behind Shock Waves, Comhusthm & Flame, 14, 37 -48 (1970)

[246] L. J. SPADACCINI and M. B. COLKET III, IGNITION DELAY CHARACTERISTICS OF METHANE FUELS, Prog. Energy Combust. Sci. VoL 20, pp. 431-460, 1994

[248] MARIA U. ALZUETA, RAFAEL BILBAO, PETER GLARBORG, Inhibition and Sensitization of Fuel Oxidation by SO2, COMBUSTION AND FLAME 127:2234–2251 (2001)

[249] TAE J. KIM, RICHARD A. YETTER AND FREDERICK L. DRYER, NEW RESULTS ON MOIST CO OXIDATION: HIGH PRESSURE, HIGH TEMPERATURE EXPERIMENTS AND COMPREHENSIVE KINETIC MODELING, Twenty-Fifth Symposium (International) on Combustion/The Combustion Institute, 1994/pp. 759 766

[250] M.S. Skjøth-Rasmussen, P. Glarborg, M. Østberg, J.T. Johannessen, H. Livbjerg, A.D. Jensen, T.S. Christensen, Formation of polycyclic aromatic hydrocarbons and soot in fuel-rich oxidation of methane in a laminar flow reactor, Combustion and Flame 136 (2004) 91–128

[251] CHRISTIAN LUND RASMUSSEN, JON GEEST JAKOBSEN, PETER GLARBORG, Experimental Measurements and Kinetic Modeling of CH4/O2 and

CH4/C2H6/O2 Conversion at High Pressure, International Journal of Chemical Kinetics DOI 10.1002/kin

[252] Pino Sabia, Mariarosaria de Joannon, Antonio Picarelli, Raffaele Ragucci, Methane auto-ignition delay times and oxidation regimes in MILD combustion at atmospheric pressure, Combustion and Flame 160 (2013) 47–55

[253] Fikri Sen, Bo Shu, Tina Kasper, Jürgen Herzler, Oliver Welz, Mustapha Fikri, Burak Atakan, Christof Schulz, Shock-tube and plug-flow reactor study of the oxidation of fuel-rich CH4/O2 mixtures enhanced with additives, Combustion and Flame 169 (2016) 307–320

[254] R. Sivaramakrishnan, A. Comandini, R.S. Tranter, K. Brezinsky, S.G. Davis, H. Wang, Combustion of CO/H2 mixtures at elevated pressures, Proceedings of the Combustion Institute 31 (2007) 429–437

[255] A. El Bakali, P. Dagaut, L. Pillier, P. Desgroux, J.-F. Pauwels, A. Rida, and P. Meunier, Experimental and modeling study of the oxidation of natural gas in a premixed flame, shock tube, and jet-stirred reactor, Combustion and Flame 137 (2004) 109–128

[256] Tanh Le Cong & Philippe Dagaut (2008) Experimental and Detailed Kinetic Modeling of the Oxidation of Methane and Methane/Syngas Mixtures and Effect of Carbon Dioxide Addition, Combustion Science and Technology, 180:10-11, 2046-2091, DOI: 10.1080/00102200802265929

[257] T. Le Cong, P. Dagaut, G. Dayma, Oxidation of Natural Gas, Natural Gas/Syngas Mixtures, and Effect of Burnt Gas Recirculation: Experimental and Detailed Kinetic Modeling, Journal of Engineering for Gas Turbines and Power JULY 2008, Vol. 130

[258] T. Le Cong, P. Dagaut, Experimental and Detailed Modeling Study of the Effect of Water Vapor on the Kinetics of Combustion of Hydrogen and Natural Gas, Impact on NOx, Energy & Fuels 2009, 23, 725–734

[259] Tanh Le Cong, Philippe Dagaut, Oxidation of H2/CO2 mixtures and effect of hydrogen initial concentration on the combustion of CH4 and CH4/CO2 mixtures: Experiments and modelling, Proceedings of the Combustion Institute 32 (2009) 427–435

[260] PHILIPPE DAGAUT , JEAN-CLAUDE BOETTNER & MICHEL CATHONNET (1991) Methane Oxidation: Experimental and Kinetic Modeling Study, Combustion Science and Technology, 77:1-3, 127-148, DOI: 10.1080/00102209108951723

[261] PHILIPPE DAGAUT, FRANCK LECOMTE, JACOB MIERITZ, PETER GLARBORG, Experimental and Kinetic Modeling Study of the Effect of NO and SO2 on the Oxidation of CO–H2 Mixtures, DOI 10.1002/kin.10154

[262] Philippe Dagaut, Guillaume Dayma, Hydrogen-enriched natural gas blend oxidation under high-pressure conditions: Experimental and detailed chemical kinetic modelling, International Journal of Hydrogen Energy 31 (2006) 505 – 515

[263] Edoardo Ramalli, Gabriele Scalia, Barbara Pernici, Alessandro Stagni, Alberto Cuoci, and Tiziano Faravelli. Data ecosystems for scientific experiments: managing combustion experiments and simulation analyses in chemical engineering. Frontiers in big Data, page 67, 2021.

List of Figures

List of Tables

POLITECNICO
MILANO 1863

SCUOLA DI INGEGNERIA INDUSTRIALE
E DELL'INFORMAZIONE

EXECUTIVE SUMMARY OF THE THESIS

Reconciling theory, experiments and models for hydrogen combustion: an integrated theoretical and optimization approach

TESI MAGISTRALE IN CHEMICAL ENGINEERING – INGEGNERIA CHIMICA

AUTHOR: Claudio Averoldi

ADVISOR: Prof. Matteo Pelucchi

CO-ADVISOR: Dr. Andrea Bertolino

ACADEMIC YEAR: 2020-2021

1. Introduction

In the modern society, major problems are related to energy demand and human activities in general, which produce many consequences on the environment. Pollutant emissions such as CO2 and greenhouse gases, affect many aspects such as climate change, and effects are already visible proving that an immediate step change is needed [1].
In this context, decarbonization becomes one of the main challenges nowadays, with the development of green energy sector, and the use of smart energy carriers, such as hydrogen, instead of fossil fuels.
If produced from renewable sources (i.e. via water electrolysis using renewable energy, or through reactor electrification with cracking or steam reforming processes), hydrogen can guarantee the achievement of a green energy economy being applicable to many applications. For this reason, hydrogen is a molecule of interest for future developments of both the process and the energy industry, also in the short-medium perspective.
In order to design new facilities optimized for hydrogen combustion technology, as pure or in mixture with other hydrocarbons, the importance of having a predictive chemical kinetic model that can guarantee accurate simulations becomes necessary. The proposal of this work is to provide the state-of-the-art model for hydrogen combustion through a multiscale approach.
Some progresses in this direction have already been done, this work in fact inherits the efforts of a project by Politecnico di Milano, RWTH Aachen University, Argonne National Laboratory, National University of Ireland Galway, Technical University of Denmark and Eötvös Loránd University, the goal is to define a common state-of-the-art model for hydrogen combustion to the chemical kinetics community, starting from theoretical bases and then reconciling it with experimental data, including both rate constant and combustion properties measurements.
From this work, a modified H_2 model has been produced, by updating rate constants for many reactions.

2. Kinetic modeling

Kinetic modeling is a fundamental step in the design of new combustion technologies and new fuels that are sustainable and applicable to already existing devices. Indeed, a deep knowledge of chemical kinetics allows to predict how the system evolves changing the operative conditions (temperature, pressure, residence time, fuel composition, etc.), and therefore to optimize the design of burners, engines and thermal machines by means of detailed chemical kinetics appropriately reduced to be coupled with Computational Fluid Dynamics simulations.
Hydrogen is also a molecule of particular importance for any fuel when modeling its combustion properties. In fact, the typical structure of combustion kinetic models is hierarchical, and hydrogen combustion, lies at the tip of this hierarchy. For this reason, despite being the simplest subset in terms of species and reactions, it is often referred to as the "core mechanism", and therefore its refinement or update its critical largely impacting also the combustion behavior of larger molecules as well as the pathways to pollutants formation [2].
Furthermore, the "simplicity" of the hydrogen subset, as well as the experimental, theoretical and modelling interest that it as received since the dawn of combustion science and engineering, allow the efficient implementation of the workflow proposed in this work.

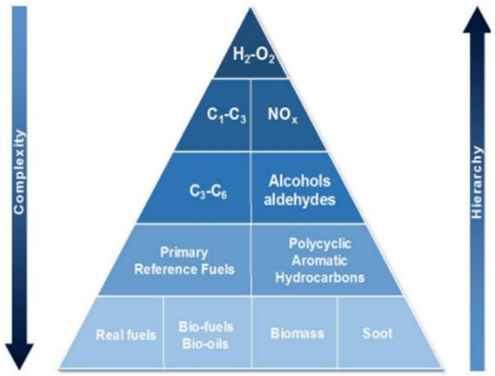

Figure 1: Hierarchy and complexity "pyramid" of combustion chemical kinetics.

3. Methods

This work deals both with pressure dependent and pressure independent reactions.
The first ones are also known as third body reactions, where a collision with a third body is required to stabilize the final products. This reaction, at intermediate pressures (i.e. between the low and the high pressure limit), and typically at high temperatures, show the so called fall-off behavior. Pressure dependent reaction rate constants are described using the PLOG formalism, which seems to give the best results in fitting experimental data, while pressure independent rate constants are written in the modified Arrhenius form. The PLOG formalism is just a set of different modified Arrhenius expressions determined at different pressures. For pressures in between a logarithmic interpolation is performed by commercial and opensource solvers such as OpenSMOKE++ [3].
For pressure independent reactions, the starting point are the Arrhenius coefficients used in the original hydrogen model, for pressure dependent reactions, the starting point is theoretical calculations, computed with Ab Initio Transition State Theory based Master Equation and Potential Energy Surface at Argonne National Laboratory. These methods are known to provide highly accurate rate constants and have become the standard in combustion kinetic model developments [4].
Experimental data for elementary reaction rate constants have been collected from the extensive literature. Out of the > 10000 experimental data points in >1000 datasets, only the most direct measurements were retained and considered in the work-flow. This was found to be typical of early studies where diagnostics limitations were evident or the lack of a comprehensive knowledge of the system led to inappropriate interpretations of the observed phenomena. This selection was also guided by theory calculations that are expected to provide a factor of 2 uncertainty in the worst case scenario. Data that were found to be outside this range were carefully analyzed before being retained or neglected.
Data used in this work cover both those on reaction rates for a single elementary reaction (microscopic data), and those used for the validation step instead. These latter are typically ideal reactor experiments, and the observable of most industrial

interest are typically flame velocities and ignition delay times (macroscopic data).
The optimization step has been performed using OptiSMOKE++, a toolbox developed by Fürst, Bertolino et al. [5] for the optimization of chemical kinetic models, it uses the algorithms contained in DAKOTA [6] (Design analysis kit for optimization and terascale applications). For the scopes of this work an evolutionary algorithm was used, and the objective functions defined based on L1 and L2-norm.
The optimized reactions have been tested singularly on some macroscopical experiments, to assess the effect of a single modified reaction on the simulation.
Once all the reactions have been reviewed, the new model has been assembled and the comprehensive validation performed. Simulations of premixed laminar flames, shock tubes, PFRs and PSRs, where performed using the OpenSMOKE++ suite of programs, with both the original model and the new model, in order to see overall effect of the revisions from this effort.

4. Results

For each reaction the Potential Energy Surfaces (PES) is investigated with gold-standard methods [7].
Microscopic data for every reaction are summarized in tables that report the literature references, the operative conditions (T, p) and the bath gas involved in the case of pressure dependent reactions.
Then, for every reaction investigated, an optimization step is performed, in which the starting model (i.e. the rate constant from theory calculations for pressure dependent reactions, or the rate constant from the old model for temperature dependent only cases), the experimental data and the optimized model are reported, as follows:

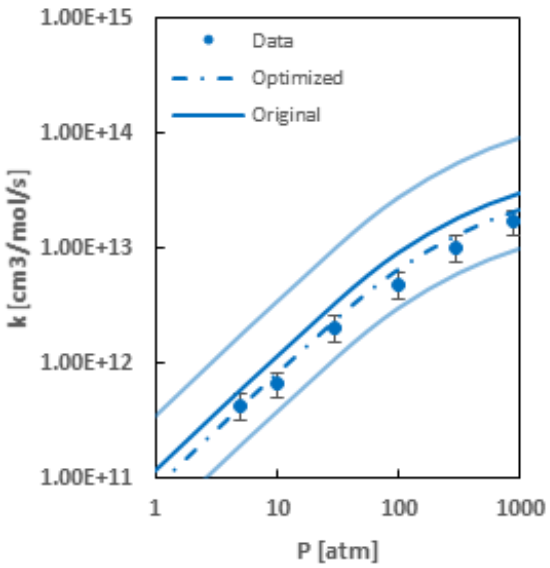

Figure 2: Optimization step for reaction $R17a: H\cdot + O_2 + M \rightarrow HO_2\cdot + M$ with He as a bath gas, data reported are at fixed temperature T=500 K

For these reactions, data can be represented (following how experiments have been carried out) as in Figure 2, varying pressure freezing temperature value or freezing pressure varying temperature, as in the following example:

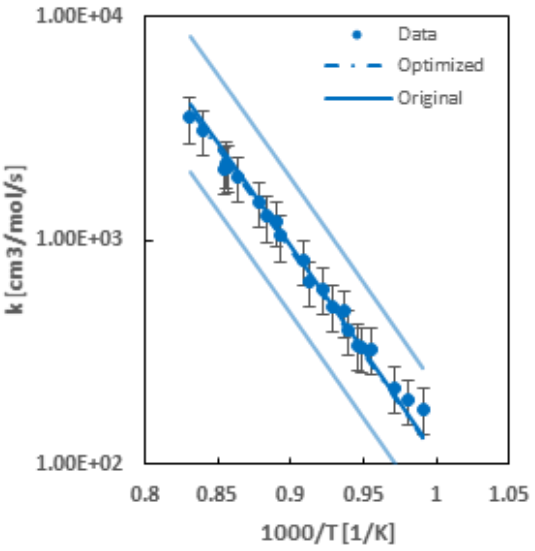

Figure 3: Optimization step for reaction $R18a: H_2O_2 + M \rightarrow 2OH\cdot + M$ with AR as a bath gas, data reported are at a fixed pressure P=1.98 atm

While, for pressure independent reactions, T is the only variable:

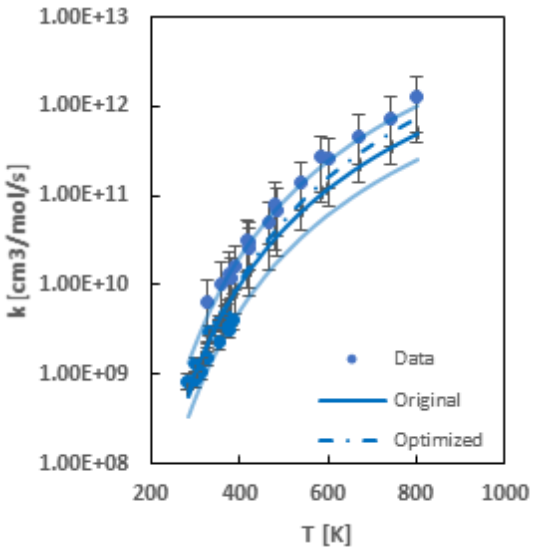

Figure 4: Optimization step for pressure independent reaction $R26b: H_2O_2 + O(^3P) \rightarrow OH\cdot + HO_2\cdot$

As is in the legend, blue line represents the starting point for optimization, dash-dotted line is the optimized model and light blue lines are the bounds for the optimizer.
Then every single reaction is tested on a few cases of the macroscopic experiments database so as to provide insights on the effects, as reported in Figure 5.

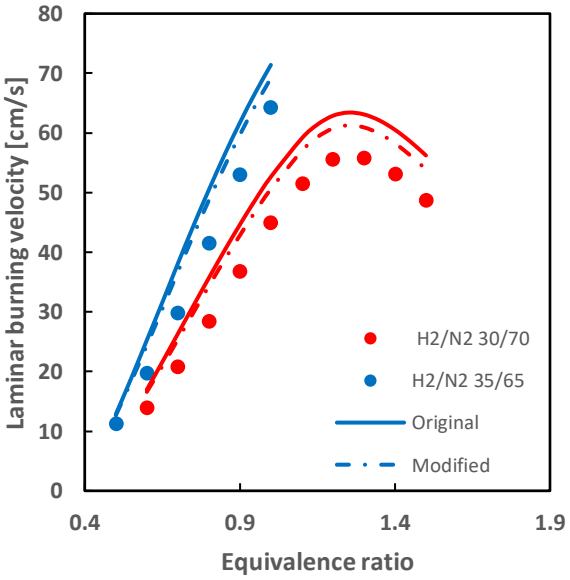

Figure 5: Optimized mechanism for reaction $R18c: H\cdot + HO_2\cdot \rightarrow H_2 + O_2$ is tested on a flame velocity (data from Voss et al. [8]) to assess the impact of the modification

As a last step, the original Polimi model (CRECK 2003, March 2020) which is largely based on the Aramco mech 2.0 [9] the final model obtained from this work is validated over the entire database of macroscopical experiments. Examples are reported in Figure 6 and 7.

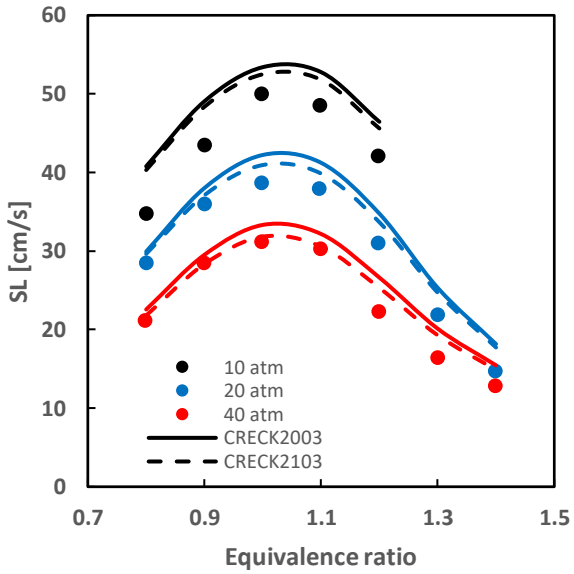

Figure 6: New model vs Polimi model on a premixed laminar flame at different pressures, experimental data are from Rozenchan et al. [10]

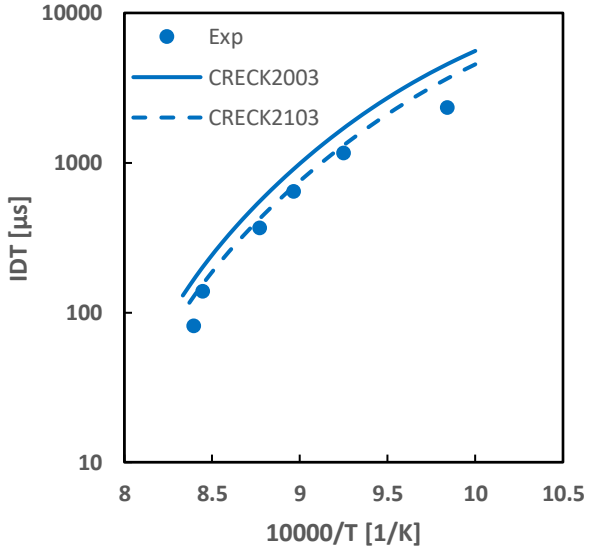

Figure 7: New model vs Polimi model in ignition delay time evaluation in a shock tube, data are from Kalitan et al. [11]

As expected from the well trained nature of the starting model the variations are not dramatic, but still notably in the desired direction showing overall important improvements of model performances in particular for high dilution cases (e.g. MILD combustion conditions) and for oxy-

fuel combustion of particular interest for the hydrogen energy economy.

5. Conclusions

This work proposes a state of the art model for hydrogen combustion, conciliating theory and experimental data.
In general, comparing the model obtained in this work with the previous version, an improvement can be seen in reproducing experimental data at medium-high pressure conditions, this is attributable to the introduction of PLOG formalism for pressure dependent reactions, and for cases with large amounts of exhaust gas recirculation.
Not in every case the results provided by the new model are better than the previous, this is reasonable, Aramco mech 2.0 is in fact a "well trained" mechanism, i.e. it has been tested on a large scale of experiments, and the kinetic constants have been gradually improved to better reproduce those data, therefore an high accuracy is expected. In other word: the starting model was already a good model.
The new model, still, can be furtherly improved, by completing the theoretical revision on the missing reactions firstly, and also deepening the experimental knowledge, especially for those reactions that show a lack of microscopic data (this also arises doubts on their reliability).
Also, more investigations (both theoretical and experimental) on different bath gases can increase the accuracy in interpretation for pressure dependent reactions.
As we believe in a growing interest on industrial use of hydrogen in the next years, a completely predictive theory-based model for hydrogen combustion will be fundamental for future perspectives on transition to green energy.
Future works in the same direction can be made for kinetic modeling of bigger species, to optimize the design of new technologies in terms of both efficiency and pollutant emissions.

6. Bibliography

[1] https://climate.nasa.gov/

[2] Matteo Pelucchi, Alessandro Stagni, Tiziano Faravelli, Addressing the complexity of combustion kinetics: Data management and automatic model validation, Computer Aided Chemical Engineering, 2019, Volume 49, pp 763-798.

[3] Alberto Cuoci, Alessio Frassoldati, Tiziano Faravelli, Eliseo Ranzi, OpenSMOKE++: An object-oriented framework for the numerical modeling of reactive systems with detailed kinetic mechanisms, Computer Physics Communications, 2015. 192: p. 237-264.

[4] Stephen J. Klippenstein, From theoretical reaction dynamics to chemical modeling of combustion, Proceedings of the Combustion Institute, 2017, Volume 36, pp. 77-111.

[5] Magnus Fürst, Andrea Bertolino, Alberto Cuoci, Tiziano Faravelli, Alessio Frassoldati, and Alessandro Parente. Optismoke++: A toolbox for optimization of chemical kinetic mechanisms. Computer Physics Communications, 264:107940, 2021.

[6] Brian M Adams, W J TBohnhoff, K R Dalbey, J P Eddy, M S Eldred, D M Gay, K Haskell, Patricia D Hough, and Laura P Swiler. DAKOTA, a multilevel parallel object-oriented framework for design optimization, parameter estimation, uncertainty quantification, and sensitivity analysis: version 5.0 user's manual. Sandia National Laboratories, Tech. Rep. SAND2010-2183, 2009.

[7] Stephen J. Klippenstein, Carlo Cavallotti, Ab initio kinetics for pyrolysis and combustion systems, Computer Aided Chemical Engineering, 2019, Volume 49, pp 115-167.

[8] S. Voss, S. Hartl, C. Hasse, Determination of laminar burning velocities for lean low calorific H_2/N_2 and $H_2/CO/N_2$ gas mixtures. International journal of hydrogen energy 39, 2014, pp.19810-19817.

[9] International Journal of Chemical Kinetics 45.10 (2013): 638-675.

[10] G.Rozenchan, D.L.Zhu, C.K.Law, S.D.Tse, Outward propagation, burning velocities, and chemical effect of methane flames up to 60 atm. Proceedings of the Combustion Institute, Volume 29, 2002, pp.1461-1469

[11] Danielle M. Kalitan, Eric L. Petersen, John D. Mertens, Mark W. Crofton, Ignition of lean CO/ H2/Air mixtures at elevated pressures. ASME Turbo Expo 2006: Power for Land, Sea, Air, May 8-11, 2006, Barcelona, Spain

7. Acknowledgements

I wish to acknowledge my advisor, Prof. Matteo Pelucchi, for costant help provided in the development of this Thesis, and my co-advisor, Dr. Andrea Bertolino, especially for his active contribution with the implementation of OptiSMOKE++ optimization routine for this work.

I also wish to acknowledge Prof. Stephen J. Klippenstein and Prof. Liming Cai, that co-operated with us in this project.